F
N
P

Journal of FOOD PROCESS ENGINEERING

Edited by D. R. Heldman, Michigan State University

FOOD & NUTRITION PRESS, INC.
WESTPORT, CONNECTICUT 06880 USA

VOLUME 1, NUMBER 1 JANUARY 1977

JOURNAL OF FOOD PROCESS ENGINEERING

Editor: D. R. HELDMAN, Chairman, Department of Agricultural Engineering, Michigan State University, East Lansing, Michigan

Editorial Board:

A. L. BRODY, Mead Packaging, Atlanta, Georgia

J. M. HARPER, Head, Agricultural Engineering Department, Colorado State University, Fort Collins, Colorado

C. G. HAUGH, Agricultural Engineering Department, Purdue University, Lafayette, Indiana

C. J. KING, Chairman, Department of Chemical Engineering, University of California, Berkeley, California

K. F. MATTIL, Food Protein Research and Development Center, Texas A. and M. University, College Station, Texas

R. L. MERSON, Department of Food Science and Technology, University of California, Davis, California

N. N. MOHSENIN, Agricultural Engineering Department, Pennsylvania State University, University Park, Pennsylvania

F. W. SCHMIDT, Department of Mechanical Engineering, Pennsylvania State University, University Park, Pennsylvania

All articles for publication and inquiries regarding publication should be sent to Prof. D. R. Heldman, Michigan State University, Department of Agricultural Engineering, East Lansing, Michigan 48824 USA.

All subscriptions and inquiries regarding subscriptions should be sent to Food & Nutrition Press, Inc., 265 Post Road West, Westport, Connecticut USA.

One volume of four issues will be published annually. The price per volume is $45.00 which includes postage to U.S., Canada, and Mexico. Subscriptions to other countries are $55.00 per year via surface mail, and $62.00 per year via airmail.

Subscriptions for individuals for their own personal use are $25.00 per volume which includes postage to U.S., Canada, and Mexico. Personal subscriptions to other countries are $35.00 per year via surface mail, and $42.00 per year via airmail. Subscriptions for individuals should be sent direct to the publisher and marked for personal use.

JOURNAL OF FOOD PROCESS ENGINEERING

JOURNAL OF FOOD PROCESS ENGINEERING

Journal of
FOOD PROCESS ENGINEERING

VOLUME 1

Editor: D. R. HELDMAN

FOOD & NUTRITION PRESS, INC.
WESTPORT, CONNECTICUT USA

ISSN 0145-8876

Printed in the United States of America

CONTENTS

EDITORIAL

The initiation of a new technical journal is a challenging and controversial issue. The advantages and disadvantages must be carefully identified, evaluated and analyzed. Although these advantages and disadvantages will vary depending on the individual involved in the identification, the overriding issue to be considered in the case of food engineering is that a new discipline is evolving.

For nearly twenty-five years, technical research articles dealing with some aspect of food engineering have been published in a wide variety of technical journals. In most cases, the location of publication has been determined by the professional affiliation of one or more of the authors involved. This approach to the publication of technical literature in the area of food engineering has resulted in an extremely complex situation for the new researcher with an interest in food engineering. Unfortunately, literature reviews have become time consuming and difficult and often the researcher overlooks an important contribution due to a lack of contact with the appropriate journal.

It is not the purpose of the *Journal of Food Process Engineering* to serve as the single location for all literature in food engineering. In fact, such a result could detract significantly from the overall impact that researchers in the area of food engineering will have in the next twenty-five years. Hopefully, this new Journal can serve as the focal point for the new researcher in the area of food engineering and reduce significantly the complex and time-consuming efforts devoted to literature reviews. In the *Journal of Food Process Engineering*, an achievement of this purpose will be attempted by publication of review manuscripts in selected areas of food engineering and by publication of lengthy research papers. The emphasis will be on *quality* of technical research literature.

Although the first emphasis of the *Journal of Food Process Engineering* is on serving the researcher, the food engineer employed in the food industry should benefit as well. As processes and equipment become more complex, the sophistication of the food engineer serving the industry must improve. The food engineer working in the food industry is faced with many of the same problems as the researcher when considering the importance of maintaining contact with current technical

literature. With a focal point for food engineering research literature, the food engineer will be able to maintain contact with a major portion of the research developments as they occur.

In addition to review manuscripts and research papers, the *Journal of Food Process Engineering* will be establishing additional features in future issues. These features will include book reviews to assist the reader in maintaining an awareness of the latest technical food engineering literature published in book form. A calendar of events section will be established to include a limited listing of technical meetings which relate to food engineering. The third feature being considered would be a listing of food engineering references in order to provide citations of the literature being published in related discipline areas.

In the final analysis, the intent of the *Journal of Food Process Engineering* is to serve any reader with an interest in technical food engineering literature. We will look forward to fulfilling this intent and we will look forward to reactions from the reader. The scope of subject matter areas to be considered for publication in the Journal has been established and printed. A tentative guide to authors has been included in this issue as well.

The *Journal of Food Process Engineering* is initiated to serve the interests of those who are dedicated to improving processes and equipment design for the most important industry; that which must handle, process and distribute the food for an increasing world population. It seems very appropriate that this Journal evolve in the last quarter of the twentieth century.

D. R. Heldman

HEAT AND MASS TRANSFER FUNDAMENTALS APPLIED TO FOOD ENGINEERING[1]

C. JUDSON KING

Department of Chemical Engineering
University of California
Berkeley, California 94720

Received for Publication January 4, 1977

ABSTRACT

There is a need for deeper qualitative and quantitative understanding of the heat and mass transfer mechanisms underlying various techniques for food production, processing, preservation and storage. This is important for the development of new food sources, for more economical and energy-efficient processing of food from existing sources, for better food quality and quality control, and for adherence to new regulations such as nutritional labeling and shelf-life dating.

Several classes of food-processing problems are presented where advances can be made on the basis of improved understanding of heat and mass transfer mechanisms. These include cases of competing transport, cases where transport competes with kinetics of chemical or biochemical reactions, and cases where determination and understanding of the rate-determining factor are needed. Specific examples are drawn from drying processes, leaching and extraction, freezing, sterilization and enzyme deactivation, and artificial cultivation.

INTRODUCTION

There is a rapidly growing need for better qualitative and quantitative understanding of fundamental phenomena and mechanisms underlying food processing. This includes the production, transformation, preservation and storage of foods. Through a deeper understanding processes can be designed with greater confidence and reliability, and improved processes can be created. The incentives for developing this knowledge have recently substantially increased and will continue to grow. These incentives include

(1) the need for more quantitative control of product quality, as

[1] This paper was presented at Symposium on Improved Unit Operations in Food Engineering, Institute of Food Technologists Annual Meeting, Anaheim, California, June 8, 1976.

Journal of Food Process Engineering 1 (1977) 3–14.

related to nutritional labeling and shelf-life dating;
(2) the need for more energy-efficient and economical processing, as costs of energy and materials increase;
(3) the need for lessening environmental impact through alteration of processes and/or better identification and control of constituents in effluents; and
(4) the need for developing food supplies from new sources, where costs must be kept low if these sources are to be attractive and useful.

Costs of food processing have risen and no longer contribute as small a percentage to the total cost of the food cycle as once was the case. This fact also calls for an improved and more fundamental approach to the engineering of food processes.

Figure 1 shows the central role that an understanding of mechanisms of processes can play. The interpretation of mechanisms relies upon the fundamental principles of transport (fluid dynamics, heat and mass transfer), of thermodynamics (phase equilibrium, chemical-reaction equilibrium, etc.), of chemical kinetics, and of whatever other phenomena may come into play. Although existing knowledge gives much guidance in determining and extending mechanisms, it is often necessary to establish or distinguish between mechanisms through fundamental research. If the mechanism of a process is well-understood, we can represent the process through (hopefully simple) mathematical process models and can generalize so as to extend our knowledge to a wider class of processes or process possibilities. With process models we can make quantitative calculations and predictions which will lead to more reliable design, optimization of design and operating conditions, and less overdesign. Finally, both the mechanistic understanding and the wider scope afforded by generalizing should lead to the generation of new and better processing approaches. The methodology outlined in Fig. 1 has become commonplace in many other industries, but has only begun to be used in the food industry.

Much of the determination of mechanisms reduces to distinguishing between limitations imposed by fundamentally different phenomena, for example, transport as opposed to thermodynamic equilibria. Another important aspect is determining which out of a number of different candidate transport mechanisms is dominant. The purpose of the remainder of this paper is to present several classes of problems in food processing where knowledge of mechanisms of heat and mass transfer is needed, and to explore for some of the ways in which this improved understanding would help.

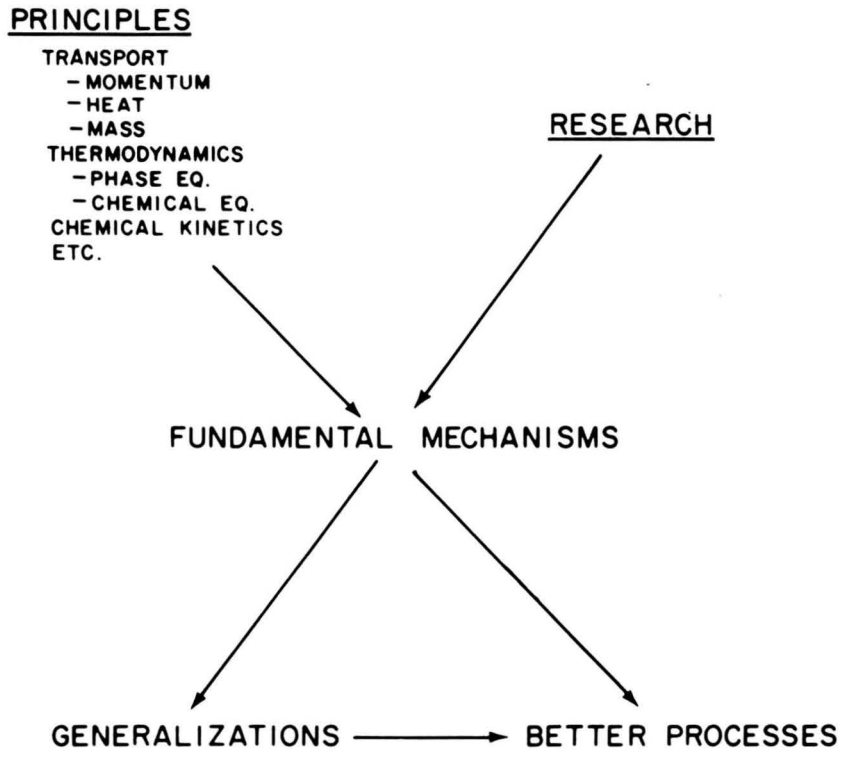

FIG. 1. THE CENTRAL ROLE OF UNDERSTANDING MECHANISMS

COMPETING TRANSPORT

Often the goals of a food process relate directly to favoring one form of transport over another, such as promoting heat transfer while retarding mass transfer of at least some species, or promoting mass transfer of one substance but not of others.

Selective Leaching or Extraction

Leaching or extraction may be carried out so as to recover a particular substance (e.g., soy protein) while leaving others behind, or to remove an undesirable substance (e.g., caffeine, gossypol, arsenic, lactose) while leaving food material behind. In these cases it is desirable to achieve as selective a removal as possible. Another common incentive when non-aqueous solvents are used is for as little of the solvent as possible to be left in the food substance.

Selectivity in leaching or extraction can be achieved through the use

of a solvent which trades upon favorable phase equilibrium — i.e., a high equilibrium distribution coefficient for what is to be extracted, and a low distribution coefficient for what is not to be extracted. Alternatively, selectivity can be achieved through selective transport. Cell membranes themselves give a certain transport selectivity. The transport selectivity can thereby be influenced by the degree of subdivision, by the degree of swelling of a solid matrix by a solvent, and by the temperature, among other causes. It is important to distinguish between transport-rate limits, on the one hand, and equilibrium limits, on the other hand. The relative removals of substances that are rate-limited as opposed to those which are equilibrium-limited can be influenced through changes in temperature, through changes in the solvent-to-feed ratio, and through changes in the flow configuration of the extraction device.

Freezing

The size, shape and location of ice crystals in a frozen substance are influenced by the relative rates of nucleation and growth of ice crystals, as they reflect the temperature history and the rate of freezing. Controlling ice-crystal morphology is one of the more promising avenues for improving freeze concentration processes (Huige *et al.* 1973; Stocking and King 1976). The ice-crystal morphology also has a strong influence upon the retention of volatile flavors and aromas in freeze drying (Flink and Karel 1970; Rulkens and Thijssen 1972; King 1971).

For structured foods the ice-crystal size and location has much to do with quality factors such as texture and drip tendency. Figure 2 shows an idealization of the number, size and location of ice crystals reported by Koonz and Ramsbottom (1939) for chicken meat frozen at different rates of cooling. The number of crystals and the position inside or outside the fibers probably depend upon balances between inherent crystal nucleating and growth rates, the rate of heat conduction to a crystallite site, the rate of moisture diffusion within a fiber, and the rate of moisture diffusion through the wall (sarcolemma) of a fiber.

Selective Dewatering

Drying and concentration processes are typically situations where one strives for removal of water and nothing else. This is often difficult, because of the volatility of many flavor and aroma substances, the permeability of natural or synthetic membranes to substances other than water, and the solubility of other substances in water-extracting solvents. Some avenues toward selective water removal are using a

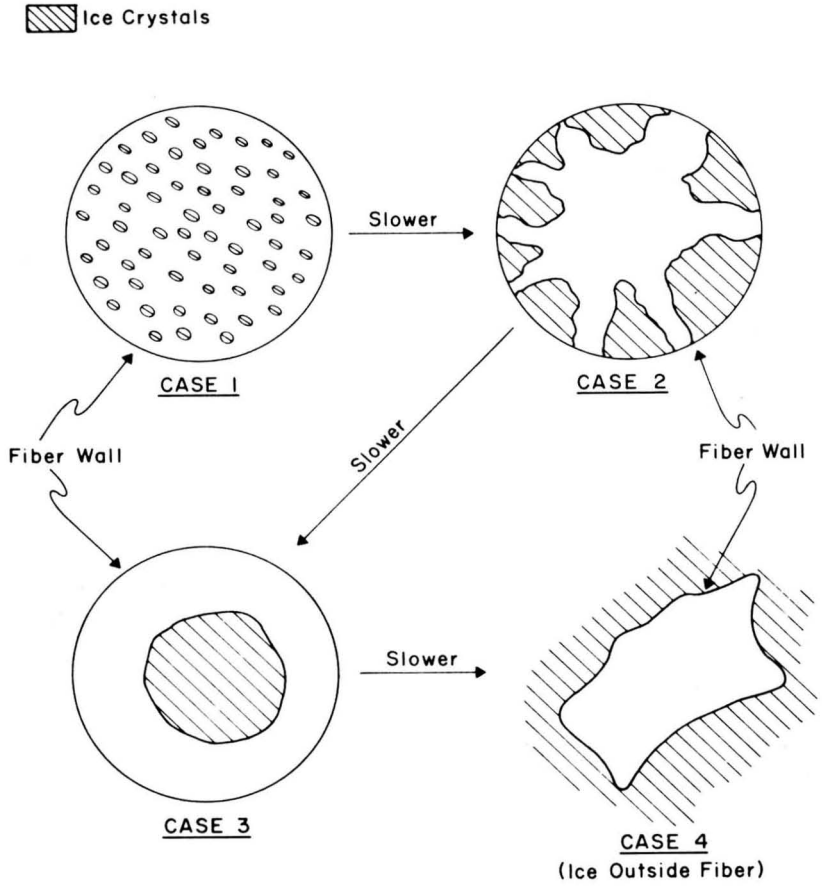

FIG. 2. IDEALIZATION OF ICE-CRYSTAL MORPHOLOGIES IN FIBERS OF FROZEN POULTRY MEAT (AFTER KOONZ AND RAMSBOTTOM 1939)

The freezing velocity is greatest for Case 1, and decreases sequentially from case to case.

process, such as freezing, where water is the only substance in a second phase at equilibrium, or imposing a selective transport barrier (King 1974a, 1974b). A particularly useful result of fundamental mass-transfer studies over the past ten years is the finding that high concentrations of carbohydrates or some other substances at the surface of a food particle exert a highly water-selective barrier (Thijssen and Rulkens 1968; Thijssen 1971).

Balanced Flavor Retention

There is also an incentive for achieving a balanced flavor removal if some of the flavor constituents are lost through processing. Loss of most of some components with nearly complete retention of others can result in an off-flavor. In cases (e.g., evaporation or extraction) where flavor loss is caused by equilibration with a vapor phase or a solvent, it is important to know the different equilibrium distribution coefficients or relative volatilities of the various important flavor components. When flavor loss is transport limited, it then becomes important to judge the mobilities of different substances. Fortunately, many important flavor compounds seem to have about the same diffusivities as one another in water and in concentrated aqueous solutions.

Structure Retention in Drying

Product collapse or shrivelling in air drying is caused by surface-tension forces involving liquid water. There have been numerous processing approaches (puffing, etc.) proposed which effectively serve to negate or counterbalance the surface-tension contractive force. Clearly, an understanding of the mechanisms of the various phenomena involved can lead to a better balance between prevention of shrinkage; loss of nutrients, flavor, etc.; and structure disruption in such processes. As but one example, the pressure-freeze, air-dry process of Haas *et al.* (1972) can be interpreted in terms of a mechanism involving equilibrium dissolution of gases and counterdiffusion with air across cell-wall membranes (King 1974c). Understanding of the mechanism can then lead to optimum process operation and modifications to increase process workability or reduce expense.

COMPETING TRANSPORT AND CHEMICAL REACTION

In other cases the goals of a process have to do with favoring or discouraging the rate of one or more chemical or biochemical reactions in comparison with transport rates.

Enzyme Deactivation

Blanching is a process wherein the goal is usually to cause the reaction of enzyme deactivation, while minimizing other reactions and loss of food constituents. Since enzyme deactivation is usually accomplished through heat, the goals devolve (1) to promoting heat transfer while discouraging mass-transfer processes leading to leaching, and (2)

to supplying the heat through a program which is optimal for achieving enzyme deactivation while discouraging side reactions or transport. Achieving these goals requires quantitative understanding of mechanisms and rates (including activation energies) of enzyme deactivation reactions and reactions altering nutrients, color, texture, etc., as well as an understanding of mechanisms of leaching in the case of water blanching.

Sterilization

Similar goals hold for sterilization, where rates of destruction of undesirable organisms must be promoted preferentially to rates of destruction of various quality factors. This usually leads to a desire for quite uniform heat-transfer conditions.

Packaging

If respiration continues in storage, it is desirable to allow for controlled exchange of oxygen and carbon dioxide with the environment, while guarding against undesired exchange of water vapor or invasion by other, undesirable substances. This has led to a considerable amount of research on competitive transpiration rates, which obviously must have a strong foundation in mechanisms (see, for example, Karel 1973).

RATE-DETERMINING FACTORS

Acceleration of the rate of a process or promotion of a desired phenomenon over undesired phenomena often requires a determination of the rate-determining step. The rate-determining step may be defined as the factor which principally controls the overall rate of the process concerned.

Drying

Figure 3 is a schematic of the various rate factors involved in drying processes. Heat must be transferred from a heat source to the evaporation zone, usually by way of the piece surface. External heat transfer, from the source to the surface, may occur by any of the three principal heat-transfer mechanisms. Internal heat transfer, from the piece surface to the evaporation zone (if it is located within the piece), is usually by conduction, but can also occur by radiation, particularly if a penetrating radiation (e.g., microwave) is used. Water vapor, generated at the evaporation zone, must first travel to the piece surface by any of a

variety of internal mass-transfer mechanisms. Then water vapor must travel from the piece surface to the moisture sink (condenser or desiccant) by external mass-transfer processes such as convective mass transfer or diffusion.

For the various potential mechanisms operating in *parallel*, such as the three different mechanisms of external heat transfer, the rate-governing mechanism will be that which affords the *fastest* rate of transfer. On the other hand, for the mechanisms in series — external heat transfer, internal heat transfer, internal mass transfer and external mass transfer — the step with the greatest effect on the rate will be the one which is inherently the *slowest*, or which requires the largest concentration-difference or temperature-difference driving force. Thus the rate-determining step will be that mechanism which is inherently the slowest out of the assembly of fastest mechanisms for each step. As an example, in ordinary freeze-drying conduction is dominant over radiation for internal heat transfer. However, for a well-designed freeze dryer, internal heat transfer is inherently slow compared to external heat transfer after an initial period, meaning that, to give the same heat flux, internal heat transfer requires a greater temperature difference than external heat transfer. Furthermore, heat and mass transfer are coupled in such a way and the relative values of heat and mass transfer coefficients are such that the partial-pressure difference of water vapor required to give a mass flux equivalent to the heat flux is small. Therefore, the heat-transfer processes are more rate-limiting than the mass transfer processes. Hence the rate-determining step is internal heat transfer by conduction.

This situation can be changed, however. For example, early in a freeze-drying run heat must be conducted only a short distance from the piece surface to the sublimation plane. Internal heat transfer is inherently a faster process, and external heat transfer — by a combination of conduction and radiation — is then usually rate-determining. As another example, adding a modest pressure of an inert gas to a freeze drying process will accelerate internal heat transfer. But in an ordinary freeze dryer there is little convection for external mass transfer, and the presence of inerts slows external mass transfer by diffusion. The result is that, beyond a certain partial pressure of inerts, an ordinary freeze dryer will become rate-limited by external mass transfer, and as pressures increase the external diffusion process will be slowed so much as to have a severe rate-reducing effect on the whole process. The secret of using inerts is then to promote external convective mass transfer, by means of appropriate dryer design.

For ordinary air drying, on the other hand, external heat transfer is

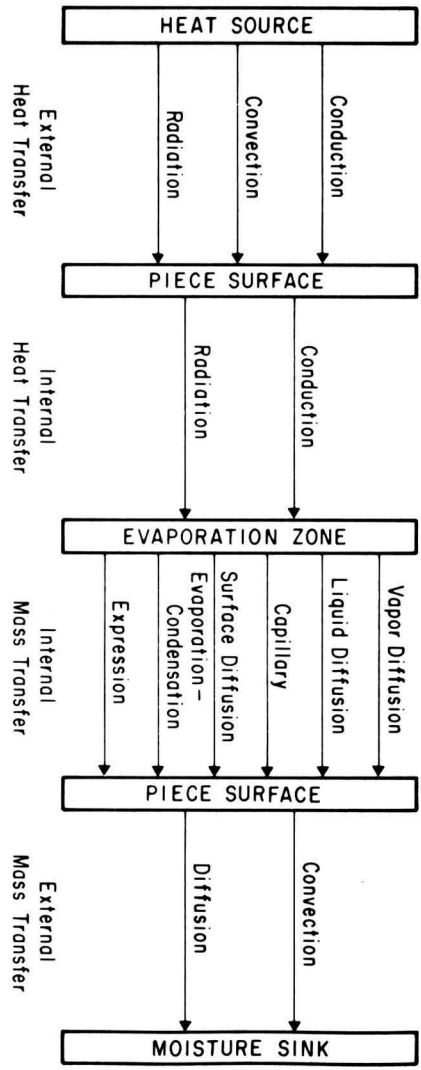

FIG. 3. RATE FACTORS IN DRYING

accelerated through convection, conductive internal heat transfer is accelerated by the use of higher pressure than in freeze drying, and external mass transfer is accelerated through convection. The result is that the principal rate-determining step, for most foods, is internal mass transfer. But by which of the six mechanisms indicated in Fig. 3? Although these six mechanisms for moisture migration within foods during drying have been suggested in various combinations by different authors, there has been very little work directed toward establishing which of the mechanisms prevails under various circumstances. Without a knowledge of mechanism, there is no sound way to predict methods for increasing rates, or for improving product quality without harming rates, or for selecting processes and process conditions which minimize loss of nutrients, flavor, etc.

Artificial Cultivation

Figure 4 depicts a process which has been installed by Marine Colloids, Inc., for artificial production of types of seaweed which are desirable feedstocks for the manufacture of carrageenan, a prominent food additive. Seaweed is suspended in a slant-bottom tank by means of an air lift which causes circulation. Carbon dioxide for photosynthesis is supplied with the air or as dissolved bicarbonate. The tank is exposed to sunlight and/or an artificial source of light. A nutrient solution is continuously supplied, and a purge solution is continually withdrawn, so as to remove metabolites.

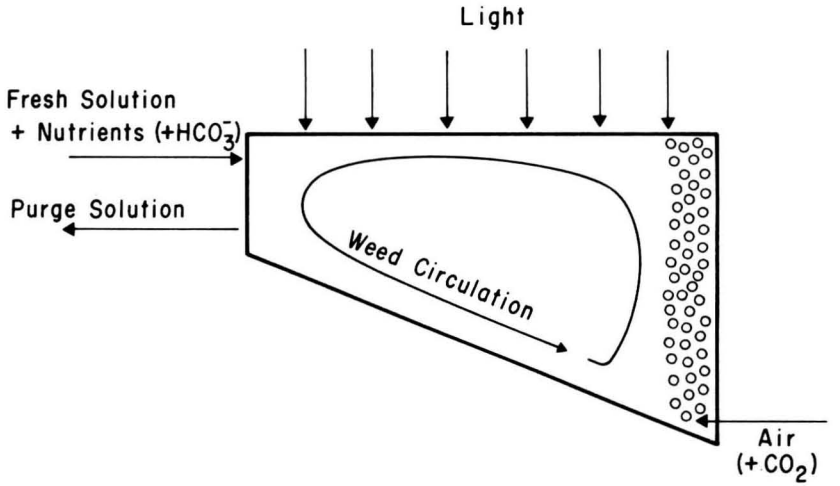

FIG. 4. ARTIFICIAL CULTIVATION OF SEAWEED

Table 1 lists candidate rate-determining steps for this process. It is apparent that there are many such factors, and that careful applications of principles and experiments to distinguish between them is important for optimizing the design of the tank reactor and maximizing growth rates of seaweed.

Table 1. Potential rate-determining factors for artificial seaweed-cultivation process

Rate of supply of light
Rate of supply of nutrients
Rate of supply of carbon
Rate of removal of seaweed (e.g., as it affects light extinction)
Rate of removal of metabolites
Rate of mass transfer of CO_2 from air to solution
Rate of mass transfer of dissolved carbon from solution to seaweed
Rate of mass transfer of nutrients from solution to seaweed
Rate of mass transfer of metabolites from seaweed to solution
Bulk mixing of solution
Bulk mixing of seaweed
Inherent growth kinetics of seaweed

Similar analyses of mechanism underlie the development of successful and economical processes for the manufacture of synthetic protein, the conversion of cellulosic substance to foods, and similar applications.

CONCLUSION

These various examples should indicate the importance of understanding heat and mass transfer and other mechanism factors for the improvement of existing food processes, and for the development of new and better processes.

ACKNOWLEDGMENT

Dr. H. J. Bixler, President, Marine Colloids, Inc., Rockland, Maine, kindly made the seaweed-cultivation example available.

REFERENCES

FLINK, J. and KAREL, M. 1970. Effects of process variables on retention of

volatiles in freeze-drying. J. Food Sci. *35*, 444–447.
HAAS, G. J., PRESCOTT, H. E., JR. and D'INTINO, J. 1972. Pressure freezing-air drying: a new technique to reduce deterioration in drying tissue. J. Food Sci. *37*, 430–433.
HUIGE, N. J. J., SENDEN, M. M. G. and THIJSSEN, H. A. C. 1973. Nucleation and growth kinetics for the crystallization of ice from dextrose solutions in a continuous stirred tank crystallizer with supercooled feed. Kristall u. Technik *8*, 785–801.
KAREL, M. 1973. Quantitative analysis of food packaging and storage stability problems. AIChE Symp. Ser. *69*(132), 107–113.
KING, C. J. 1971. *Freeze Drying of Foods*. CRC Press, Chemical Rubber Co., Cleveland, Ohio.
KING, C. J. 1974a. Novel dehydration techniques. In *Advances in Preconcentration and Dehydration of Foods*, (A. Spicer ed.), Applied Science Publishers, London.
KING, C. J. 1974b. Understanding and conceiving chemical processes. AIChE Monograph Series No. 8, American Institute of Chemical Engineers, New York.
KING, C. J. 1974c. Pressurized freezing for retarding shrinkage after drying: a quantitative interpretation. Cryobiology *11*, 121–126.
KOONZ, C. H. and RAMSBOTTOM, J. M. 1939. A method for studying the histological structure of frozen poultry. Food Res. *4*, 120–128.
RULKENS, W. H. and THIJSSEN, H. A. C. 1972. Retention of model aromas in freeze-drying slabs of maltodextrin. J. Food Technol. 7, 79–93.
STOCKING, J. H. and KING, C. J. 1976. Secondary nucleation of ice in sugar solutions and fruit juices. AIChE Jour. *22*, 131–140.
THIJSSEN, H. A. C. 1971. Flavour retention in drying preconcentrated food liquids. J. Appl. Chem. Biotechnol. *21*, 372–376.
THIJSSEN, H. A. C. and RULKENS, W. H. 1968. Retention of aromas in drying food liquids. De Ingenieur *80*(47), 45–56.

PROCESSING WHEY-TYPE BY-PRODUCT LIQUIDS FROM COTTONSEED PROTEIN ISOLATION WITH ULTRAFILTRATION AND REVERSE OSMOSIS MEMBRANES

J. T. LAWHON, S. H. C. LIN[1], D. W. HENSLEY, C. M. CATER AND K. F. MATTIL

Texas A&M University
Food Protein Research and Development Center
College Station, Texas 77843

Received for Publication September 28, 1976

ABSTRACT

Cottonseed wheys resulting from protein isolation from cottonseed flour were processed by semi-permeable ultrafiltration (UF) and reverse osmosis (RO) membranes. The UF membrane fractionated the soluble whey constituents by retaining protein and passing through salts, carbohydrates and other non-protein components along with most of the water. The UF membrane effluent was then processed through an RO membrane to recover a secondary product containing the whey materials not retained in the protein product from the UF membrane.

The feasibility of recycling effluent from the RO membrane for reuse in subsequent protein extractions was demonstrated. Thus, the threat of water pollution from effluent disposal could be eliminated completely and process water requirements drastically reduced.

Spray-dried UF protein concentrates were tested for utilization in protein fortification of breads and noncarbonated beverages and as whipping products. They exhibited commercial potential for use in these food applications.

The economics of processing the whey-type liquids by the membrane process under investigation were analyzed. Membrane processing of wheys by each of two alternative whey processing systems proved to be economically attractive.

INTRODUCTION

Regulations governing disposal of processing wastewaters, especially those high in organic matter, have become more stringent in recent

[1] Present address: Ralston-Purina Company, Checkerboard Square, St. Louis, MO, 63188

years. Disposal of cheese whey, while perennially presenting a problem to cheese producers, has drawn increased attention as a result of these regulations. The same issue which has confronted cheese manufacturers for so long is potentially facing food processors isolating protein from cottonseed and other oilseeds. Cottonseed protein isolation processes result in whey-type by-product liquids that retain a significant portion of the extracted flour nitrogen (from 21 to 31% using continuous centrifugation), carbohydrates and other nutrients (Lin *et al.* 1974).

In work conducted at Texas A&M University's Food Protein Research and Development Center (FPRDC), cottonseed wheys were processed with semi-permeable membranes to recover valuable protein constituents and to simultaneously prevent water pollution which would ensue if these wheys were discarded into domestic water bodies. By selecting ultrafiltration (UF) membranes of proper pore sizes, whey components were fractionated. The protein materials (having larger molecular weights) were retained while constituents that were lower in molecular weight such as carbohydrates, salts, free amino acids and short-chain peptides passed through with most of the water. This effluent from the UF membrane was then processed with a reverse osmosis (RO) membrane which concentrated essentially all the organic matter and salts into a secondary product. The effluent water (RO permeate) from the RO membrane was demonstrated at the FPRDC to be sufficiently low in solutes to permit recycling it to the front end of the isolation process for reuse as process water (Lawhon *et al.* 1973).

COMPOSITION OF EXPERIMENTAL MATERIALS

Data from processing cottonseed wheys generated by the two protein isolation processes considered to be of greatest commercial significance will be presented herein. These two processes were each applied to glandless cottonseed flour and liquid cyclone process (LCP) deglanded cottonseed flour. However, only glandless flour whey data will be presented. Except for increased color in LCP wheys and their products and some differences in the amounts of solute present in LCP wheys, results from that flour were not importantly different.

The first process, the Single Extraction, Selective Precipitation Procedure (Berardi *et al.* 1972) (designated herein as Process B) produces a single whey. The second process, the Two-Step Extraction Procedure (Berardi *et al.* 1969) (designated herein as Process C) produces two wheys. The whey from Process B will be identified as B whey while wheys from Process C are identified as C-NSP and C-SP wheys. NSP and SP stand for non-storage protein and storage protein, respectively. In

Process B solvent to solids ratios of 10–1 and 8–1 were used during its extraction and re-extraction steps, while ratios of 15–1, 10–1, and 8–1 were used in the extraction and re-extraction steps of Process C. Therefore, Processes B and C yield different quantities of whey. Also, due to these and other inherent features of the two processes (as detailed in the references cited), their wheys have different compositions, and products recovered from them possess different characteristics.

Proximate Analysis

Wheys contain water-soluble cottonseed flour constituents that are extracted but not precipitated in the protein isolation processes. Table 1 contains analytical data on unfractionated whey solids procured by freeze drying the three wheys referred to above. The constituents shown do not add up to 100% because of the indirect methods used in quantitation. These data reveal the peculiar characteristics of each whey and reflect its process dependency. Process B whey might be considered a combination of C-NSP and C-SP wheys. C-NSP whey is derived from the first-step extraction of Process C and thus contains more carbohydrates and less protein (N × 6.25) than C-SP whey which comes from the second extraction step in that process. Oil, crude fiber and gossypol contents are negligible since the wheys are composed of water-soluble substances. Ash contents were noticeably high as anticipated. The ash was largely contributed by sodium hydroxide and phosphoric acid used in the protein extraction and precipitation steps of the isolation procedures. The total phosphorus is mostly inorganic in nature and comes from phosphoric acid. C-SP whey solids were considerably higher in protein mainly due to their low carbohydrate content.

Table 1. Analytical data on unfractionated whey solids from glandless cottonseed flour for Processes B and C

Whey Identification	Protein Nitrogen (N × 6.25)		Ash	Phosphorus Total	Phosphorus Inorganic	Carbohydrates
			% Dry Weight Basis			
Process B	5.7	35.6	25.0	5.1	4.4	35.9
Process C-NSP	5.1	31.9	16.0	3.9	3.2	46.1
Process C-SP	9.2	57.5	14.2	5.8	3.1	17.9

Amino Acid Analyses

An amino acid analysis of the unfractionated whey solids is given in Table 2 along with corresponding analyses of fractionated solids (i.e., products from ultrafiltration of wheys). The latter products will be discussed subsequently.

Table 2. Amino acid analyses of unfractionated whey solids and UF protein concentrates from cottonseed wheys

Amino Acids	Unfractionated Solids			UF Protein Concentrates		
	Process B	Process C				
		NSP	SP	UF B	UF C-NSP	UF C-SP
	g/16gN					
Lysine	5.5	6.0	4.2	6.1	6.9	5.9
Histidine	2.0	1.8	2.3	3.2	1.7	2.7
Ammonia	1.9	1.8	2.0	1.8	1.7	1.8
Arginine	12.7	12.4	13.0	12.8	12.3	10.6
Tryptophan	1.0	1.2	1.2	1.3	1.3	1.6
Cystine	5.0	4.4	3.0	5.7	5.2	2.3
Aspartic acid	7.1	7.0	6.7	6.3	6.6	8.4
Threonine	2.5	2.5	2.8	2.5	2.8	3.9
Serine	2.4	1.2	3.2	2.5	2.4	4.1
Glutamic acid	24.3	17.3	21.5	26.3	23.7	19.3
Proline	2.9	4.1	3.1	3.1	2.9	3.9
Glycine	3.6	3.3	4.2	3.4	3.1	4.6
Alanine	2.6	2.9	3.1	2.4	2.9	4.6
Valine	1.7.	2.1	2.9	1.9	1.9	4.5
Methionine	0.9	0.8	1.8	1.4	1.2	2.2
Isoleucine	1.1	1.3	2.1	1.2	1.1	3.4
Leucine	2.1	2.5	4.4	2.3	2.2	6.5
Tyrosine	2.7	2.5	2.4	3.1	2.8	3.6
Phenylalanine	2.0	2.0	3.1	1.9	1.9	4.7
Totals	84.0	77.1	86.9	88.3	84.6	98.6
Available lysine	5.2	5.6	4.1	6.1	6.4	5.6

Protein is certainly the most important constituent of cottonseed wheys. Protein is conventionally calculated as total nitrogen multiplied by 6.25. This practice is not entirely accurate, especially in this case, since some cottonseed whey nitrogen may not be related to proteins. Comparison of the analysis of Table 2 with amino acid analysis of the

parent glandless flour (not shown) revealed an increase in the lysine and cystine contents in Process B and C-NSP whey solids over that of the source flour. Since the deficiency or lack of availability of lysine and sulfur amino acids (cystine plus methionine) is a primary concern in most legumes and cereals, higher lysine and sulfur amino acids in cottonseed wheys is of interest to food manufacturers because of their nutritional importance.

Cottonseed wheys also contain non-protein nitrogen (NPN) which may include peptides, free amino acids, nucleic acid materials and other nitrogenous compounds. Most of this NPN, however, is amino acid nitrogen (since 75 to 80% of the total nitrogen was determined to be amino acid nitrogen).

Carbohydrates

The carbohydrates in cottonseed wheys are shown by thin layer and gas chromatography techniques to consist principally of raffinose, sucrose, stachyose and glucose, in that order. Raffinose comprised approximately one-half of the carbohydrates in Process B and C-SP wheys, and one-third of those in C-NSP whey.

EXPERIMENTAL PROCEDURES AND PRODUCTS PRODUCED

Membrane Process Utilized

The process investigated for use with the cottonseed wheys employed a UF membrane stage followed by an RO membrane stage as shown schematically in Fig. 1.

Pilot plant scale operations were conducted with a ROpak Single-Core Reverse Osmosis Machine manufactured by Rev-O-Pak, Inc., Newbury Park, CA. For functional purposes the unit was divided into two banks of tubular cells. An upper bank was outfitted with tubular UF membrane cores and a lower bank contained tubular RO membranes. Each bank contained 24 sq ft of membrane surface area. The cellulose-based membranes used were supported on the exterior of 5/8″ diameter ceramic cores. The UF membranes had a molecular weight cutoff range of 5,000 to 10,000. The RO membranes were rated for 90% NaCl rejection.

Processing Technique

Each whey, irrespective of isolation procedure, was pasteurized by heating to 145°F for 30 minutes, cooled and then fed unfiltered into

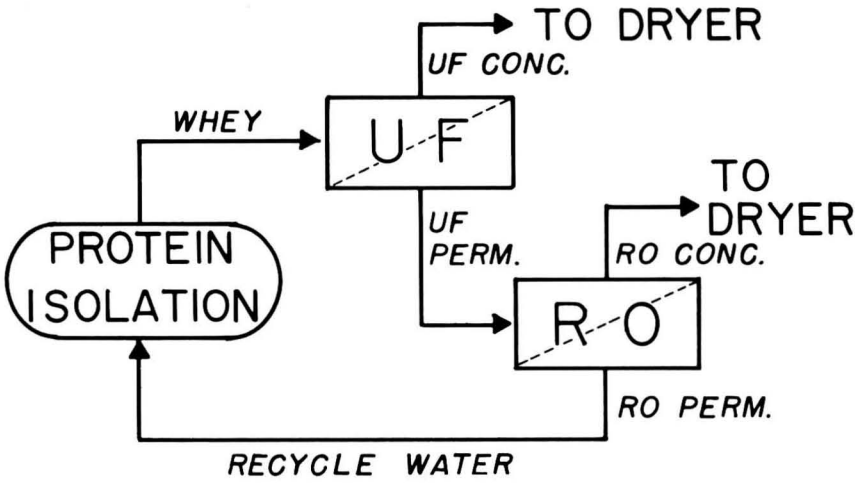

FIG. 1. SIMPLIFIED FLOW SCHEMATIC ILLUSTRATING MEMBRANE PROCESSING OF COTTONSEED WHEY AND ITS RELATIONSHIP TO THE PROTEIN ISOLATION PROCESS

UF membranes at 115–120°F. Pilot plant wheys contained a small amount of suspended solids due to incomplete separation of protein curd from liquid whey by the continuous centrifuge used in the isolation process. Process B whey contained 0.013% suspended solids.

In the UF step, wheys were fractionated and concentrated by batches. The original volume (usually 60 to 75 gal.) was circulated across the membranes until reduced by four-fifths. It was then diluted with a volume of tap water equal to the remaining one-fifth and concentrated again to one-fifth of the original volume to achieve the equivalent of a 10 to 1 volume reduction for the original whey and maintain a higher permeation rate while doing so. When processing UF permeate with the RO membrane, permeation rates were generally higher and tended to decline more slowly than for UF membranes. UF concentrates were spray dried with an Anhydro Spray Dryer Type III-A No. 2. An inlet air temperature of 300–310°F and an outlet air temperature of 185–195°F were used. A sufficient quantity of RO concentrate was freeze dried for making yield calculations and analytical determinations on the dry RO product.

Membrane Performance

Table 3 contains sample analyses which show the fractionation and removal of whey constituents from stage to stage throughout the membrane processing cycle for each whey. Solids reduction in each whey

Table 3. Fractionation and removal of constituents from cottonseed wheys by ultrafiltration and reverse osmosis membranes

Sample Description	Total Solids %	Ash %	Nitrogen, %		Carbohydrates %	COD ppm
			Total	NPN[1]		
Process B:						
Original whey[2] (Feed to UF)	1.64	0.410	0.094	0.070	0.589	12,000
UF permeate (Feed to RO)	0.99	0.356	0.024	0.020	0.407	6,700
RO permeate	0.01	0.006	0.000	—	0.003	65
Process C:						
Original NSP whey[2] (Feed to UF)	1.88	0.267	0.078	0.096	0.829	17,000
UF permeate (Feed to RO)	1.23	0.219	0.101	0.410	0.620	11,000
RO permeate	0.02	0.006	0.001	—	0.007	210
Original SP whey[2] (Feed to UF)	0.84	0.119	0.077	0.013	0.150	9,100
UF permeate (Feed to RO)	0.29	0.101	0.011	0.008	0.088	3,000
RO permeate	0.01	0.005	0.000	—	0.001	420

[1] Non-protein nitrogen
[2] BOD values for Process B, C-NSP and C-SP wheys were 8,600, 9,400, and 5,000 ppm, respectively

was variable because of differences in whey compositions (i.e., wheys having higher salt contents had less solids retained by UF membranes, etc.). COD was reduced from 12×10^3 ppm to only 65 ppm in Process B whey.

Chemical oxygen demand (COD) was used throughout these investigations in preference to biological oxygen demand (BOD) for measuring the pollution potential (organic matter) of an effluent. COD values were found to correlate highly with total solids minus ash determinations made on the same samples (see Fig. 2). This demonstrated that reliable predictions of COD values could be obtained from relatively simple determinations of total solids and ash. However, all COD values shown herein were from actual determinations.

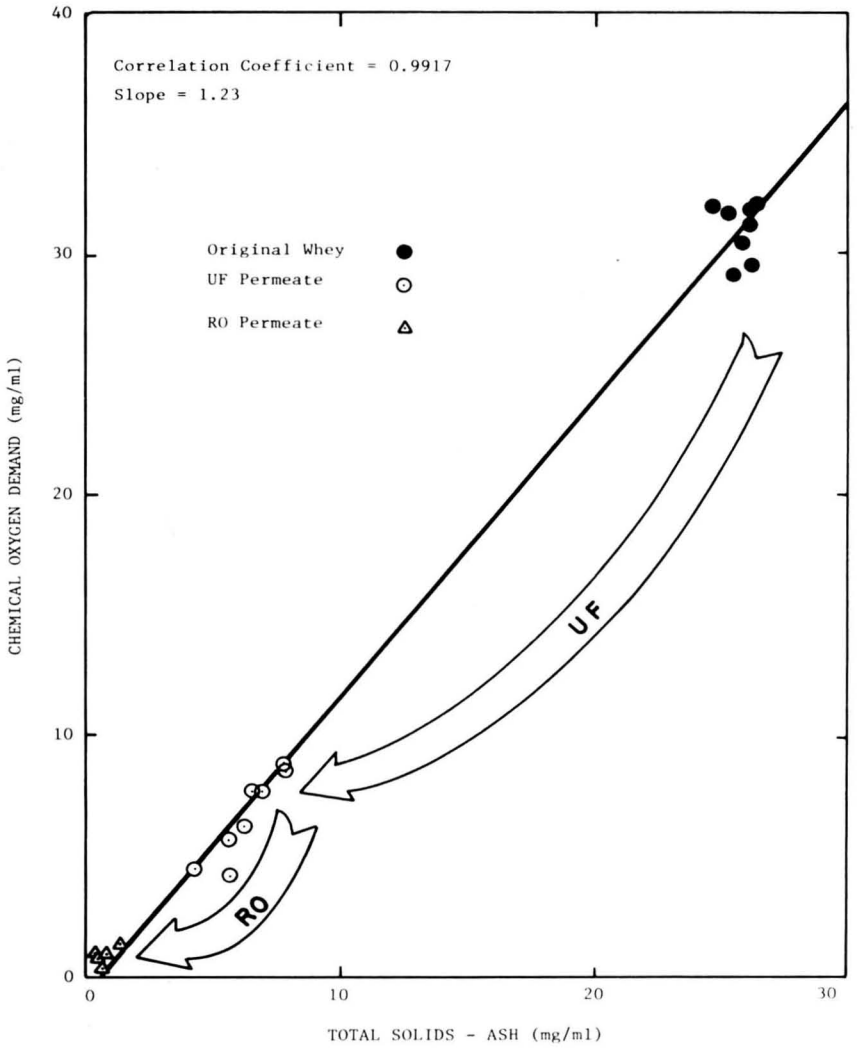

FIG. 2. CORRELATION OF COD WITH TOTAL SOLIDS MINUS ASH

Composition of Products from UF and RO Membranes

Two types of products were obtained from the membrane process. Besides the primary product (protein concentrate from the UF membrane) a secondary product was recovered from the RO membrane. Presumably, the secondary product would be dried by drum drying or some drying method less expensive than spray drying. It was not within the scope of the work conducted at the FPRDC to investigate marketable uses for the secondary product.

Proximate analyses of each type product recovered are given in Table 4. Only one of the UF products, the UF C-NSP, was not sufficiently high in protein to be designated a true protein concentrate (i.e., 70% protein on dry weight basis). Comparison of analytical data given in Table 1 with the data of Table 4 shows the reduction in carbohydrates and ash and enrichment in protein of whey solids achieved with the UF membranes.

The UF C-SP product contained 3.4% oil. Oil in the other two products was negligible. Again, this compositional difference may be attributed to differences in the origins of the wheys. Gossypol contents of the UF products were sufficiently low to be of no concern. The phosphorus present was mostly inorganic from phosphoric acid used in the isolation process.

Amino acid analyses on whey solids before and after UF processing were presented in Table 2. From those data it may be noted that the quality of protein in whey constituents was increased slightly by UF as reflected by the increase in percentage amino acid nitrogen. In each UF product, lysine, cystine, and methionine were further increased by the UF membrane processing.

Recycling the Effluent from the Final Membrane Stage

Oilseed protein isolation processes, unlike cheese manufacturing processes which produce wheys, do not have a constant supply of liquid raw material entering the process. Oilseed protein processes conventionally begin with a dry flour. Thus, the possibility of recycling the effluent (RO permeate) from membrane processing of cottonseed wheys back to the front end of the protein isolation process for reuse in subsequent extractions was investigated. By handling the RO permeate in this way, water pollution from whey disposal could be eliminated and process water requirements drastically reduced.

The question sought to be answered was, "What effect would the repeated use of RO permeate in flour extractions have on the quality of protein isolates produced?" To answer this question, a laboratory-prepared Process B whey (containing higher percent total solids than pilot plant B whey) was processed using an Aquamosis Mark XXV Laboratory Reverse Osmosis Unit manufactured by Fre-Del Engineering Corporation, Santa Anna, CA. The unit contained cellulose-based membranes rated for 10,000 molecular weight and 90% rejection of NaCl for UF and RO, respectively. The membranes were 4 in. in diameter and of a flat, circular configuration. They were supported on flat, porous, stainless steel circular plates.

Quantities of glandless cottonseed flour were extracted in four

Table 4. Analytical data on products from membrane processing cottonseed wheys

Product Identification[1]	Moisture	Ash	Oil	Gossypol		Nitrogen		Protein	Phosphorous		Carbohydrates
				Total	Free	Total	Non-Protein	(N X 6.25)	Total	Inorg.	
	%	% Dry Weight Basis									
UF B	6.1	8.4	0.10	0.02	0.00	11.6	3.6	72.3	2.30	2.08	23.3
UF C-NSP	6.7	6.2	0.60	0.02	0.01	10.3	2.6	64.3	1.49	1.17	33.8
UF C-SP	5.5	6.5	3.4	0.02	0.01	12.1	1.4	75.9	1.47	0.74	8.3
RO B	13.2	34.3	0.06	—	—	2.3	2.3	13.9.	11.0	10.5	46.6
RO C	9.3	20.3	0.15	—	—	3.9	3.9	24.2	5.36	4.83	36.1

[1] Products designated by membrane type, isolation process, and whey type.

extraction cycles (see Fig. 3). Each extraction in the series was repeated on the following day to give duplicate sets of data throughout. Conductivity, total solids, ash, total nitrogen, non-protein nitrogen, carbohydrates, and COD were determined on all wheys, UF permeates and RO permeates. Tapwater adjusted to pH 10 with NaOH was used to make the initial extraction. The three succeeding extractions were made at the same pH using a combination of tapwater and recycled RO permeate. Mean values from four sets of measurements for conductivity, percent solids, ash, and COD on the tapwater used were 733 μmhos, 0.055%, 0.0355%, and 20.7 ppm, respectively.

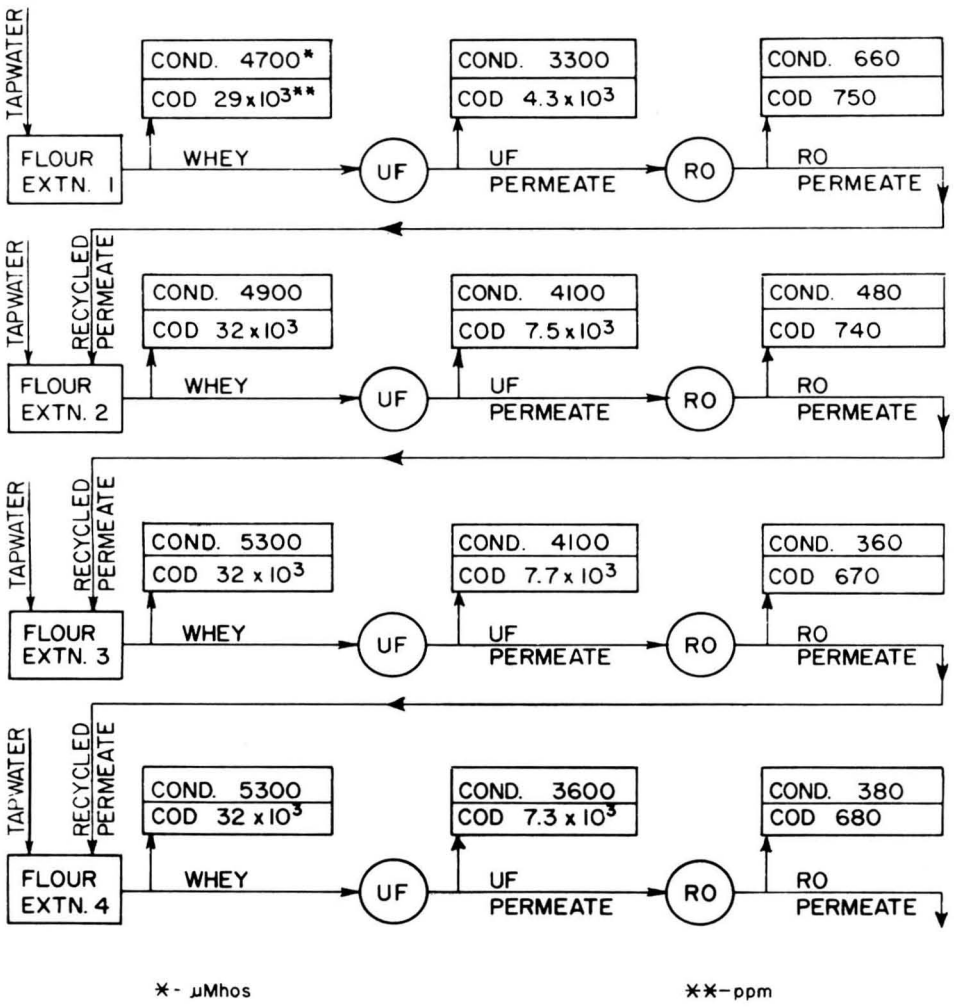

FIG. 3. FLOW DIAGRAM WITH ANALYTICAL DATA FROM FOUR FLOUR EXTRACTION-WHEY PROCESSING CYCLES

Results. Of primary interest was the behavior of salt concentration (as reflected by conductivity) and COD in the RO permeates from cycle to cycle as this RO effluent was reused in succeeding extractions. It is evident from Fig. 3 that the salt level in each of the RO permeates was less than that of the tapwater used. Through four extraction cycles, performed in duplicate, the conductivity of RO permeates dropped from an average of 660 μmhos in the initial extractions to 380 μmhos in the fourth pair of extractions. The COD in RO permeates remained relatively constant.

The extraction cycles performed as described to obtain the data shown in Fig. 3 were essentially repeated to obtain data on the NSP and SP isolates prepared using recycled RO permeate. However, in the latter series, only a single extraction was made for each of the four extraction-whey processing cycles. The data obtained are given for inspection in Table 5. Upon examination of these data for any quality changes, the variations noted from cycle to cycle appeared to be only random variations.

Table 5. Analytical data on NSP and SP protein isolates from permeate recycle investigations

Extraction Cycle No.	Isolate Type	Moisture (%)	Ash[1] (%)	Total[1] Nitrogen (%)
1	NSP	85.2	1.33	12.3
	SP	64.0	1.41	17.0
2	NSP	85.0	1.01	12.2
	SP	64.9	0.92	16.2
3	NSP	85.8	1.08	12.1
	SP	63.7	0.95	16.8
4	NSP	85.3	1.88	12.3
	SP	66.5	0.99	16.7

[1] Dry weight basis

Observations. It is apparent from Fig. 3 that the conductivity of the original wheys never exceeded 5400 μmhos. If no more than approximately 10% of the original whey salts may be expected to pass into RO permeate, then the estimated conductivity of RO permeate would be about 540 μmhos (less than that of the tapwater used). It becomes evident therefore, that unless the conductivity of a whey is 10 times higher than the conductivity of tapwater, the RO permeate may be expected to contain less salts than tapwater. It should be recognized

that the conductivity of tapwater varies from one geographical location to another and for that reason these numbers may not be the same everywhere. If it had been necessary tighter membranes rated to reject 95 to 98% of the salts could have been used in these tests.

No adverse effects on NSP and SP isolate quality were observed from the proximate analyses performed on these products from extractions using recycled RO permeate. Thus, the recycling concept definitely appears to be a process innovation to prevent water pollution and reduce process water requirements by more than one-half.

Data obtained in this study indicated that the UF/RO recycling concept demonstrated would also be applicable to other oilseed protein isolation processes where water is used for protein extraction. This is one of the methods which should help achieve the Federal "zero discharge" goal of 1985.

UTILIZATION OF WHEY PROTEIN CONCENTRATES RECOVERED

The three UF products from Process B and C wheys were evaluated for potential use in protein fortification of bread and non-carbonated "ade"-type beverages or instant fruit drinks, and as whipping products (Lawhon *et al.* 1974). The results of these evaluations will be summarized briefly.

Protein Fortification of Breads

The UF products were tested for protein enrichment of wheat flour breads in wheat flour-whey protein blends proportioned to contain 17.5% protein on a 14% moisture basis. Glandless cottonseed flour was also blended with wheat flour in the same manner and included in a statistically designed experiment for comparative purposes. An all-wheat flour (12.4% protein in the flour) bread was baked as a control.

Ten treatments consisting of the five materials or blends, mentioned above, with and without 1.5% sodium stearoyl-2 lactylate (SSL) added as a dough conditioner were baked in random order and compared. Representative loaves of bread from the comparisons are shown in Fig. 4. The upper row of loaves contain no SSL. Loaves in the lower row contain SSL added to determine its affect on loaf volume.

Loaf volumes were analyzed statistically by the analysis of variance. Loaf A (the control) with SSL added was larger than the test loaves. However, Loaf A without SSL was not larger than Loaf D without SSL. The UF product from the C-SP whey proved to be best for protein enriching breads. Although, the other experimental products tested

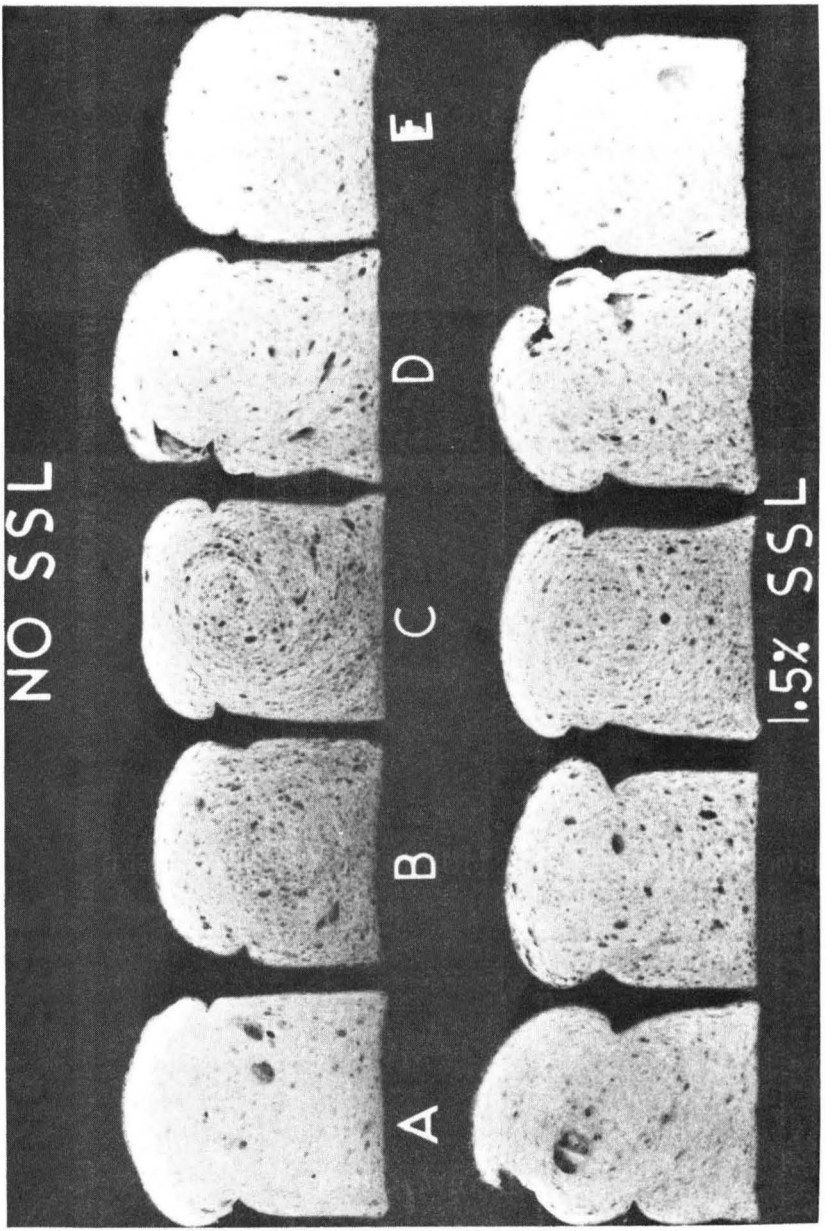

FIG. 4. LOAVES OF BREAD BAKED WITH BLENDS OF WHEAT FLOUR AND EITHER UF PROTEIN PRODUCTS OR GLANDLESS COTTONSEED FLOUR WITH AND WITHOUT SSL ADDED

Loaf A contains 100% wheat flour, Loaf B contains Rogers GL-7 glandless cottonseed flour, Loaf C contains UF B, Loaf D contains UF C-SP, and Loaf E contains UF C-NSP.

performed satisfactorily if used with SSL. UF C-SP bread was not significantly improved in loaf volume by the use of SSL.

Protein Fortification of Beverages

The UF B protein product was selected for fortifying an "ade"-type beverage and an instant fruit drink which are sold as powder to be reconstituted with water. UF B product was dispersed in distilled water and the resulting protein solution-suspension centrifuged to obtain a clear supernatant for use (instead of water) in reconstitution. The UF B product was not 100% soluble due to some slight change in the solubility of its nitrogen possibly resulting from the drying treatment given the product or solubility change induced by removal of salts, etc. during the UF operation. A reconstituted orange-flavored "ade" beverage and an orange-flavored fruit drink were sensory tested by a panel of ten untrained taste judges.

Mean scores of each beverage tested are given in Table 6. An analysis of variance showed no significant difference between treatments in either set of values at the 1% level of significance (i.e., the taste judges could not detect the presence of the protein in either drink at the protein levels tested).

Table 6. Mean scores from sensory evaluation of protein-fortified non-carbonated "ade" and instant fruit drinks

Beverages Tested	Protein Levels 0%	1%	2%	3%
Orange-flavored "ade" drink	7.47	7.60	7.37	7.10
Orange-flavored instant fruit drink	7.63	7.13	7.40	7.23

Although drinks with protein levels in excess of 3% were not sensory tested, it was found to be possible to incorporate higher levels of protein if desired. Cloudiness in commercial drinks of the types tested is not necessarily undesirable.

Whipping Property Evaluations

Whipping property evaluations were made on five cottonseed whey materials as shown in Table 7. Each material was whipped at 12%

Table 7. Whipping data on products from cottonseed wheys

Materials Whipped	Foam Viscosities with Sugar Added, cps		
	12% Product Conc		6% Protein Conc
	pH 4.5[a]	pH 7.0	pH 4.5[a]
UF B	107,900ab	64,100	91,600b
UF C-NSP	71,900b	57,600	53,700d
UF C-SP	13,700c	2,000	2,400e
UF B-dialyzed	138,300a	69,300	72,100c
Process B whey solids	93,200b	68,100	114,000a

[a]Means followed by same alphabetical letter were not significantly different at the 5% level

product concentration and also at the product concentration required to give 6% protein in a solution-suspension from each material. Foam viscosities from tests at pH 4.5 were analyzed by statistical techniques. As indicated in Table 7, the two products whipped in addition to the three UF products assessed throughout the study were (1) UF B product with additional salts and carbohydrates removed by exhaustive dialysis and then freeze dried, and (2) a product from spray drying Process B whey without membrane treatment (i.e., unfractionated whey solids).

The foams obtained from UF products B and C-NSP were pleasant tasting and very stable. Foams from spray-dried, unfractionated whole whey solids had a noticeably bitter taste although the foam viscosity was desirably high. This bitterness was attributed to the high ash content of whole whey solids. Whipping properties of protein products from cottonseed wheys prove to be definitely superior to those of either protein isolates or whippable extracts from cottonseed flours previously tested at the FPRDC. They exhibited definite commercial potential for use in some applications as whipping agents.

To provide a control for comparison, a commercial whipping product, spray-dried egg white solids (containing 1% sodium lauryl sulfate as a whipping aid), was whipped and measured by the same procedures. It yielded a foam with a viscosity of 158,100 cps. Egg white foams were less stable than foams from UF B and UC C-NSP products at room temperature. However, foams from the whey products were noncoagulable by heat as were egg white foams.

ECONOMIC ANALYSIS OF THE MEMBRANE PROCESS

Uncertainty about the economic feasibility of membrane processing has been a principal factor inhibiting its widespread adoption. Thus, an economic analysis was made with the membrane process described herein being utilized to process wheys from two hypothetical protein isolation plants employing the different isolation procedures (Lawhon *et al.* 1976). However, in the abbreviated treatment of the total study as given herein, only the analysis made on the smaller of the two plants will be presented.

In addition to analyzing the membrane process actually utilized throughout the investigations, a possible alternative whey processing system was also analyzed for comparative purposes. The primary system (designated System 1) consisted of ultrafiltration followed by reverse osmosis. The alternative system (System 2) consisted of ultrafiltration followed by vacuum evaporation to concentrate UF permeate.

Capital and operating costs were developed as of July 1, 1974. Estimates of revenue from product sales were calculated based on product yield data from the FPRDC pilot plant runs and various assumed market prices using prices of competitive products as of July, 1974 as a guide in making the assumptions. Membrane processing equipment requirements were based on achieving a mean permeation rate of 14 gallons per square foot per day (gfd) for the UF membranes and 22 gfd for the RO membranes.

The hypothetical whey processing plant presented herein was designed to process whey resulting from the production of 7,000,000 pounds of storage protein (SP) isolate (0% H_2O basis) annually, using Process B. It was designated Plant B for simplicity. It was sized to process 700,000,000 pounds of whey annually. This is the amount of whey that would be generated from processing 15,556 tons of flour. An operating period of 20 hours per day was assumed with 4 hours per day allowed for membrane cleaning. Calculations were based on 310 days of plant operation per year.

Cost Estimation Methods

The costs of Plant B, were estimated in considerable detail to obtain its total plant capital and operating costs. Capital costs as developed consisted of six cost elements, i.e., major process equipment, auxiliary process equipment, plant materials, field labor, freight, and engineering and design services, plus contingencies. Major process equipment and installation were priced from purchase prices supplied by manufacturers or from a process equipment cost manual. Auxiliary process equipment

cost before installation was taken as 42.5% of installed major equipment cost (Popper 1970). The "plant materials" cost element was costed by breaking it down into the individual categories comprising it and applying cost ratios obtained from Popper *et al.* (1970) for each category relative to total process equipment (major plus auxiliary). Field labor which includes labor costs associated with accessory equipment and plant materials was estimated as 22% of the combined amount of these two cost elements. Freight costs were included as 1.5% of all process equipment cost. Engineering and Design Services were included as 10% of the other cost elements excluding contingencies. Contingencies were provided for by including 5% of the sum of the cost elements excluding Engineering and Design Services.

Operating costs were separated into five cost elements. These were: major process equipment, auxiliary process equipment, plant materials, property taxes and insurance, and administrative expenses. The first three cost elements were further divided into fixed and variable expenses. Fixed expenses included depreciation, membrane replacement, and maintenance. Variable expenses were made up of operating labor, electrical power, steam, fuel, water, supplies and cleaning.

The straight line method of depreciation was employed with varying lengths of useful life assigned to different types of equipment. Membrane life was considered to be 18 months. Property taxes and insurance were included as 2% of the total capital costs. Administrative expense was estimated as 6% of gross product sales. Contingencies were provided for with an allowance of 3% of variable expenses on major and auxiliary process equipment and plant materials.

Cost Analysis Results

In Fig. 5, a simplified flow diagram for Plant B using either System 1 or 2 is given. Weights of each fraction existing from the various unit operations are also shown. A combined loss of 1% of UF concentrate dry solids weight was assumed to occur in the drying and packaging steps. Weights of products for sale were based on 6% moisture.

Capital costs for Plant B were $8,828,977 and $9,108,751 for Systems 1 and 2, respectively. Capital costs for System 2 were $279,824 higher than corresponding costs for System 1. However, total annual operating costs for System 1 ($2,038,069) were slightly higher than those for System 2 ($2,031,821).

Estimation of Profitability

The profitability of a business venture is measured chiefly by the return realized on funds invested. For this study, the Explicit

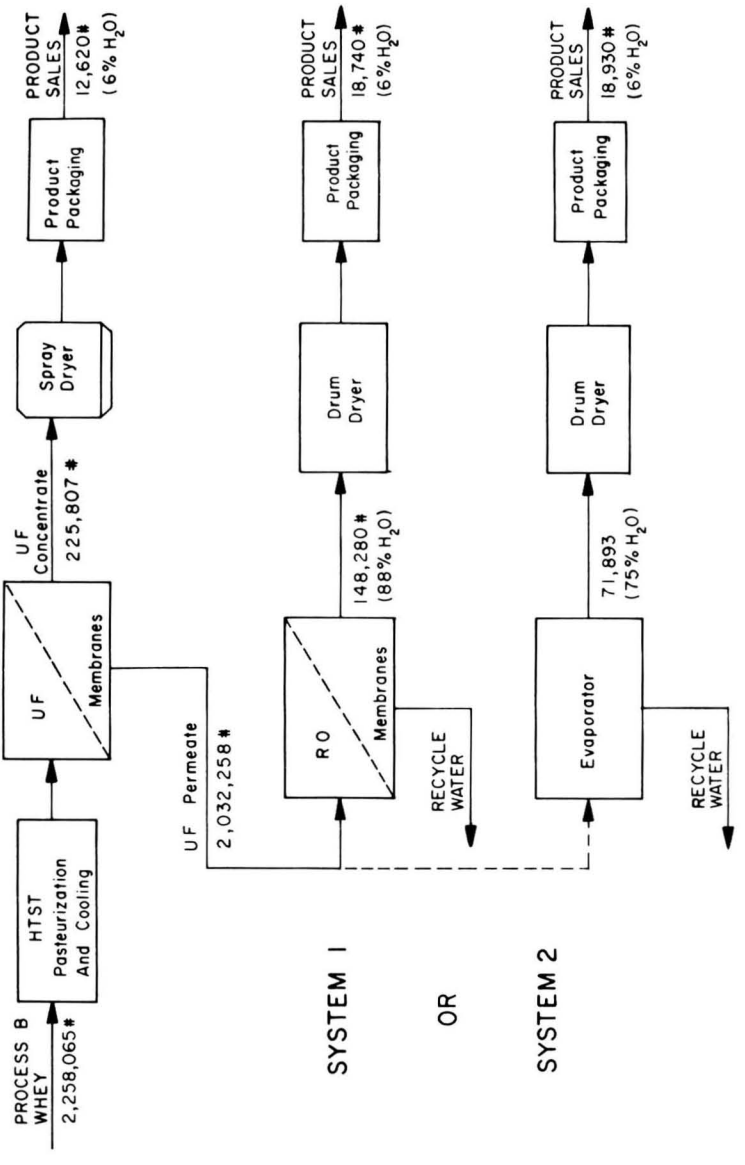

FIG. 5. SIMPLIFIED FLOW DIAGRAM FOR COTTONSEED WHEY PROCESSING — PROCESS B, SYSTEMS 1 OR 2

Reinvestment Rate of Return Method (E.R.R.) of DeGarmo and Canada (1973) was used (DeGarmo and Canada 1973). Table 8 shows profitability calculated for Plant B using System 1 or System 2 as annual rate of return on total capital invested (i.e., total plant capital costs plus working capital) before income taxes. Considering selling prices of $1.50 per pound of UF protein and $0.07 per pound for drum-dried product to be consistent with current price levels, System 1 would show an E.R.R. of 25.7% and System 2, a return of 25.0%. E.R.R.'s assuming other selling prices are shown also.

Table 8. Profitability of cottonseed whey processing assuming various market prices per pound of ultrafiltration protein and drum-dried product — Process B, Systems 1 and 2

Market Prices	UF Protein	$1.30/lb.	1.50	1.70	1.90	2.10
	Drum-dried Product	$0.06/lb.	0.07	0.08	0.09	0.10
Annual Rate of Return	System 1	19.7%[a]	25.7	31.5	37.3	43.1
	System 2	19.2%[a]	25.0	30.7	36.3	41.9

[a]Annual rate of return on total capital invested before income taxes

System 1 was found to give a slightly higher rate of return than System 2 throughout. Another consideration that recommends this type system is that it requires less energy input than System 2 since the concentration of UF permeate solids with RO membrane is accomplished without a phase change.

CONCLUSIONS

Pilot plant work at the FPRDC and the subsequent economic analysis based on operating data from plant runs have confirmed that cottonseed wheys from protein isolation can be profitably processed with UF and RO membranes to recover food and/or feed protein products and simultaneously prevent environmental pollution.

Although cellulose acetate membranes were used in these investigations, a new ("second generation") non-cellulosic type of UF membranes has since emerged which gives noticeably superior permeation rates. The new type membranes may be operated over a wide pH range (1–14) and at temperature up to the boiling point of water without damage to the membranes. Thus, better microbial control is possible.

Operating constraints with these new UF membranes may now be the heat sensitivity of protein-containing feed materials and the temperature limitations of other processing equipment involved.

Non-cellulosic RO membranes are currently under development by membrane manufacturers and researchers in the field.

ACKNOWLEDGMENT

This research was funded in part by USDA Research Agreement No. 12-14-100-11021 (72) and by the Natural Fibers & Food Protein Commission of Texas.

REFERENCES

BERARDI, L. C., FERNANDEZ, C. J. and MARTINEZ, W. H. Cottonseed protein isolates: Selective precipitation procedure. Abstract No. 68 from program of the 32nd Annual Meeting of the Institute of Food Technologists, May, 1972, Minneapolis, Minn.

BERARDI, L. C., MARTINEZ, W. H. and FERNANDEZ, L. J. 1969. Cottonseed protein isolates: Two-step extraction procedure. Food Technol. *23*(10), 75–82.

DEGARMO, E. P. and CANADA, J. R. 1973. Engineering Economy, 5th Ed., Chap. 10, The Macmillan Co., New York.

LAWHON, J. T., HENSLEY, D. W., CATER, C. M. and MATTIL, K. F. 1976. An Economic Analysis of Cottonseed Whey Processing. J. Food Sci. *41*(2), 365–369.

LAWHON, J. T., LIN, S. H. C., CATER, C. M. and MATTIL, K. F. 1973. Recycling of effluent from membrane processing of cottonseed wheys. Food Technol. *27*(2), 26–34.

LAWHON, J. T., LIN, S. H. C., ROONEY, L. W., CATER, C. M. and MATTIL, K. F. 1974. Utilization of cottonseed whey protein concentrates produced by ultrafiltration. J. Food Sci. *39*(1), 183–187.

LIN, S. H. C., LAWHON, J. T., CATER, C. M. and MATTIL, K. F. 1974. Composition and characteristics of glandless and liquid cyclone process deglanded cottonseed wheys. J. Food Sci. *39*(1), 178–182.

POPPER, HERBERT and the Staff of Chemical Engineering. 1970. *Modern Cost-Engineering Techniques*. McGraw-Hill Book Company, New York.

MODELLING HEAT TRANSFER IN FOODS USING THE FINITE-ELEMENT METHOD

J. DE BAERDEMAEKER AND R. P. SINGH

Department of Agricultural Engineering
University of California
Davis, California

AND

L. J. SEGERLIND

Department of Agricultural Engineering
Michigan State University
East Lansing, Michigan

Received for Publication October 15, 1976

The use of finite-element method as a numerical procedure for solving differential equations in physics and engineering has increased considerably since a publication by Turner, Clough, Martin and Topp (1956). The theoretical basis of the method and its application to structural and solid mechanics problems have been discussed by several researchers in recent years. Early publications related to heat transfer include Zienkiewicz and Cheung (1965), Visser (1965), and Wilson and Nickell (1966). Application of the finite-element method to heat conduction is discussed in books by Zienkiewicz (1971), Desai and Abel (1972), and Norrie and DeVries (1972). Comini *et al.* (1974), gave a finite-element formulation for nonlinear problems of phase changes found in freezing.

In the finite-element method the region under consideration is divided into small elements. Probably the most popular two-dimensional element is the triangle, although rectangles, higher-order triangles, and curved quadrilaterals are also available for solving two-dimensional problems. All elements are assumed to be connected at nodal points located along the boundaries. The element equations are obtained by minimizing a functional or a residual. This aspect differs considerably from the finite-difference method, which approximates the derivatives at a point. The finite-element method has some definite major advantages contributing to its popularity. These advantages in food related problems are described by Singh and Segerlind (1974).

This paper demonstrates the application of the finite-element method to analysis of some important time-dependent thermal food-processing problems. The important aspects of the finite-element

Journal of Food Process Engineering 1 (1977) 37–50.

formulation of time-dependent axi-symmetric heat-transfer problems are summarized first. Discussed next are the results of this formulation as applied to heat transfer in foods. *Theoretical aspects of the finite-element method for axi-symmetric bodies:*

Heat conduction in axi-symmetric bodies is governed by:

$$\frac{\partial}{\partial r}\left(rk_{rr}\frac{\partial T}{\partial r}\right)+\frac{\partial}{\partial z}\left(rk_{zz}\frac{\partial T}{\partial z}\right)=r\rho\,C_p\frac{\partial T}{\partial t} \tag{1}$$

where r and z are the coordinate directions,

k_{rr} and k_{zz} are the conductivities in the coordinate directions,
T is the temperature,
ρ is the density of the material,
C_p is the specific heat, and
t is the time.

Equation (1) is valid as long as there is no internal heat generation.

The boundary conditions for (1) are either a prescribed temperature

$$T = T_B \text{ on a surface } S_1 \tag{2}$$

or convection gains or losses through the surface

$$k_{rr}\frac{\partial T}{\partial r}\ell_r + k_{zz}\frac{\partial T}{\partial z}\ell_z + h(T - T_\infty) + q = 0 \text{ on surface } S_2 \tag{3}$$

where ℓ_r and ℓ_z are the direction cosines,

h is the surface heat-transfer coefficient
T_∞ is the fluid temperature surrounding the body, and
q is a boundary heat source.

It is assumed that ρ, C_p, q, and h are rotationally symmetric. Also, S_1 and S_2 are mutually exclusive, with their sum equalling the total surface area.

The Galerkin Residual Method (Crandall 1956; Strang and Fix 1973) can be used to transform Equation (3) into a finite-element form. A trial function for T which satisfies the boundary conditions is substituted into (3), and the resulting residual is made orthogonal with respect to a weighting function W:

$$\int_V \left[\frac{\partial}{\partial r}\left(rk_{rr}\frac{\partial T}{\partial r}\right)+\frac{\partial}{\partial z}\left(rk_{zz}\frac{\partial T}{\partial z}\right)-rC_p\frac{\partial T}{\partial t}\right]W\,dV = 0 \tag{4}$$

Integrations by parts of (4) and applying the divergence theorem yields:

$$-\int \left[rk_{rr} \frac{\partial T}{\partial r} \frac{\partial W}{\partial r} + rk_{zz} \frac{\partial T}{\partial z} \frac{\partial W}{\partial z} + \rho C_p r \frac{\partial T}{\partial t} W \right] dV$$

$$+\int \left[rk_{rr} \frac{\partial T}{\partial r} \ell_r + rk_{zz} \frac{\partial T}{\partial z} \ell_z \right] WdS = 0 \qquad (5)$$

In the finite-element method the solution domain is subdivided into smaller elements to which Equation (5) is applied. Such an axi-symmetric triangular element is illustrated in Fig. 1. The variable temperature $T^{(e)}$ in the element is approximated as a function of the temperature values at the nodes (Segerlind 1976):

$$T^{(e)} = T_1 N_1 + T_2 N_2 + T_3 N_3 \qquad (6)$$

whereby T_1, T_2, and T_3 are the nodal temperatures and N_1, N_2, and N_3 are element shape functions which are derived from the geometry of the elements.

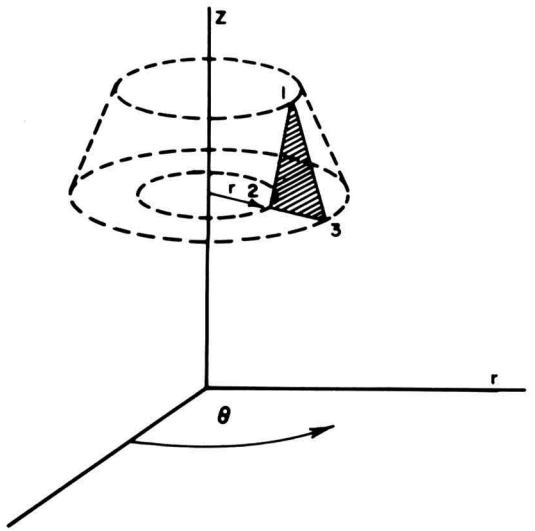

FIG. 1. A TRIANGULAR AXI-SYMMETRIC FINITE-ELEMENT WITH NODAL VALUES

Equation (6) can be rewritten in vector notation as:

$$T^{(e)} = [N] \{T\} \tag{7}$$

where [N] is a row vector of interpolating functions or shape functions, and $\{T\}$ is the value of the field variable at the nodal points associated with the element. It is also convenient to choose weighting functions, W, that are identical to the interpolating functions, N_1, N_2, and N_3. Equation (7) is then substituted into (5), resulting in a matrix equation for one element. If the interpolating polynomial satisfied some conditions of continuity and compatibility (Segerlind 1976), then the integrals (5) of all the elements can be summed together. The resulting matrix equation is of the form:

$$[K] \{T\} + [C] \frac{\partial \{T\}}{\partial t} - \{F\} = 0 \tag{8}$$

[K] and [C] are square matrices, respectively involving the thermal conductivity and the specific heat of the material. These matrices also depend on the geometry of the elements. $\{F\}$ is a column vector of known values of heat input, while $\{T\}$ is the vector of the unknown nodal temperatures.

In solving differential Equation (8) a finite-difference scheme is used to evaluate time elements. This study uses a Galerkin approach or weighted residual method with linear time elements (Warzee 1974). The procedure calculates the temperature $\{T\}_1$ at the present time from the temperature $\{T\}_0$ at the previous time, using a variable time-step size, Δt:

$$\left(\frac{2}{3}[K] + \frac{1}{\Delta t}[C]\right) \{T\}_1 = \frac{1}{3}\{F\}_0 + \frac{2}{3}\{F\}_1 - \left(\frac{1}{3}[K] - \frac{1}{\Delta t}[C]\right) \{T\}_0 \tag{9}$$

$\{F\}_0$ and $\{F\}_1$ are heat inputs at the beginning and the end of the time step.

The matrix operations in (9) are simplified somewhat by the fact that [K] and [C] are positive definite symmetric banded matrices. Some storage and solution techniques for banded matrices are discussed by Segerlind (1976).

APPLICATIONS TO PHYSICAL PROBLEMS

The following applications use the most simple element, the triangle. Subdivision of the content of a cylindrical can is shown in Fig. 2. Since symmetry exists around the axis, elements are shown in only one quarter of the region. Also, the elements in axi-symmetric problems should be considered as ring-shaped elements, with a triangular as cross section. Division of a region into triangles was performed with a separate program described by Segerlind (1976). An optimum relationship for stability and numerical oscillations was found to exist between element size, time step, and thermal diffusivity. Since the Biot number is usually very high for convective heat transfer in thermal processing, a negligible surface resistance to heat transfer was assumed.

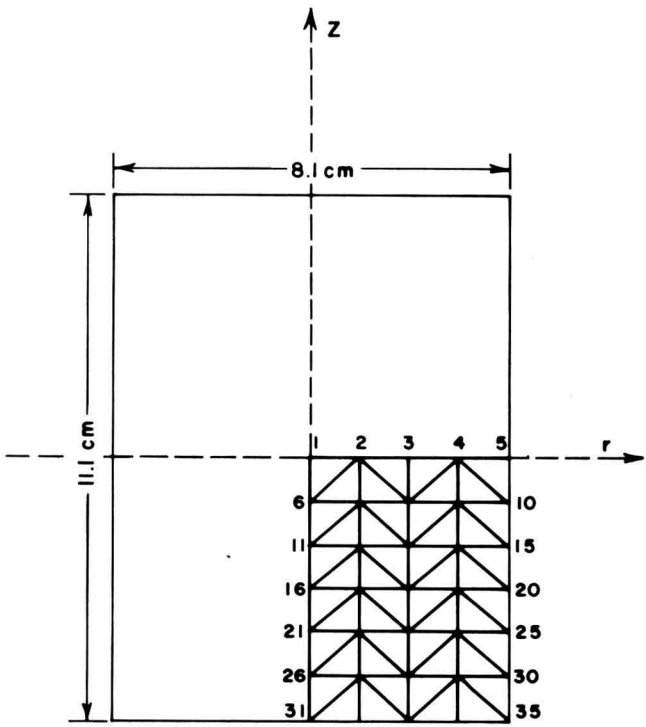

FIG. 2. DIVISION OF A CYLINDRICAL CAN INTO TRIANGULAR RING-SHAPED ELEMENTS

Heat Transfer in Cylindrical Cans

The temperature history of conductively heated food packaged in a

cylindrical can (with a height of 11.1 cm and a diameter of 8.1 cm) was calculated. The following thermal properties were used: thermal conductivities, $k_{zz} = k_{rr} = 0.521$ watt/m°C, specific heat, $C_p = 3766$ J/kg°C and density, $\rho = 1040$ kg/m^3. The can was assumed to have an initial uniform temperature of 21.1°C and was dropped at time t = 0 in a medium with a temperature of 93.3°C. Figure 3 shows the temperature history at the center of the can and at a point 2.03 cm from the side and 1.85 cm from the bottom (node 23 in Fig. 2).

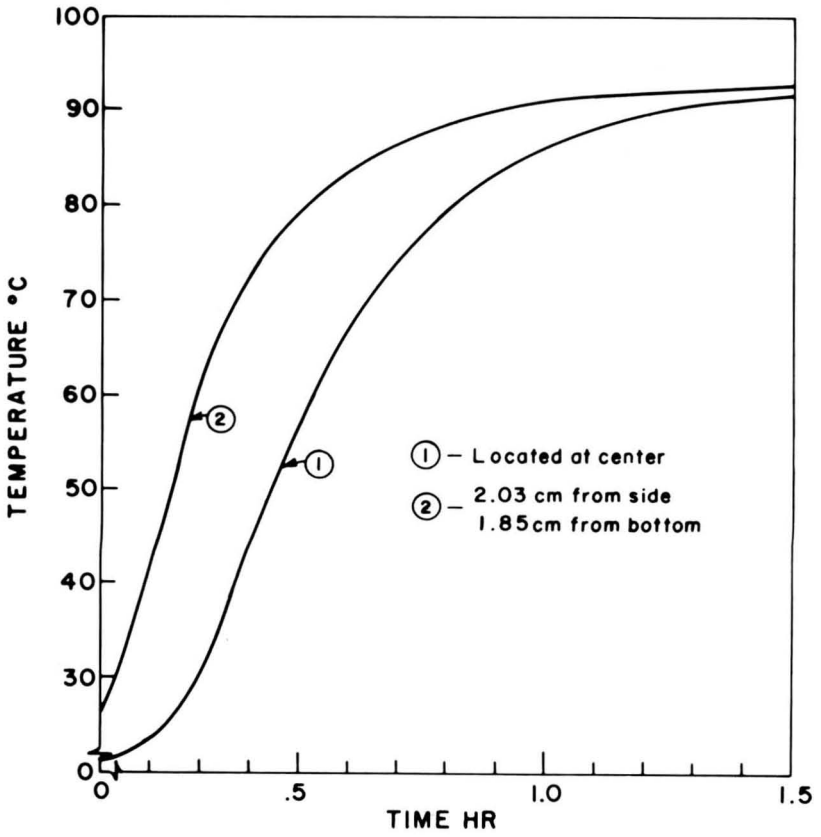

FIG. 3. PREDICTED TEMPERATURE HISTORY AT TWO LOCATIONS IN A CYLINDRICAL CAN (WITH FOODSTUFF) INITIALLY AT 21.1°C EXPOSED SUDDENLY TO A MEDIUM AT 93.3°C

The accuracy of a finite-element solution can be verified by comparing results with analytical solution. A one-dimensional (infinite-slab) problem was programmed on the computer using the same grid and

material properties as assumed in the above example. The only change necessary in input data was to make the temperature gradient along the side of the can zero. The result is shown in Fig. 4 along with the analytical solution for this problem as obtained from Myers (1971). Similar results were obtained for analytical and finite-element solutions to infinite cylinder and finite cylinder geometries.

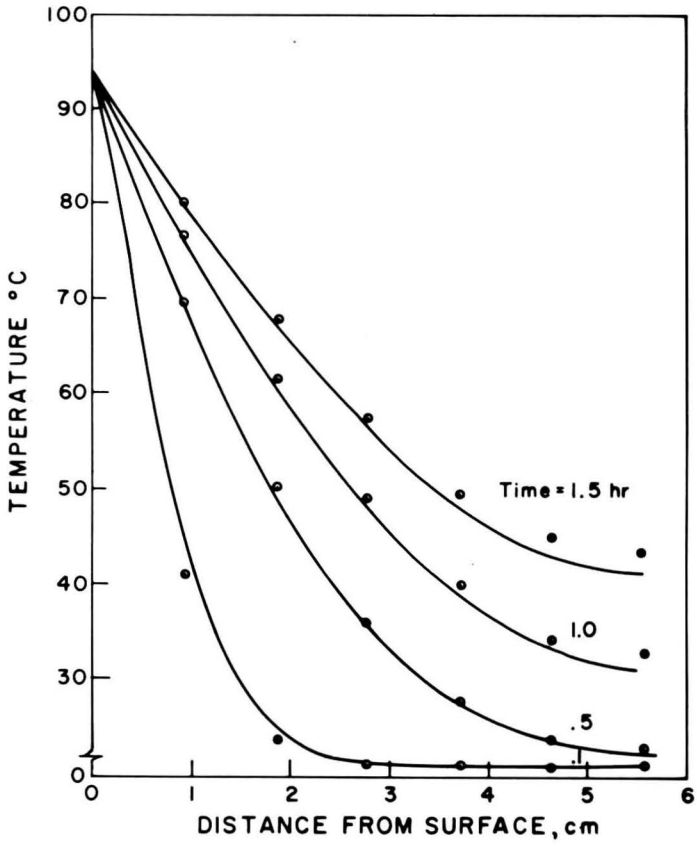

FIG. 4. PREDICTED TEMPERATURE DISTRIBUTION IN AN INFINITE SLAB INITIALLY AT 21.1°C AND SUDDENLY SUBJECTED TO A SURROUNDING TEMPERATURE OF 93.3°C

The predicted temperature values, identified by ⊖, are compared with the analytical solution.

Agreement between the numerical and the analytical solutions is generally good, even for this rather coarse grid. It should also be noted

that the above stepwise change of the temperature ($\partial(T)/\partial t = \infty$ on the boundary) puts unusual requirements on the stability and the oscillating behavior of any numerical method.

The Cooling of Fruit

To illustrate use of the finite-element method in problems involving irregular boundaries, the temperature distribution was calculated in a pear during cooling. The 78 node points associated with 120 elements are indicated in Fig. 5. The thermal properties are from Sweat (1974) and Riedel (1951): thermal conductivity, $k_{zz} = k_{yy} = 0.595$ W/m°C, density 1000 kg/m^3, and specific heat 3,598 J/kg°C. The initial pear temperature was assumed to be 22°C and the surrounding temperature 2°C. The temperature evolutions at nodes 28 and 37 are indicated in Fig. 6. The center temperature (node 37) has a considerable lag with respect to temperature variation toward the outside. Under the given circumstances, it will take more than 35 minutes to cool the center below 3°C, neglecting the effect of heat of respiration.

The Cooking of a Chicken Leg

A chicken leg is an example of a body composed of several materials with different thermal properties; i.e., skin, meat, bone, bone marrow. The shape can be considered approximately axi-symmetric. To reduce the number of calculations, the composition of the leg was somewhat simplified and only the meat and bone were considered. The grid included 96 nodes for 148 elements (60 for the bone, 88 for the meat). The thermal properties of the meat were (Walters 1963): conductivity $k_{zz} = k_{rr} = 0.411$ W/m°C, specific heat, $C_p = 3{,}431$ J/kg°C, and density $\rho = 1070$ kg/m^3. The bone properties were: conductivity, $k_{zz} = k_{rr} = 0.346$ W/m°C, specific heat, $C_p = 2{,}970$ J/kg°C, and density $\rho = 860$ kg/m^3. Initial temperature was 4.4°C, and the leg was dropped in a liquid at 100°C. Figures 7a, 7b, and 7c, respectively illustrate the isotherms in the leg after 0.15, 0.5, and 0.75 hour.

The meatless part of the bone has a fast increase in temperature. Otherwise, the difference in thermal properties between the meat and the bone is not readily noticeable. The isotherm lines indicate the location for monitoring temperature during cooking.

A further refinement of this example would include different thermal properties for the cooked and uncooked meat. This is, however, a nonlinear problem, and iterative temperature calculations would be required at each time step.

Isotherms were computer-drawn using the nodal temperatures as calculated by the finite-element program and the interpolating

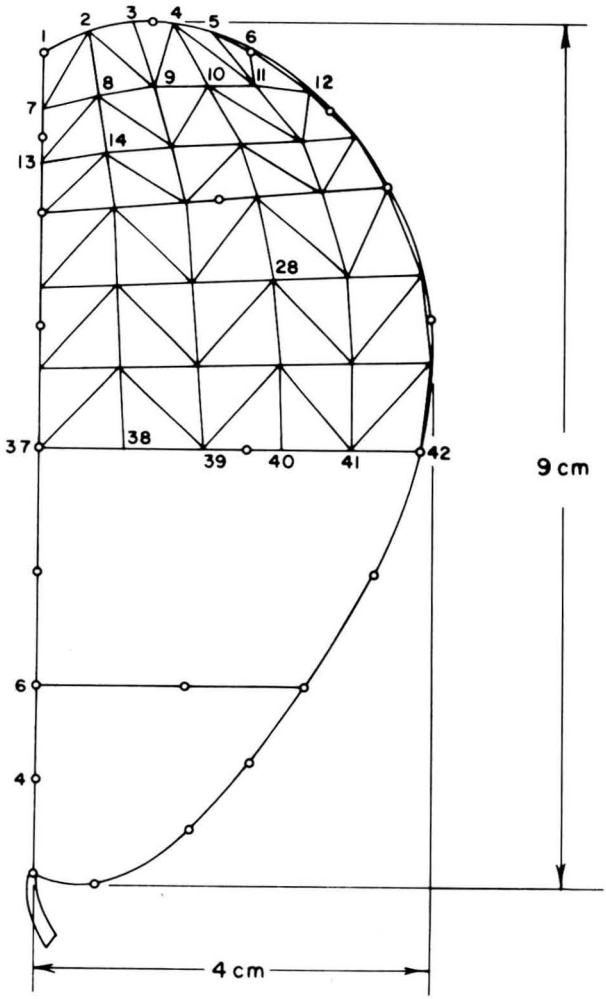

FIG. 5. A HALF-PEAR DIVIDED INTO TRIANGULAR ELEMENTS. THE POINTS DESIGNATED AS 'O' WERE USED TO GENERATE THE GRID FROM QUADRILATERAL REGIONS

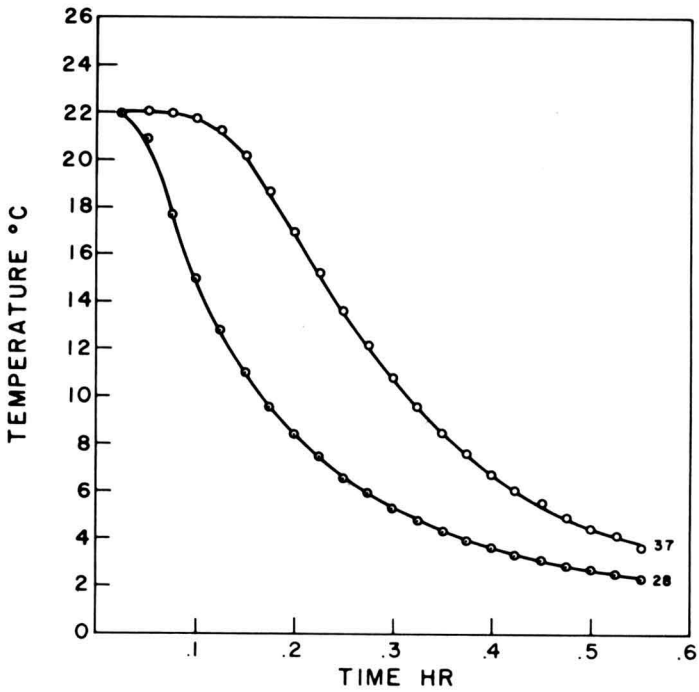

FIG. 6. PREDICTED TEMPERATURE HISTORY AT TWO INTERIOR POINTS IN A PEAR DURING COOLING (FOR LOCATIONS OF NODES 28 AND 37, SEE FIG. 5)

functions, Equation (5). It should be noted here that computer graphics are readily used in output of the results of finite-element calculations when disk files are used for the temporary storage of element-data information and results. It is an efficient way of analyzing and reducing the flood of numbers resulting from finite-element analysis.

Nonisotropic Material Properties, and Time-Dependent Boundary Conditions

The thermal properties for meat vary with direction because of its fibrous nature. The thermal conductivity of beef, for example, is 0.434 W/m°C in the direction of the fibers, but only 0.346 W/m°C in the direction normal to the fibers (Kopelman 1969). The specific heat is 3500 J/kg°C and the density is 1160 kg/m^3. The pan frying of a steak was simulated for two cases: cut parallel to the fiber and cut normal to the fiber. The beef steak considered in this example was 2.54 cm thick and assumed to be round, with a diameter of 12.2 cm (Fig. 8). Seventy

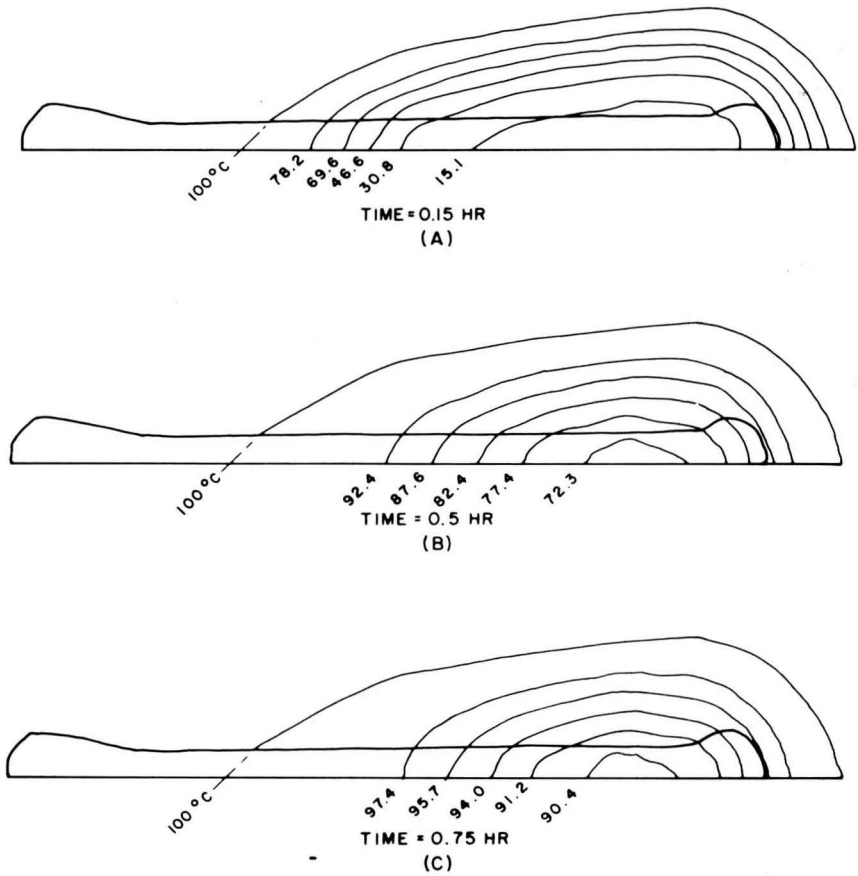

FIG. 7. PREDICTED TEMPERATURE DISTRIBUTION AT DIFFERENT TIME INTERVALS IN A HALF-AXI-SYMMETRIC CHICKEN LEG

(Leg dimensions: overall length = 14.1 cm, bone length = 11.56 cm, leg half-thickness = 2.67 cm).

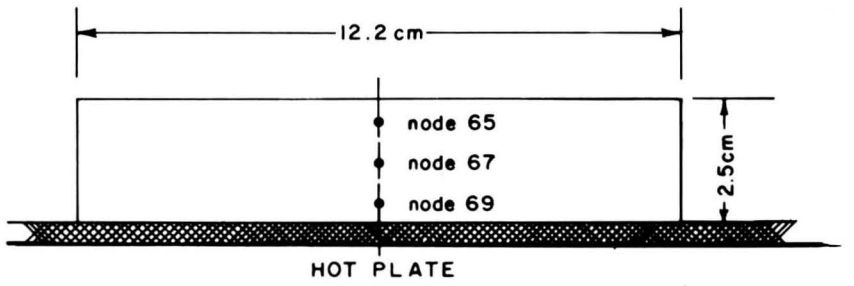

FIG. 8. LOCATIONS OF SOME NODES OF INTEREST IN A BEEF STEAK 2.5 CM THICK PLACED ON A HOT PLATE

nodes and 108 elements were used. The following nodes along the axis of symmetry (r = 0) were observed: node 67 at the center (z = 1.27 cm) and a node at each side of node 67; i.e., node 65 (z = 2.12 cm) and node 69 (z = 0.42 cm). The simulation assumes that the steak is placed on a hot plate at 177°C. Initially, the side z = 0 is heated, and after 9 minutes the node with z = 2.54 cm was heated. This process was repeated to simulate the turning of the steak in a frying pan. No heat is lost from the side opposite to the hot plate.

The temperature history at the mentioned nodes is shown in Fig. 9 for the fibers parallel to the z direction and in Fig. 10 for the case of fibers normal to the z direction. It can be seen that in both cases the center temperature increases uniformly in time although the temperature at other locations vary greatly.

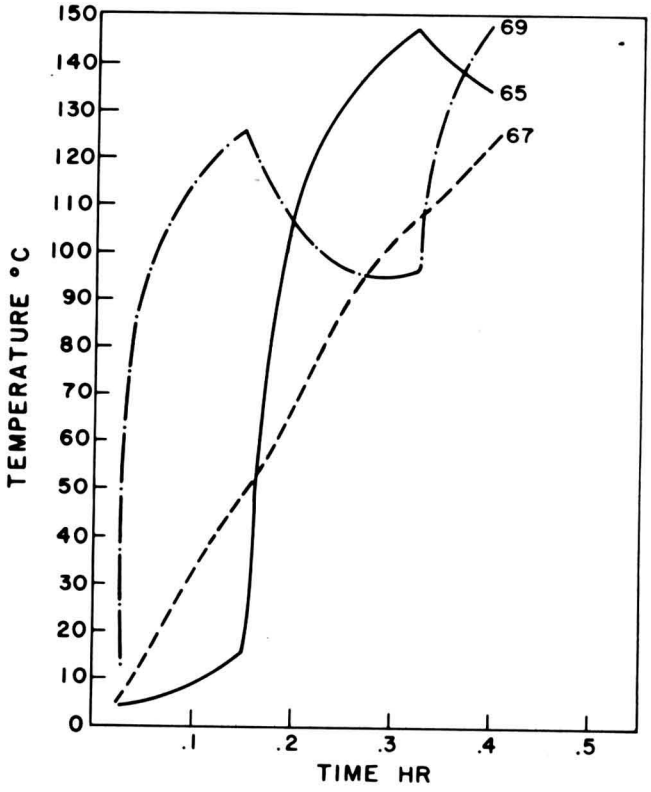

FIG. 9. PREDICTED TEMPERATURE HISTORY IN A BEEF STEAK WITH FIBERS NORMAL TO THE HOT PLATE

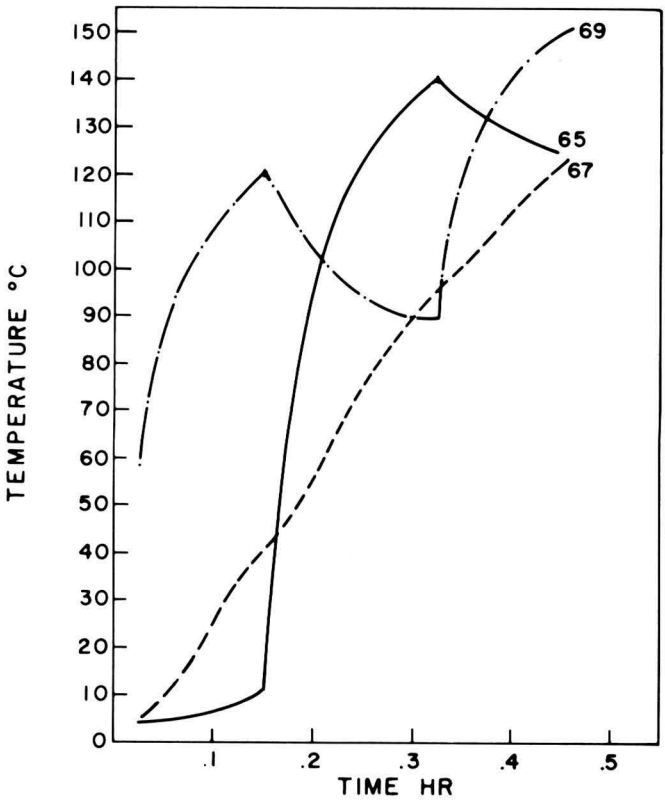

FIG. 10. PREDICTED TEMPERATURE HISTORY IN BEEF STEAK WITH FIBERS PARALLEL TO THE HOT PLATE

SUMMARY

This paper illustrates applications of the finite-element method to the calculation of heat transfer in foodstuffs. It shows how the method can easily accommodate a wide variety of shapes, thermal properties, and boundary conditions within a single simple program. This makes it of great value; the user has only to divide the region into elements and provide the thermal properties and the specified boundaries.

The computer program can easily be adapted for use in quality studies involving bacterial inactivation of nutrient degradation. Diffusion problems in solids can be studied with some minor modifications.

REFERENCES

COMINI, G., DEL GUIDICE, S., LEWIS, R. W. and ZIENKIEWICZ, O. L. 1974. Finite element solution of non-linear heat conduction problems with special emphasis on phase changes. Intern. J. Num. Meth. Engr. *8*, 613–624.

CRANDALL, S. H. 1956. *Engineering Analysis*, McGraw-Hill Book Co., New York.

DESAI, C. S. and ABEL, J. F. 1972. *Introduction to the Finite Element Method*, Van Nostrand Reinhold Co., New York.

KOPELMAN, I. J. 1966. Transient heat transfer and thermal properties in food systems. Ph.D. Thesis, Michigan State University, E. Lansing.

MELOSH, R. J. 1963. Basis for derivation of matrices for the direct stiffness method. J. Am. Inst. Aeron. Astron. *1*(7), 1631–1637.

MYERS, G. E. 1971. *Analytical Methods in Heat Conduction*, McGraw-Hill Book Co., New York.

NORRIE, D. H. and DEVRIES, G. 1972. The Finite Element Method, Fundamentals and Applications, Academic Press, New York.

RIEDEL, L. 1951. The refrigeration effect required to freeze fruits and vegetables. Refrig. Eng. *59*, 670–673.

SEGERLIND, L. J. 1976. *Applied Finite Element Analysis*, John Wiley & Sons, New York.

SINGH, R. P. and SEGERLIND, L. J. 1974. The finite element method in food engineering. ASAE Paper No. 74-6015.

STRANG, G. and FIX, G. 1973. *Analysis of the Finite Element Method*, Prentice Hall, Englewood Cliffs, N.J.

SWEAT, V. E. 1974. Experimental values of thermal conductivity of selected fruits and vegetables. J. Food Sci. *39*, 1080–1083.

TURNER, M. J., CLOUGH, R. W., MARTIN, H. C. and TOPP, L. J. 1956. Stiffness and deflection analysis of complex structures. J. Aeron. Sci. *23*(9), 805–824.

VISSER, W. 1965. A finite element method for determination of non-stationary temperature distribution and thermal deformations. Proc. Conf. Matrix Methods in Struct. Mech., Air Force Inst. Tech., Wright Patterson A. F. Base, Dayton, Ohio.

WALTERS, M. 1963. Thermal conductivity and density of chicken breast meat and skin. Food Tech. *17*(6), 808–811.

WARZEE, G. 1974. Finite element analysis of transient heat conduction: explication of the weighted residual process. Comp. Methods in Applied Mech. and Engr. *3*, 255–268.

WEAVER, W., JR. 1967. Computer Programs for Structural Analysis, D. Van Nostrand Co., pp. 64–66, New York.

WILSON, E. L. and NICKELL, R. E. 1966. Application of the finite element method to heat conduction analysis. Nuclear Eng. Design *4*, 276–286.

ZIENKIEWICZ, O. C. 1971. The Finite Element Method in Engineering Science, McGraw-Hill Book Co., New York.

ZIENKIEWICZ, O. C. and CHEUNG, Y. K. 1965. Finite elements in the solution of field problems. The Engineer, pp. 507–510.

ZIENKIEWICZ, O. C. and PAREKH, C. J. 1970. Transient field problems: two-dimensional and three-dimensional analysis by isoparametric finite elements. Intern. J. Numerical Methods in Eng. *2*, 61–71.

EFFECT OF STORAGE AND PROCESSING CONDITIONS ON SORGHUM KERNEL STRENGTH

D. A. SUTER, R. A. RUPP[1], G. T. LANE[1] AND R. D. SULLINS[2]

Department of Agricultural Engineering
Department of Animal Science[1]
Department of Soil and Crop Sciences[2]
Texas Agricultural Experiment Station
Texas A&M University
College Station, Texas 77843

Received for Publication October 1, 1976

ABSTRACT

Compressive strength of sorghum kernels was measured to determine the effect of storage conditions on processing for animal feed. Ensiling grain affected a larger decrease in kernel compressive strength than did storage at a high moisture level. Results similar to the above were noted for tests conducted on kernels obtained from animal feces. Microscopic examination of kernels from each treatment revealed greater removal of kernel structure for those of lower compressive strength.

INTRODUCTION

Much progress has been made in identifying some of the basic variables which influence silage nutritive value of various sorghum grain varieties. Variables studied include maturity, dry matter content, grain content, grain passage, digestibility, seed size, and seed hardness. The latter two variables have been scarcely studied with respect to their influence on silage nutritive value.

Studies have been conducted to evaluate passage of whole grain with time. Becker and Gallup (1927) reported fecal losses of 26 to 49 percent of grain ingested with sorghum silages. Ward *et al.* (1965) found that sorghum variety affected the amount of whole seed in feces of cattle fed sorghum silage.

Scanning electron microscopy has been used to detect physical differences in seed structure which might be related to digestibility. Sullins and Rooney (1971) have found relationships existing between structural differences in the sorghum kernel and digestibility. The corneous, floury and intermediate textured kernels are nonwaxy and contain more peripheral endosperm than the waxy sorghum. The waxy

Journal of Food Process Engineering 1 (1977) 51–73.

starch is more susceptible to enzymes, has less peripheral endosperm, and the protein matrix is more susceptible to enzymatic digestion.

Through microscopy they have found the structure of peripheral endosperm of the kernel to be highly indicative of kernel digestibility. Funderburk (1974) reported on the relationship between structural differences in the sorghum kernel and maximum compressive strength values. He found that less force was required to cause failure in the waxy kernel microstructure due to compression load kernels of the other types.

The objectives of this research were:

(1) To determine the physical differences in grain sorghum kernels resulting from storage, ensiling, and digestion.
(2) To determine the effect of storage, ensiling, and digestion on the bioyield strength, ultimate strength, and modulus of deformability of grain sorghum kernels.

EXPERIMENTAL

Materials

Oro variety grain sorghum was harvested in the hard grain stage of maturity at an average moisture content of 25 percent (dry basis). Physical properties of samples are given in Table 1.

Table 1. Effect[1] of storage and processing methods on feed and fecal whole grain weights (dry basis)

	Grain Treatment Means				
	1	2	3	4	5
Parameter	Control	Silage	High Moisture	Fecal Silage	Fecal High Moisture
Test weight (Kg/m^3)	699.2a[1]	650.3b	719.8a	574.3b	674.8c
Thousand kernel weight (gm)	24.5a	21.3bc	24.5a	20.5b	22.2c
Kernel size index (KSI)	66.84	66.93	66.07	66.35	66.81
Kernel diameters (cm)					
D_1	0.403	0.408	0.409	0.409	0.398
D_2	0.364	0.374	0.378	0.376	0.361
D_3	0.251	0.234	0.239	0.242	0.230

[1] Values in the same row with different letters differed significantly ($P < .05$).

Treatment 1 (control) consisted of kernels dried soon after harvest. Treatment 2 consisted of grain taken from silage which had been stored in sealed polyethylene bags for 90 days. Treatment 3 consisted of grain stored 60 days in sealed polyethylene bags. Treatment 4 was similar to Treatment 2 except that it involved feeding silage to livestock and samples taken from the feces of animals every three hours. Treatment 5 was the same as Treatment 3 except that the grain was fed to livestock and samples taken from the feces of animals every three hours.

For each replicate, samples of the sorghum grain kernels were dried at 55°C for 72 hr in a forced draft oven. Samples were randomly selected for each treatment. Test weights of the samples were taken to conform with Official U.S. Grain Standards (1973). Twenty whole kernels were randomly selected from the dried samples for obtaining force-deformation data of each kernel. For each kernel, three diameter measurements were made (Fig. 1).

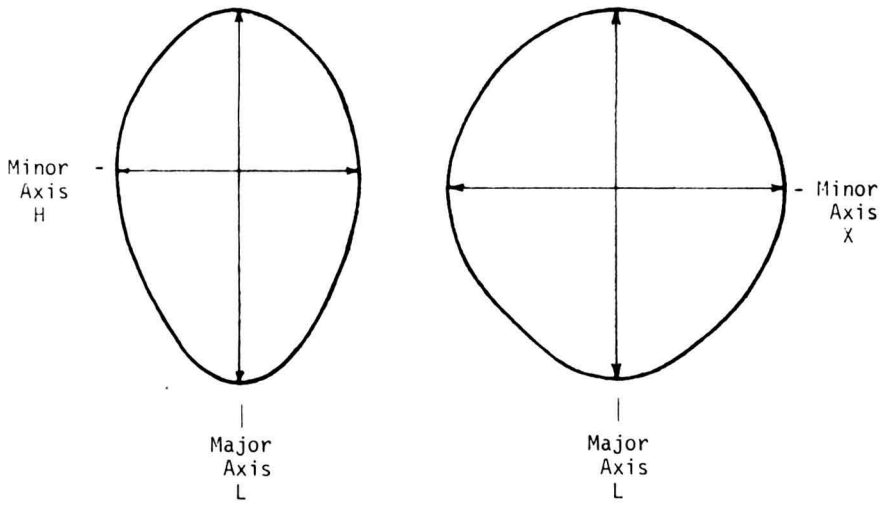

FIG. 1. MEASUREMENTS MADE ON EACH GRAIN KERNEL

Compression Tests

Force-deformation data were determined for each kernel in a loading apparatus (Funderburk 1974) at a loading rate of 5 cm/min. Force and deformation values were obtained from the force-deformation curves for the point of inflection, bioyield, and rupture values. A typical force-deformation curve is shown in Fig. 2. Test results were analyzed by a Statistical Analysis System (Barr and Goodnight 1972).

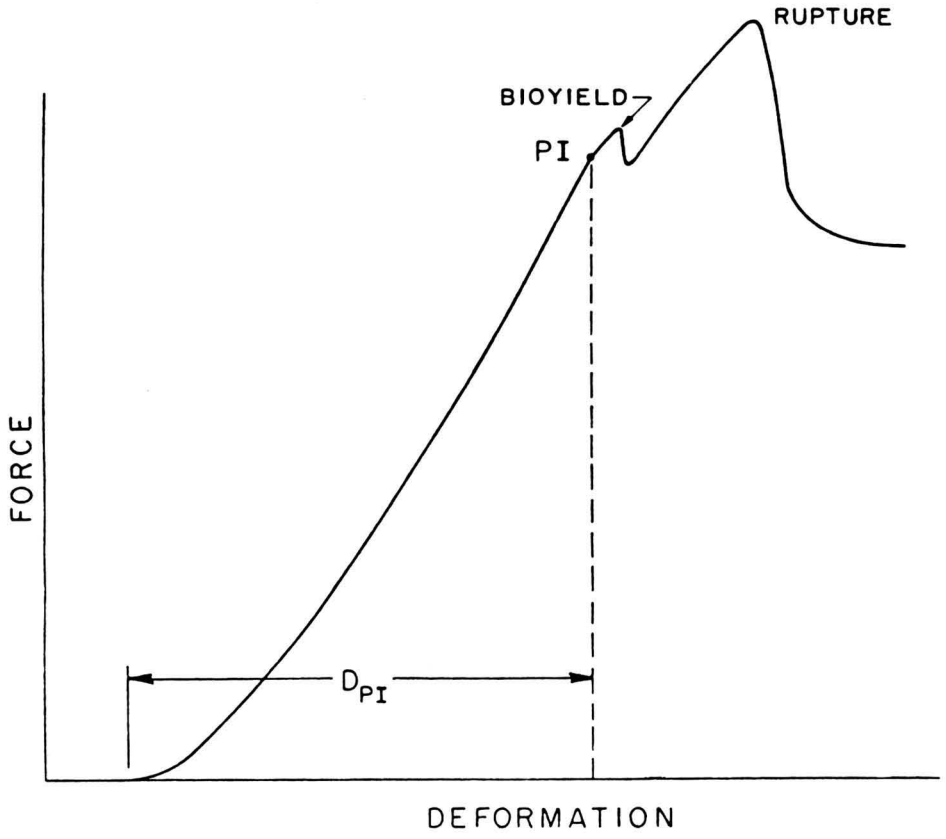

FIG. 2. FORCE-DEFORMATION CURVE FOR MATERIALS WITH BIO-YIELD POINT

PI = point of inflection; DPI = deformation at point of inflection. (Mohsenin 1973)

The modulus of deformability, E, was calculated for each kernel at the point of inflection and for the value representing one-half the force at the point of inflection. The equation used is given below as defined by Mohsenin (1972):

$$E = \frac{0.531F(1-\mu^2)}{D^{3/2}} \qquad \left(\frac{1}{R_1}+\frac{1}{R_1}\right)^{1/3} + \left(\frac{1}{R_2}+\frac{1}{R_2}\right)^{1/3\ 3/2}$$

where: E = modulus of deformability, Newtons/cm^2
F = force in Newtons (N)
μ = Poisson's ratio (assumed to be 0.3)

D = sum of both elastic and plastic deformations at both loading and supporting points of contact, cm.
R_1, R_1', R_2, R_2' = radii of curvature of the convex body at the points of contact, cm.

Test measurements indicated that R_1 and R_1' could be used as an estimate of R_2 and R_2' with less than 5 percent error.

Microscopy

Microscopic studies were directed toward relating the physical changes in the kernel to visible alterations in kernel structures and characteristics. Specimens of half-kernels of each treatment were studied with the use of a Model U-3 Jeol Scanning electron microscope. The scanning electron microscope was employed because it permitted excellent depth of field at magnifications permitting detailed observations of individual starch granules and protein structures. After a thorough study of each scanned kernel, photomicrographs were made of kernel areas which were considered representative of each sample.

RESULTS

Differences in weight of samples (Table 1) for dry, silage, high moisture, fecal silage, and fecal high moisture kernels were significantly ($P < .05$) different as determined by both Test Weight and Thousand Kernel Weight (TKW) methods. Silage grain weighed less than dry grain and lost significantly ($P < .05$) less weight during passage through the digestive tract of cows. High moisture grain weighed the same (dry matter basis) as dry grain but was significantly ($P < .05$) reduced in weight when subjected to the digestive processes.

No significant ($P < .05$) differences were found in size of grain kernels due to treatment effect as determined by the Kernel Size Index (KSI) and kernel diameters (Table 1). Kernel weight loss was not accompanied by a reduction in kernel size.

Mean values obtained in the compression tests are given in Table 2 and illustrated in Fig. 5 and 6. Statistical analysis of the mean values of measured force and deformation and calculated values of modulus of deformability at inflection, bioyield, and rupture points indicated significant differences ($P < .05$) between treatments. Orthogonal contrasts of the above mean values (Table 3) indicated significant differences between the following treatments for the parameters given.

(1) Level of significance ($P < .01$)

a. Control vs all other treatments for force and deformation at all points.

Each treatment significantly affected the amount of force required to deform the kernels to the points examined on the force-deformation curves. The measured force in Newtons (N) at the point of inflection was 17.41, 25.50, 32.47, 46.09, and 58.43 for fecal silage, fecal high moisture, silage, high moisture, and control treatment means, respectively. The measured deformation at the point of inflection was 0.11, 0.12, 0.12, 0.14, and 0.18 cm. for silage, fecal silage, fecal high moisture, high moisture, and control, respectively. Similar treatment effects were noted for force and deformation at the bioyield and rupture points.

b. Silage vs high moisture at all points.

Ensiling the grain with the entire plant decreased the amount of force required to cause failure in the microstructure and subsequent rupture of the kernels. This can be seen by comparison of the force at the point of inflection for the silage and high moisture treatment means 32.47N and 46.09N, respectively.

c. Silage vs fecal silage for force and modulus of deformability at all points.

The digestive tract decreased the amount of force required to cause failure in the silage grain kernels and also decreased their modulus of deformability. Treatment effect was significant for force but had no significant effect on deformation values.

d. High moisture vs fecal high moisture for force and modulus of deformability at all points.

The force required to cause failure in the kernels and modulus of deformability values were 46.09N, 4136.49N/cm^2, 25.50N, 2795.06N/cm^2 for high moisture and fecal high moisture, respectively.

(2) Only the contrast of silage vs high moisture for deformation at the rupture point was significant at ($P < .05$).

Microscopic examination of randomly selected kernels from each treatment revealed considerable differences between treatments with relatively little variation within treatments. Comparison of results obtained in compression tests and micrographs shown in Fig. 3 to 6 illustrate treatment effect on kernel structural change.

Table 2. Compression test means of whole grain treatments conducted to measure force and deformation and to calculate modulus of deformability at inflection, bioyield, and rupture points.

	Means								
	Inflection Point			Bioyield Point			Rupture Point		
Grain Treatment	Force (N)	Deformation (cm)	Modulus of Deformability (N/cm^2)	Force (N)	Deformation (cm)	Modulus of Deformability (N/cm^2)	Force (N)	Deformation (cm)	Modulus of Deformability (N/cm^2)
Control	58.43	0.18	3728.7	59.19	0.18	3683.52	60.17	0.19	3655.35
Silage	32.47	0.11	3928.09	32.47	0.11	3928.10	32.55	0.11	3878.31
High moisture	46.09	0.14	4136.49	46.09	0.14	4136.49	48.68	0.15	4032.95
Fecal silage	17.41	0.12	2231.56	17.41	0.12	2231.56	18.47	0.13	2007.92
Fecal high moisture	25.50	0.12	2795.06	25.50	0.12	2795.06	25.72	0.13	2671.07

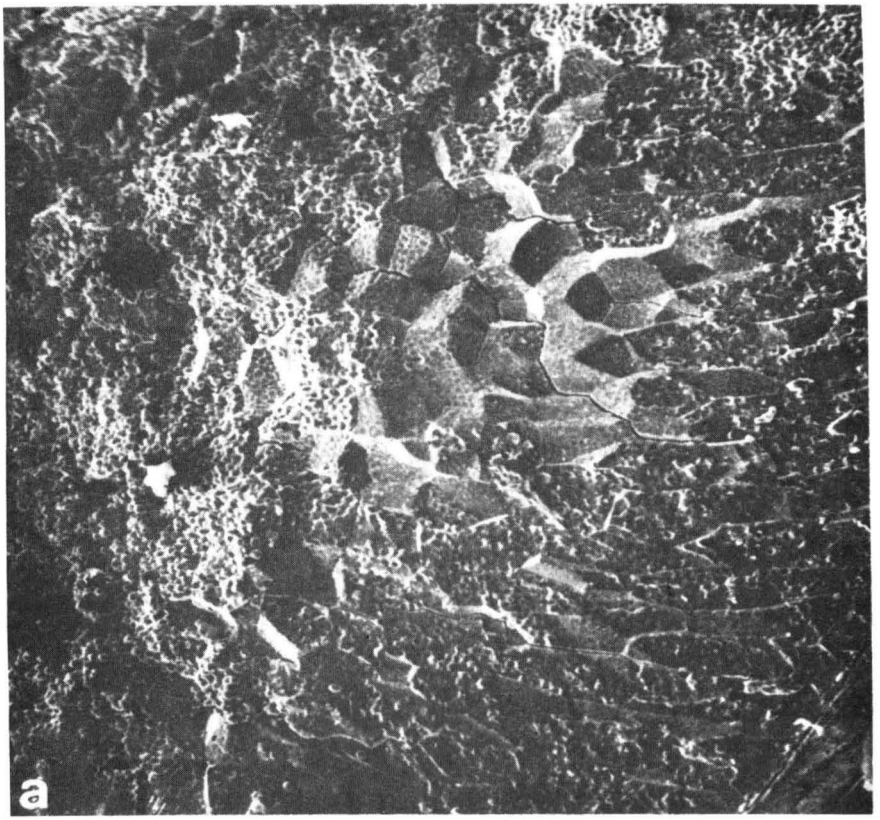

FIG. 3. SCANNING ELECTRON PHOTOMICROGRAPHS OF A GRAIN KERNEL OF CONTROL TREATMENT

(3a) longitudinal section with floury endosperm in upper left corner, corneous in center, and pericarp in lower right corner (80X).

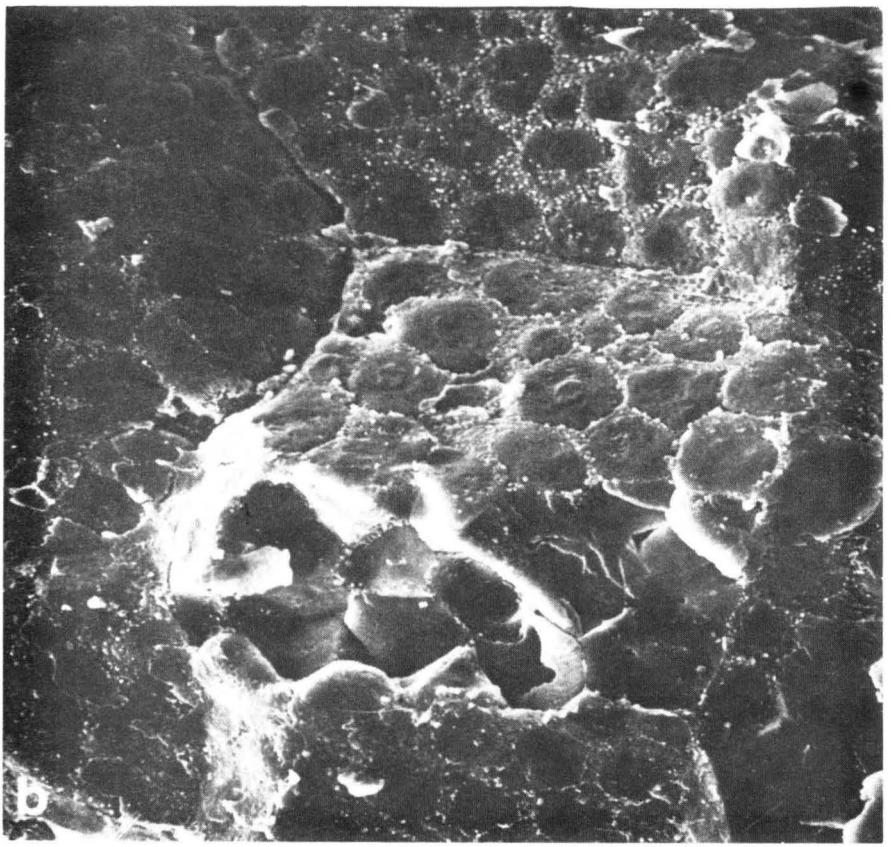

FIG. 3. SCANNING ELECTRON PHOTOMICROGRAPHS OF A GRAIN KERNEL OF CONTROL TREATMENT

(3b) corneous endosperm (1000X).

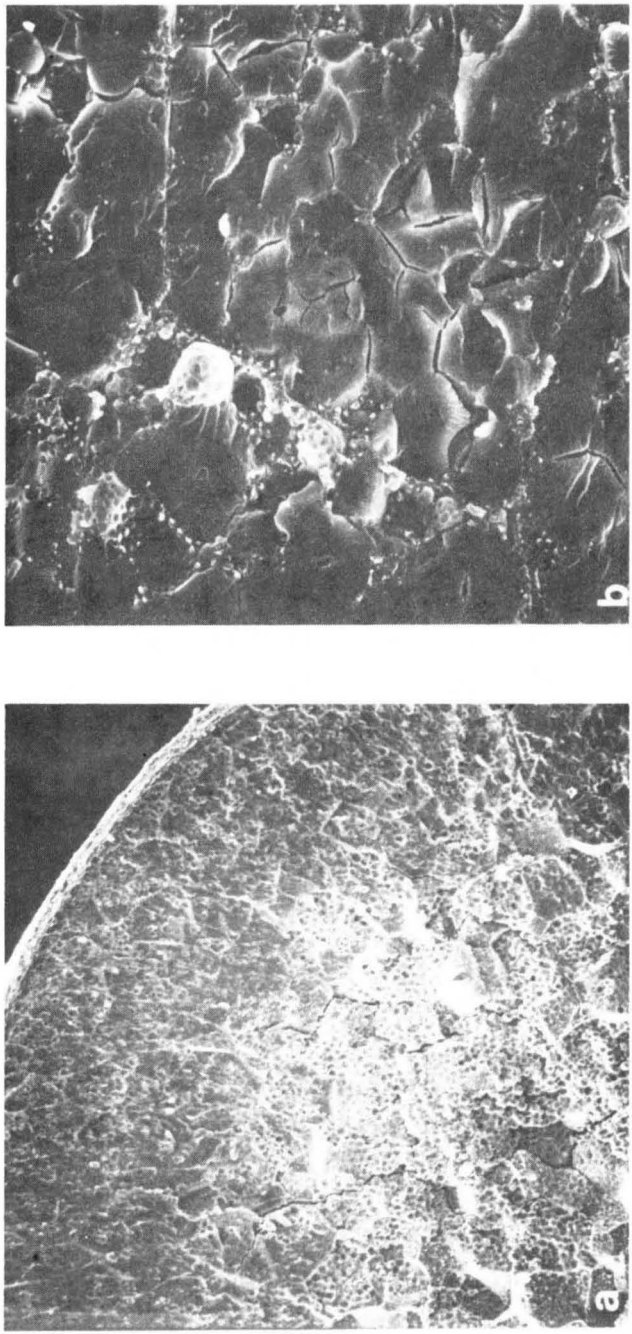

FIG. 4. SCANNING ELECTRON PHOTOMICROGRAPHS OF HIGH MOISTURE GRAIN (a–c) AND SILAGE GRAIN (d–f)

Longitudinal section, 4a, (100X); corneous endosperm, 4b, (1000X).

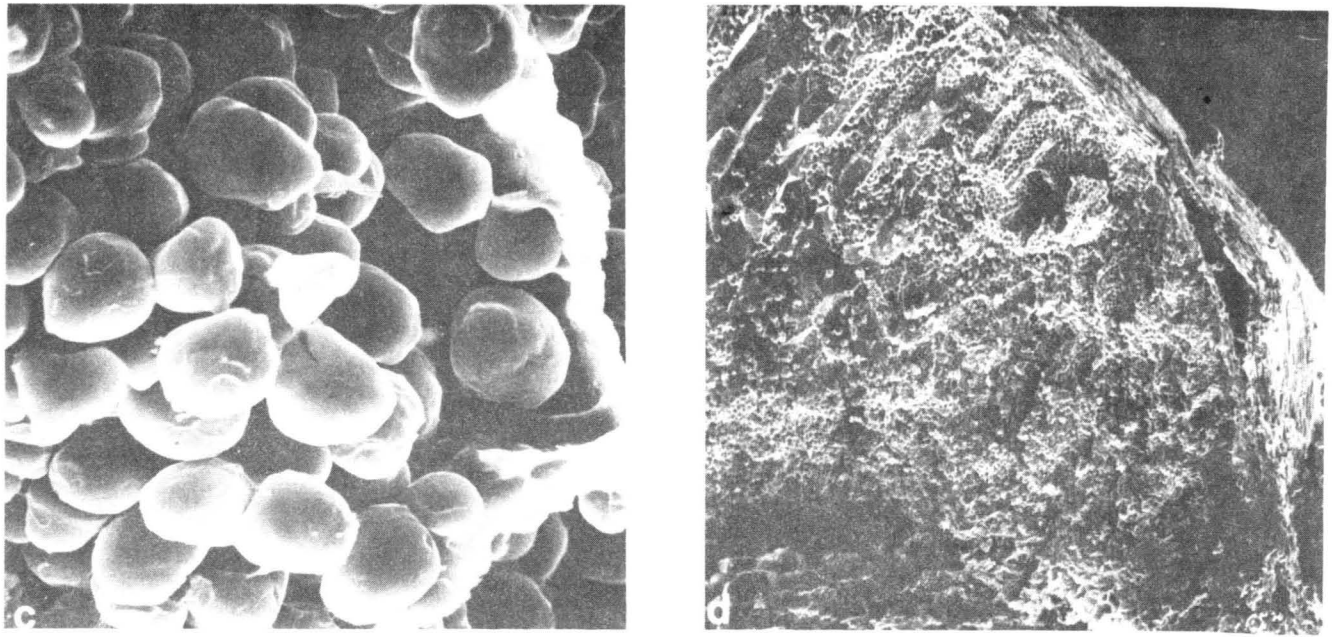

FIG. 4. SCANNING ELECTRON PHOTOMICROGRAPHS OF HIGH MOISTURE GRAIN (a–c) AND SILAGE GRAIN (d–f)

Floury endosperm, 4c, (2000X); longitudinal section, 4d, (80X).

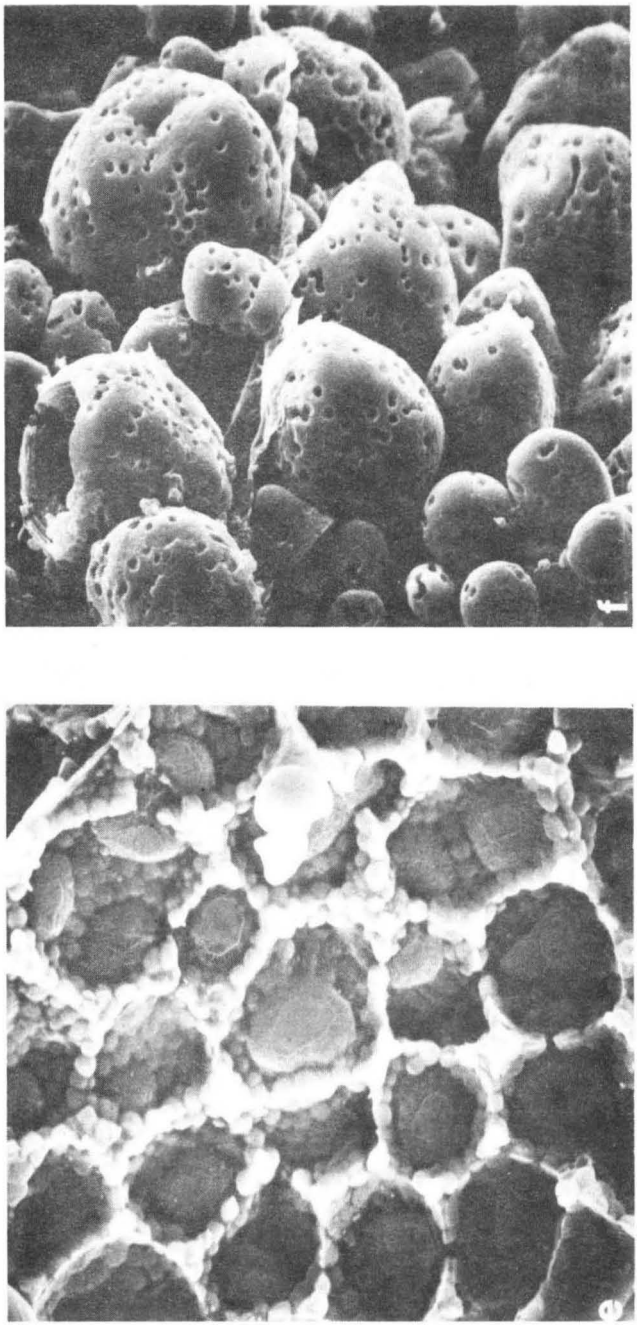

FIG. 4. SCANNING ELECTRON PHOTOMICROGRAPHS OF HIGH MOISTURE GRAIN (a–c) AND SILAGE GRAIN (d–f)

Corneous endosperm, 4e, (2000X); floury endosperm, 4f, (2000X).

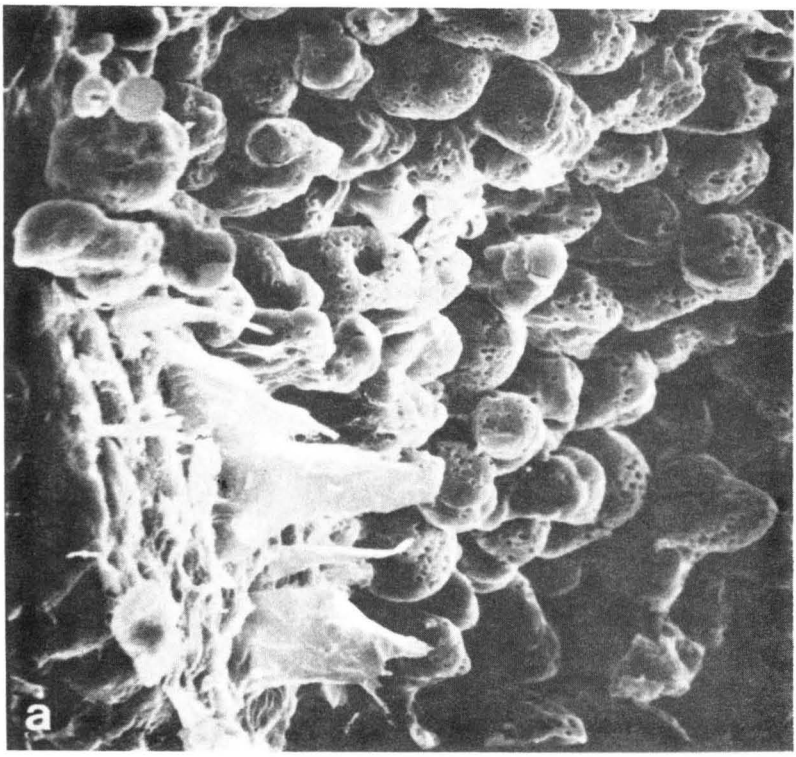

FIG. 5. SCANNING ELECTRON PHOTOMICROGRAPHS OF FECAL HIGH MOISTURE GRAIN (a, b) AND FECAL SILAGE GRAIN (c, d)

Floury endosperm, 5a, (2000X).

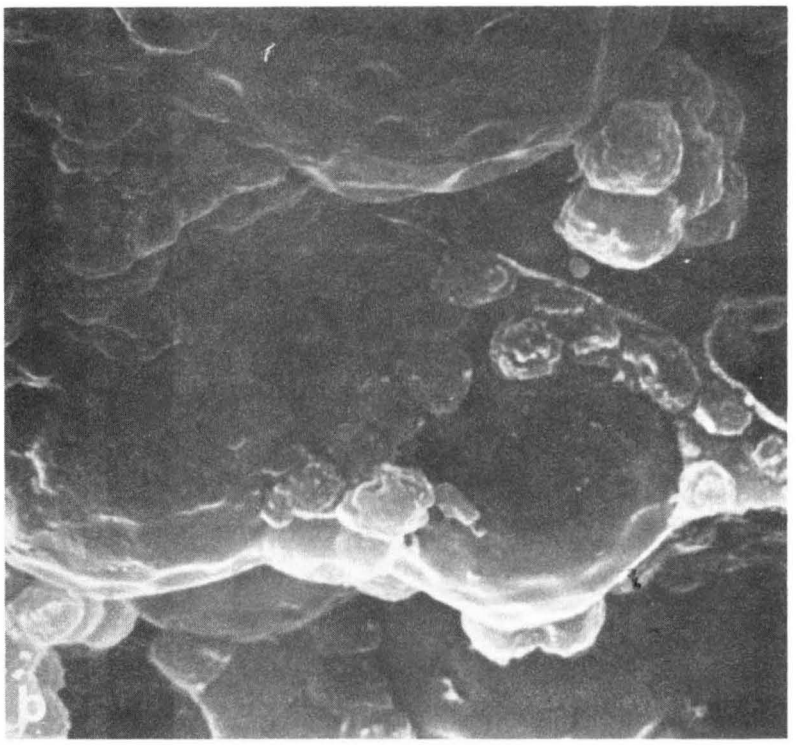

FIG. 5. SCANNING ELECTRON PHOTOMICROGRAPHS OF FECAL HIGH MOISTURE GRAIN (a, b) AND FECAL SILAGE GRAIN (c, d)

Corneous endosperm, 5b, (6000X).

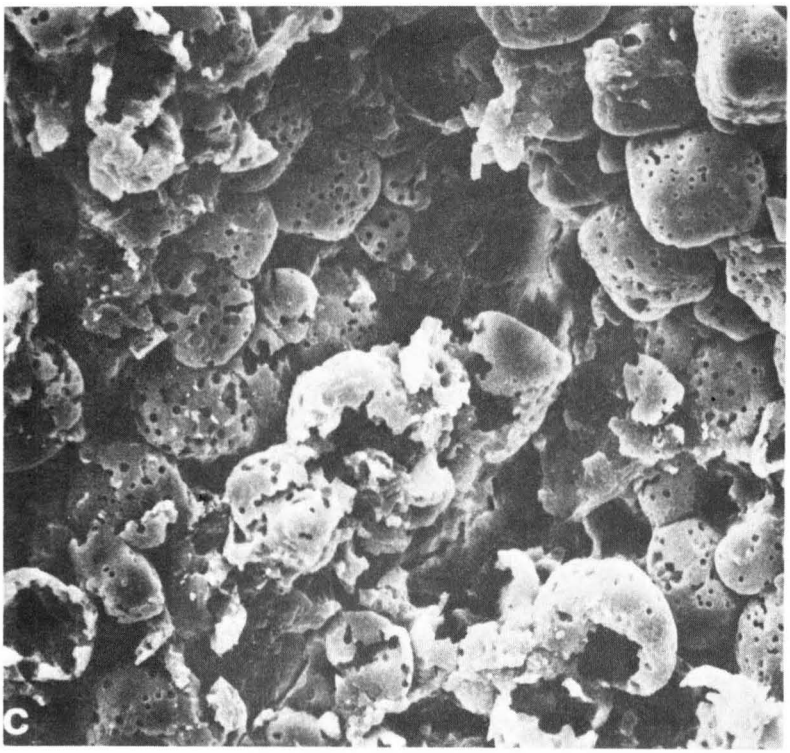

FIG. 5. SCANNING ELECTRON PHOTOMICROGRAPHS OF FECAL HIGH MOISTURE GRAIN (a, b) AND FECAL SILAGE GRAIN (c, d)

Floury endosperm, 5c, (1000X).

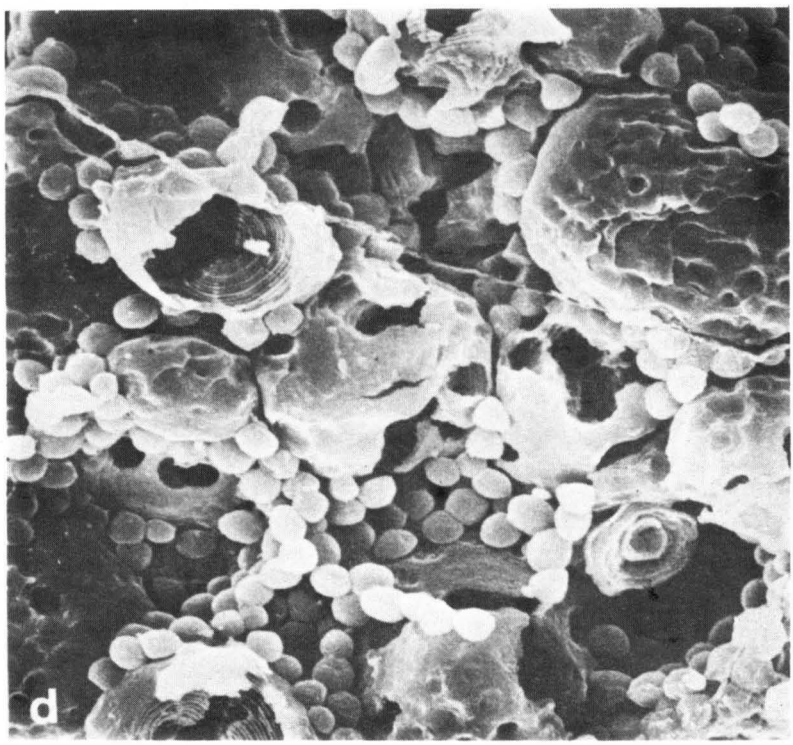

FIG. 5. SCANNING ELECTRON PHOTOMICROGRAPHS OF FECAL HIGH MOISTURE GRAIN (a, b) AND FECAL SILAGE GRAIN (c, d)

Corneous endosperm, 5d, (3000X).

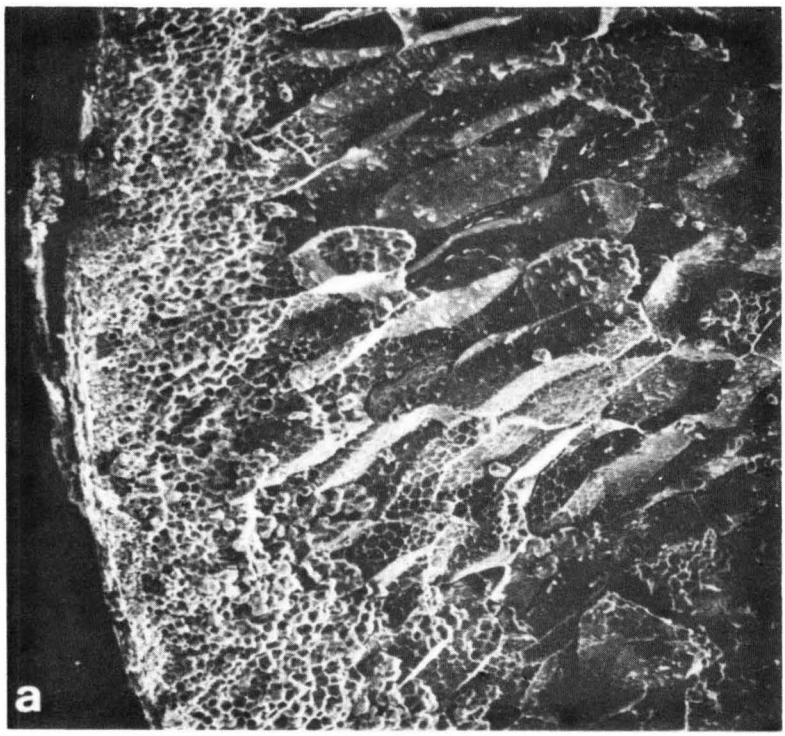

FIG. 6. SCANNING ELECTRON PHOTOMICROGRAPHS OF FECAL HIGH MOISTURE GRAIN (a, b) AND FECAL SILAGE GRAIN (c, d)

Longitudinal cross section of corneous, 6a, (100X).

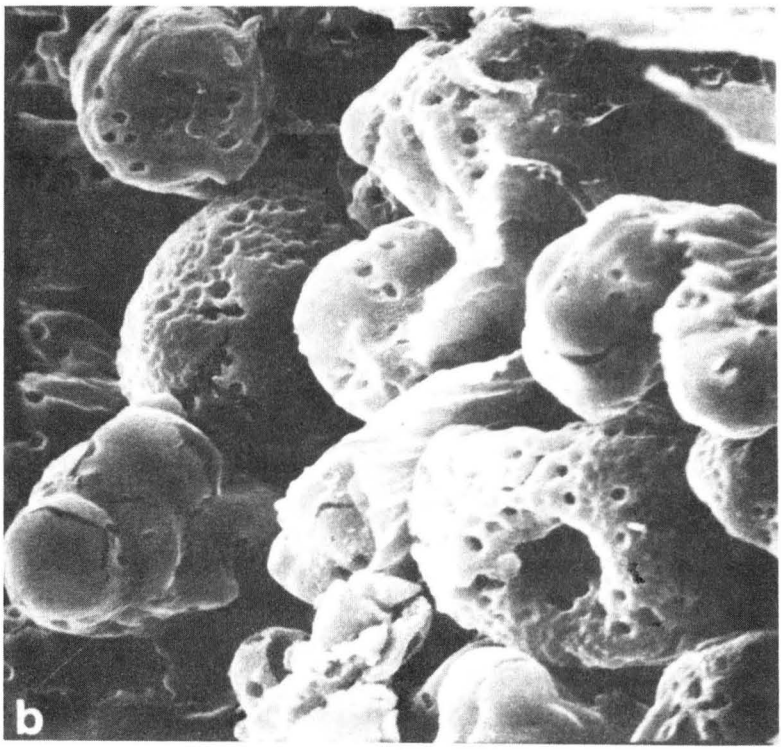

FIG. 6. SCANNING ELECTRON PHOTOMICROGRAPHS OF FECAL HIGH MOISTURE GRAIN (a, b) AND FECAL SILAGE GRAIN (c, d)

Floury endosperm, 6b, (3000X).

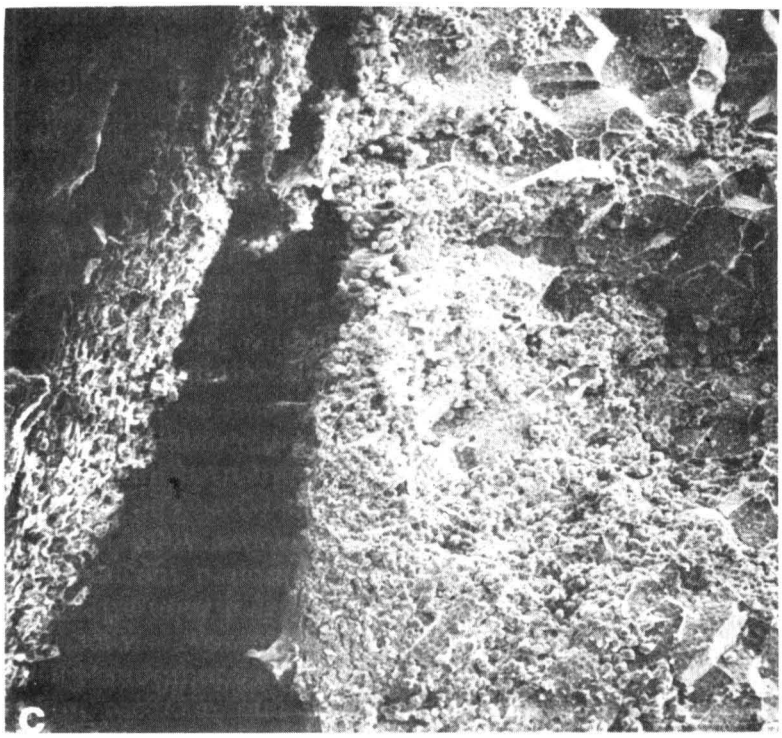

FIG. 6. SCANNING ELECTRON PHOTOMICROGRAPHS OF FECAL HIGH MOISTURE GRAIN (a, b) AND FECAL SILAGE GRAIN (c, d)

Floury endosperm adjacent to scutellum, 6c, (80X).

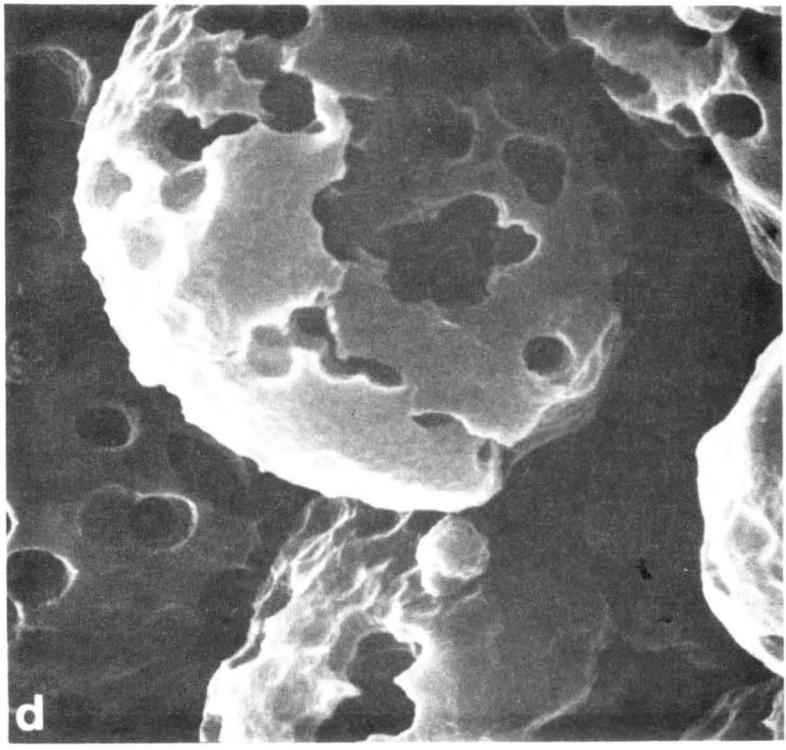

FIG. 6. SCANNING ELECTRON PHOTOMICROGRAPHS OF FECAL HIGH MOISTURE GRAIN (a, b) AND FECAL SILAGE GRAIN (c, d)

Floury, 6d, (6000X).

Table 3. Orthogonal contrasts of mean values[1] obtained for force, deformation, and modulus of deformability at inflection, bioyield, and rupture points for treatments studied

Treatment Contrasts	Parameter	t Values with 95 Degrees of Freedom		
	Force	Inflection Point	Bioyield Point	Rupture Point
1 vs 2, 3, 4, 5		7.97[a]	8.23[a]	8.28[a]
2 vs 3		3.06[a]	3.07[a]	3.66[a]
2 vs 4		3.38[a]	3.40[a]	3.20[a]
3 vs 5		4.62[a]	4.65[a]	5.21[a]
4 vs 5		1.82	1.83	1.64
	Deformation	Inflection Point	Bioyield Point	Rupture Point
1 vs 2, 3, 4, 5		4.92[a]	5.18[a]	4.83[a]
2 vs 3		1.73	1.73	2.20[b]
2 vs 4		0.63	0.63	1.10
3 vs 5		0.78	0.78	0.91
4 vs 5		0.33	0.33	0.19
	Modulus of Deformability	Inflection Point	Bioyield Point	Rupture Point
1 vs 2, 3, 4, 5		1.68	1.51	1.89
2 vs 3		0.61	0.61	0.45
2 vs 4		4.93[a]	4.94[a]	5.49[a]
3 vs 5		3.90[a]	3.91[a]	4.00[a]
4 vs 5		1.64	1.64	1.95

1[a]Significant ($P < .01$)
1[b]Significant ($P < .05$)
2Treatment numbers are: 1. Control; 2. Silage; 3. High Moisture; 4. Fecal Silage; 5. Fecal High Moisture

Cleavage in the corneous endosperm is essentially along the cell walls in the control kernels (Fig. 3a and 3b). High moisture grain (Fig. 4a) produced a rather flat cleavage surface across the kernel peripheral and corneous endosperm. By contrast, silage grain (Fig. 4d) indicates a rougher fracture surface with irregular cleavage extending throughout the peripheral endosperm. The corneous endosperm of high moisture grain (Fig. 4b) reveals cleavage across cell walls and across starch granules. High moisture grain (Fig. 4c) was characterized by spherical starch granules with only small fragments of cell walls or protein

material present. No digestion was detected in the floury endosperm of high moisture grain. Floury endosperm of silage grain (Fig. 4f) had undergone considerable starch digestion.

Fecal high moisture floury endosperm (Fig. 5a) shows evidence of considerable digestion of starch granules. Only slight digestion occurred in the fecal high moisture corneous (Fig. 5b). Considerable digestion was found in the floury endosperm of fecal silage grain (Fig. 5c). Intense digestion also was noted in some areas of the corneous endosperm of fecal silage grain (Fig. 5d). The protein matrix appears to have been digested, leaving numerous very smooth small protein bodies surrounding voids or partially digested starch granules. Some of the partially digested starch granules show concentric rings similar to tree rings.

A fecal high moisture grain kernel section is shown in Fig. 6a. Some softening of the peripheral endosperm had apparently occurred. The corneous endosperm appeared to have flat angular surfaces which indicate cleavage is along cell walls instead of across cell walls and across starch granules as was found in high moisture grain (Fig. 3a and 3b). Floury endosperm in fecal high moisture (Fig. 6b) showed evidence of surface and preferential digestion.

A portion of a fecal silage grain is shown in Fig. 6c. A small portion of corneous endosperm can be seen in upper right of micrograph. Advanced digestion in the floury endosperm of a fecal silage grain (Fig. 6d) indicates preferential with some surface digestion.

CONCLUSIONS

Possible increase in grain digestibility and decrease in processing energy may be obtained as a result of storage conditions. Ensiling grain affected a larger decrease in kernel compressive strength than did storage at a high moisture level. Kernels dried soon after harvest and not undergoing any further treatment exhibited the maximum compressive strength. Results similar to the above were noted for tests conducted on kernels obtained from animal feces. The ensilage process, therefore, offers important benefits in animal feeding. Additionally, storage of high moisture sorghum grain without expensive drying would minimize energy consumption with possible cost savings.

Further research is needed to examine economic implications of the above study. Enzymatic activity to minimize processing energy consumption may be possible for cereals used in human food.

REFERENCES

BARR, A. J. and GOODNIGHT, J. H. 1972. Statistical analysis system. North Carolina State University, Raleigh.

BECKER, R. B. and GALLUP, W. D. 1927. Utilization of the grain in kafir and cane silage by dairy cows. J. Agr. Res. *35*, 279–281.

FUNDERBURK, T. G. 1974. Evaluation of selected grain sorghum varieties in relation to the modulus of deformability. Paper presented Summer ASAE Meeting, Stillwater, Oklahoma.

MOHSENIN, N. N. 1973. Compression test of food materials of convex shape. ASAE Food Engineering Division standard adopted at 1973 Winter ASAE Meeting in Chicago (Unpublished report).

SULLINS, R. D. and ROONEY, L. W. 1971. Physical changes in the kernel during reconstitution of sorghum grain. Cereal Chem. *48*, 567–571.

WARD, G. M., NARASIMHALU, P. R., BOREN, F. W., SCHNEIDER, Verna L. and FAIRBANKS, G. E. 1965. Effect of grinding forage sorghum heads on silage starch and energy digestibility. J. Dairy Sci. *48*, 1537–1540.

U.S. Dept of Agriculture Grain Sorghum Standards. 1973. United States Department of Agriculture, Washington, D.C.

COMPACTION BEHAVIOR OF BULK WHOLE CORN KERNEL AT PRESSURES UP TO 34.6 MN/m^2

P. B. MCNULTY[1]

Agricultural Engineering Department
University College
Dublin, Ireland

AND

N. N. MOHSENIN

Agricultural Engineering Department
The Pennsylvania State University
University Park, Pennsylvania 16802

Received for Publication December 13, 1976

ABSTRACT

The compaction behavior of whole corn kernel (1.8–22.0% mc, w.b.) was investigated by axial compression in an 18.5 mm diameter die using the Amatek Universal Testing Machine at 28°C. The maximum applied pressure in each experiment was 34.6 MN/m^2 at loading rates of 0.028, 0.28, and 2.8 mm/s. Sample failure due to oil expression or sample extrusion did not occur in any test run. However, extensive physical rupture of corn kernels occurred at 1.8% moisture content and at lesser but significant levels at 6.6 and 9.7% moisture. At 15.9 and 22.0% moisture, samples were plastically deformed but little macroscopic kernel damage was evident. The effectiveness of compaction increased dramatically as moisture content increased up to 22.0% and then appeared to gradually decline with further increase in moisture. The average compression ratio at zero pressure varied from an average low of 1.70 at 1.8% to an average high of 1.92 at 22.0% mc corresponding to reductions in corn volume of 41 and 47%, respectively. In contrast, loading rate had little effect on density-pressure profiles. The latter were not adequately characterized by powder compaction models reported in the literature. Substantial volumes of internal tissue gas were estimated with an average maximum of 21% in 15.9% moisture corn kernels.

The extent of stress relaxation after termination of compaction increased as loading rate increased and was highest in 15.9% moisture

[1] Present study completed while he was a Visiting Research Associate at University Park, Pa. 16802

Journal of Food Process Engineering 1 (1977) 75–95.

corn. The pressures required for the ejection of compacted corn from the 18.5 *mm die varied from* 0.5 *to* 2.1 *MN/m*^{2} *and revealed an average maximum value at* 9.7% *moisture. Ejection pressures were substantially independent of loading rate. The most stable compacted corn samples were those produced at the* 15.9% *moisture level although the compact stability in general was very poor indeed.*

INTRODUCTION

In a preceeding paper (McNulty and Mohsenin 1977) we have discussed the behavior of low and high moisture whole corn kernel under compaction conditions leading to failure. Low moisture corn (6.6% w.b.) failed due to oil expression in the pressure range 140–310 MN/m^2 whereas high moisture corn (24.2% w.b.) failed due to sample extrusion in the pressure range 40–70 MN/m^2.

The purpose of this study was to investigate the compaction behavior of bulk whole corn kernel under conditions which would not lead to failure either by oil expression or sample extrusion. In particular we were anxious to establish criteria for the design of systems to effectively compact whole corn and other agricultural materials.

We are also investigating the effect of high pressure compaction on the microbial activity of corn and will report our preliminary data elsewhere (McNulty *et al.* 1977).

EXPERIMENTAL

Materials

Yellow dent hybrid corn was harvested in 1975 and dried with heated air to approximately 10% mc (w.b.). In June 1976, 1–2 kg batches were placed on wire mesh trays in sealed environmental chambers over saturated solutions of aqueous lithium chloride, sodium bromide, potassium chloride, and potassium sulfate. These solutions yielded equilibrium relative humidities at 23.4°C of 11.1, 58.7, 84.8, and 97.0%, respectively (Shelef and Mohsenin 1966). The low humidity sample was oven dried at 103.5°C overnight so that equilibrium would be attained by sorption as in all other cases rather than desorption. After 3–4 weeks, samples had almost reached equilibrium and, after oven drying at 103.5°C for 72 hr, yielded the moisture levels given in Table 1. The 1.8% moisture corn was obtained by oven drying at 103.5°C overnight.

Table 1. Summary of compaction tests on whole corn kernel at 28°C using $P_{max} = 34.6$ MN/m^2

Run	Corn					Compaction					Relaxation Ejection	
	% mc (w.b.)	Kernels Density kg/m^3			% U_e	Loading Rate (mm/s)	Density (kg/m^3)				$\%[1-\frac{\sigma(6s)}{\sigma(o)}]$	P_{max} (MN/m^2)
		g	ρ_B	ρ_k			ρ_o	ρ_{fP}	ρ_{fP_o}	ρ_t		
11	1.8	3.73	691	1330	48.2	0.028	616	1110	1020	1260	5.3	0.89
12	1.8	3.73	691	1330	48.2	0.28	603	1150	1060	1430	15.3	0.553
15	1.8	3.73	691	1330	48.2	2.8	649	1180	1100	1440	19.3	0.879
24	6.6	3.45	715	1370	47.8	0.028	672	1220	1130	1490	7.9	1.25
25	6.6	3.45	715	1370	47.8	0.28	673	1210	1130	1480	20.9	1.33
20	6.6	3.45	715	1370	47.8	2.8	651	1220	1130	1470	30.4	1.21
13	9.7	3.36	718	1300	44.5	0.028	633	1240	1190	1470	9.1	2.08
14	9.7	3.36	718	1300	44.5	0.28	666	1240	1180	1670	25.9	1.62
16	9.7	3.36	718	1300	44.5	2.8	693	1230	1190	1600	34.8	0.964
22	15.9	3.20	713	1280	44.3	0.028	676	1360	1260	1640	15.0	1.24
23	15.9	3.20	713	1280	44.3	0.28	664	1330	1270	1610	30.0	1.13
21	15.9	3.20	713	1280	44.3	2.8	689	1330	1270	1600	35.0	1.10
17	22.0	2.94	691	1270	45.6	0.028	654	1420	1250	1470	6.7	0.731
18	22.0	2.94	691	1270	45.6	0.28	663	1410	1240	1450	24.3	0.914
19	22.0	2.94	691	1270	45.6	2.8	641	1390	1260	1560	17.4	0.979

Pycnometer Measurements

An air comparison pycnometer was used to measure the volume of corn samples filled to the brim of the pycnometer cup. Knowing the mass of the sample, m and the volume of the cup, it was possible to evaluate the bulk and kernel densities, ρ_B and ρ_k respectively, and the external porosity U_e of the bulk corn from the following relationships:

$$\rho_B = m/V(cup) \quad (1)$$

$$\rho_k = m/V(corn) \quad (2)$$

$$U_e = 1 - \rho_B/\rho_k \quad (3)$$

Thompson and Isaacs (1967) have indicated that the "possibility of error resulting from a corn kernel . . . absorbing air during a test measurement appeared to be slight or nonexistent."

The number of kernels in each tested sample was measured. This was also done in all moisture determinations and compaction tests. These data were used to yield arithmetic averages of the number of kernels per gram of corn and the average volume of each kernel as a function of moisture content.

The high moisture sample (24.2% w.b.) used by McNulty and Mohsenin (1977) in a previous study was also tested.

Compaction Studies

The experimental procedures and analysis of data were similar to that reported by McNulty and Mohsenin (1977) with the following exceptions:

(a) All samples were compacted to exactly the same maximum pressure of 34.6 MN/m^2 which had been especially chosen to avoid major sample failure due to oil expression or sample extrusion.

(b) A new punch and die set was used which was basically similar to that reported by Kumar (1973) except that its diameter was 18.5 mm and it was machined from stainless steel. In addition, the base plug contained a thermocouple which was mounted 1.5 mm above the center of the plug.

(c) Stress relaxation was allowed to proceed for exactly 600 s after the sample had been compacted.

(d) The sample mass in all tests was 9.00 g and the number of kernels was recorded in each case.

RESULTS

The results are summarized in Table 1 and are arranged in order of ascending moisture content and loading rate.

Major sample failure due to oil expression and/or sample extrusion was not observed in any test run. However extensive physical rupture of corn kernels occurred at 1.8% moisture content and at lesser but significant levels at 6.6 and 9.7% moisture. At 15.9 and 22.0% moisture, samples were plastically deformed but little macroscopic kernel damage was evident. The initial sample height/die diameter ratio, h_o/d varied from an average high of 2.9 at 1.8% mc (w.b.) to an average low of 2.6 at 15.9% mc (w.b.). The compression ratio at zero pressure, $CR_{fP_o} = \rho_o/\rho_{fP_o}$ varied from an average low of 1.70 at 1.8% mc to an average high of 1.92 at 22.0% mc (cf Fig. 7) corresponding to reductions in corn volume of 41 and 47%, respectively. Sample temperature elevation was less than 1°C in all test runs.

Effect of Loading Rate

The effect of loading rate on the compaction behavior of whole corn is illustrated in Fig. 1–3.

Figure 1 shows that compaction behavior of low moisture corn (6.6% w.b.) was independent of loading rate thus confirming our previous data (McNulty and Mohsenin 1977). Average density values abstracted from Tables 1 and 3 revealed that the "at pressure" final density, $\rho_{fP} = 1220$ kg/m^3, was much lower than the kernel density $\rho_k = 1370$ kg/m^3 due to the relatively low value of maximum applied pressure i.e. 34.6 MN/m^2.

In contrast, high moisture corn (22.0% w.b.) subjected to a similar pressure was compacted much more easily and exceeded the kernel density $\rho_k = 1270$ kg/m^3 at pressures less than 20 MN/m^2 in all cases (Fig. 2). Even though ρ_k was exceeded no evidence of major sample failure in the form of sample extrusion or oil expression was observed. After load removal the compacted samples expanded to an average zero pressure final density $\rho_{fP_o} = 1250$ kg/m^3 which was just below the kernel density, $\rho_k = 1270$ kg/m^3. There appeared to be a slight effect of loading rate with the low loading rate producing more effective compaction.

Figure 3 shows the effect of loading rate and moisture on porosity-pressure profiles. At 6.6% moisture the apparent porosity was independent of loading rate thus confirming the data in Fig. 1. It should be noted that the estimated compact density ρ_t varied only over the small range of 1470–1490 kg/m^3 (Table 1).

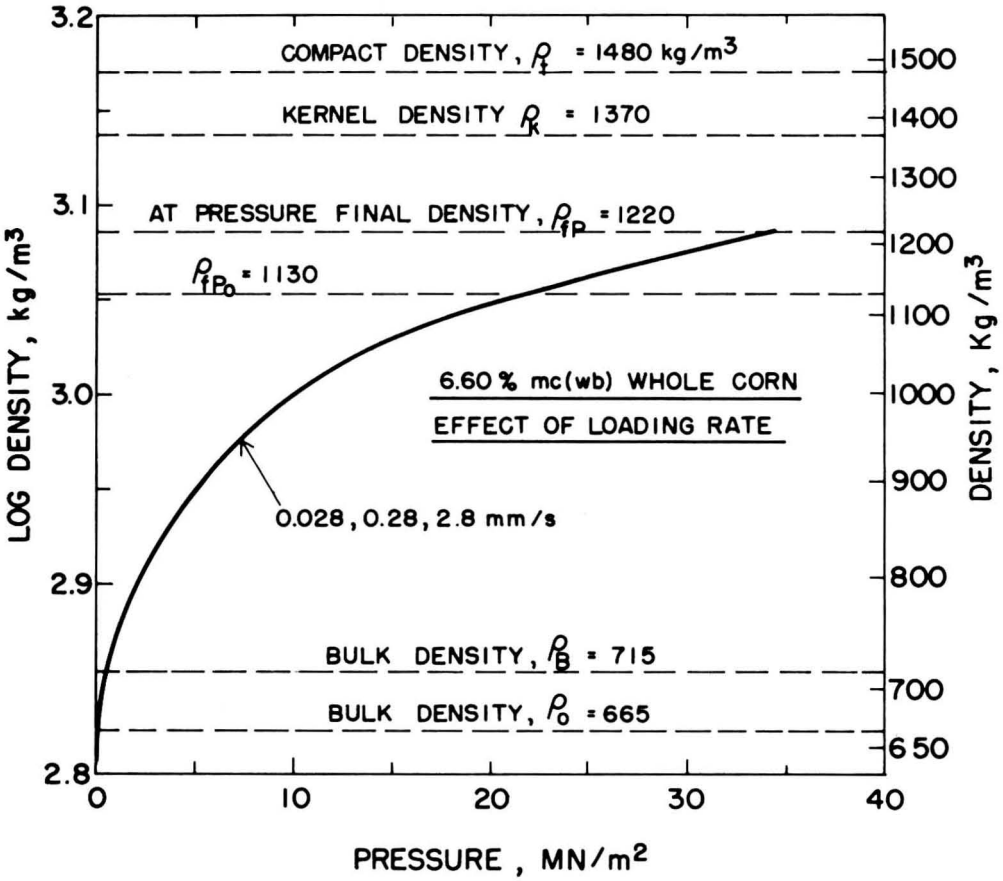

FIG. 1. EFFECT OF LOADING RATE ON COMPACTION BEHAVIOR OF LOW MOISTURE (6.6% W.B.) WHOLE CORN IN AN 18.5 MM DIAMETER DIE AT 28°C (RUNS 20, 24, AND 25)

In contrast, the porosity-pressure profile was dependent on loading rate for the high moisture corn (22.0% w.b.) i.e. the extent of "at pressure" compaction appeared to be inferior at the high loading of 2.8 mm/s. However as discussed previously (McNulty and Mohsenin 1977), this is an artifact caused by the higher predicted value of ρ_t = 1560 kg/m^3, from which porosity values, U, are evaluated i.e.

$$U = 1 - D = 1 - \rho/\rho_t \qquad (4)$$

where D = relative apparent density.

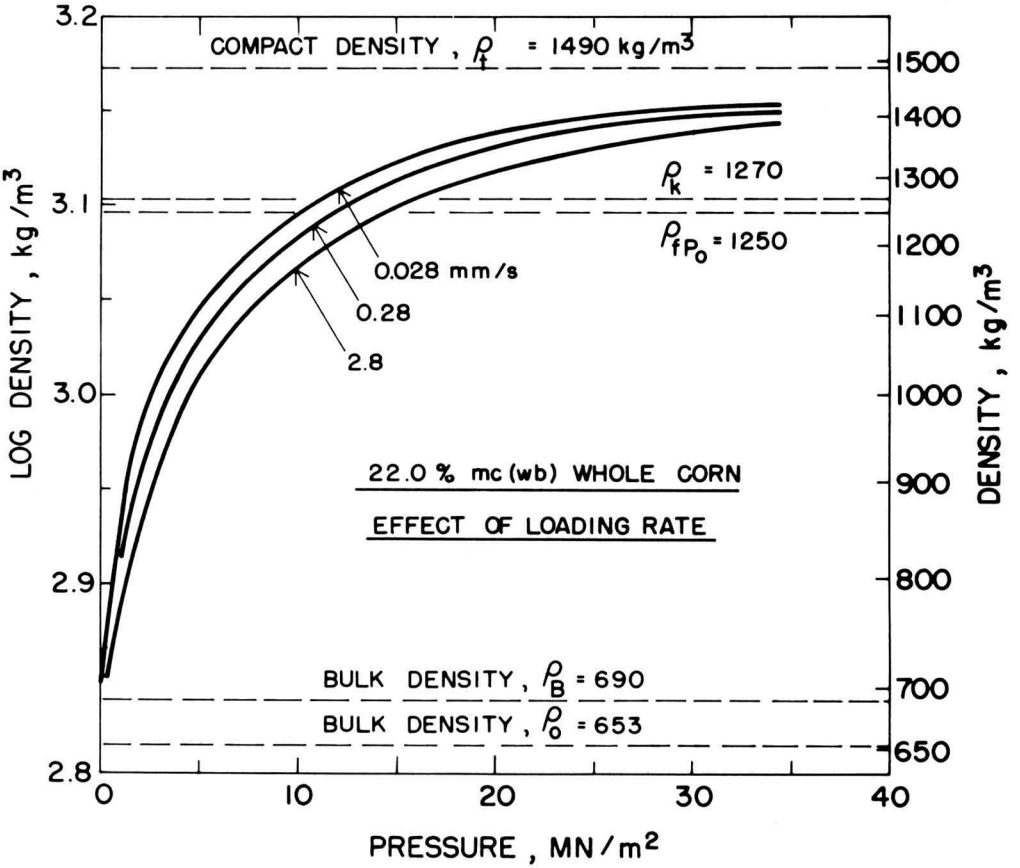

FIG. 2. EFFECT OF LOADING RATE ON COMPACTION BEHAVIOR OF HIGH MOISTURE (22.0% W.B.) WHOLE CORN IN AN 18.5 MM DIAMETER DIE AT 28°C (RUNS 17–19)

Effect of Maximum Applied Pressure, P_{max}

The effect of maximum applied pressure on densification of low moisture corn (6.6% w.b.) is presented in Table 2 which includes some data reported previously (Runs 3, 7, and 9 were abstracted from McNulty and Mohsenin 1977). In all but one case higher pressures lead to higher values of "at pressure" final density, ρ_{fP}; zero pressure final density, ρ_{fP_o}; and the zero pressure compression ratio, CR_{P_o}. The exception was run wherein the experiment had been stopped at a much lower value of P_{max} than had been originally planned.

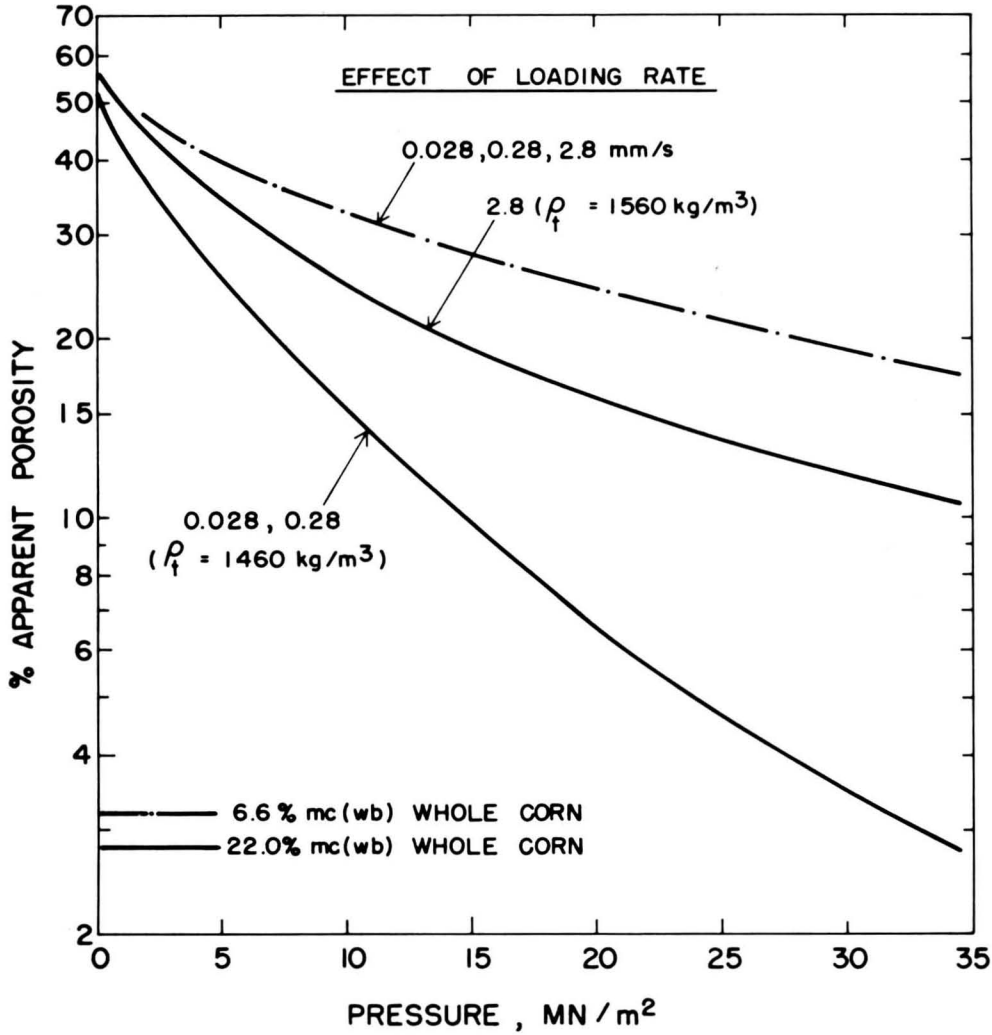

FIG. 3. EFFECT OF LOADING RATE AND MOISTURE CONTENT ON COMPACTION BEHAVIOR OF WHOLE CORN IN AN 18.5 MM DIAMETER DIE AT 28°C (RUNS 17–20, 24, AND 25)

Effect of Moisture Content

Figures 4 and 6(a) reveal that the extent of "at pressure" compaction increases as corn moisture content increased at the low and high loading rates, respectively. Figure 4 also shows a comparison with the data of Kumar (1973) on ground corn which suggests that: (a) a simple density-pressure exponential relationship does not adequately characterize the

Table 2. Effect of maximum applied pressure, P_{max}, and loading rate on densification of whole corn kernel (6.6% mc (w.b.) at 28°C

Run	Loading Rate (mm/s)	P_{max} (MN/m^2)	Density (kg/m^3)				CR_{P_o}
			ρ_o	ρ_{fP}	ρ_{fP_o}	ρ_t	
3	0.028	258	703	1490	1360	1620	1.94
24	0.028	34.6	672	1220	1130	1490	1.68
7	0.28	252	679	1460	1260	1570	1.86
25	0.28	34.6	673	1210	1130	1480	1.68
9	2.8	69.6	694	1310	1210	1360	1.74
20	2.8	34.6	651	1220	1130	1470	1.73

Table 3. Estimation of internal tissue gas in whole corn kernels from compaction data at 28°C

P_{max} MN/m^2			Density (kg/m^3)			% Porosity			
			ρ_B	ρ_k	ρ_t	U_e	U_i	U	U_k
34.6	1.8	1.70	691	1330	1380	48.1	1.8	49.9	3.6
34.6	6.6	1.70	715	1370	1480	47.8	3.9	51.7	7.4
314	6.6	2.06	715[a]	1370[a]	1600	47.8	7.5	55.3	14.4
34.6	9.7	1.78	718	1300	1580	44.8	9.8	54.6	17.7
34.6	15.9	1.87	713	1280	1620	44.3	10.3	56.0	21.0
34.6	22.0	1.92	691	1270	1490	45.6	8.0	53.6	14.8
84.3	24.2	1.83	671	1260	1400	46.7	5.4	52.1	10.0[b]

[a]Values assumed
[b]May be an overestimate due to extrusion

compaction behavior of ground or whole corn; (b) slightly greater energy is required to compact ground than whole corn; (c) the effect of moisture content on the extent of "at pressure" compaction is much more pronounced at moisture contents above 10% than below it. Figure 6(a) also confirms the latter observation.

In contrast, the effect of moisture content on porosity-pressure profiles does not follow a similar systematic pattern (Fig. 5 and 6(b)). For example, the low moisture corn (1.8% w.b.) appears to be compacted more extensively than the 9.7% corn at both low and high loading rates in sharp contrast to the behavior revealed in the density-pressure profiles (Fig. 4 and 6(a)). This apparent contradiction is best explained by referring to Fig. 7 which shows the effect of moisture content on various corn densities.

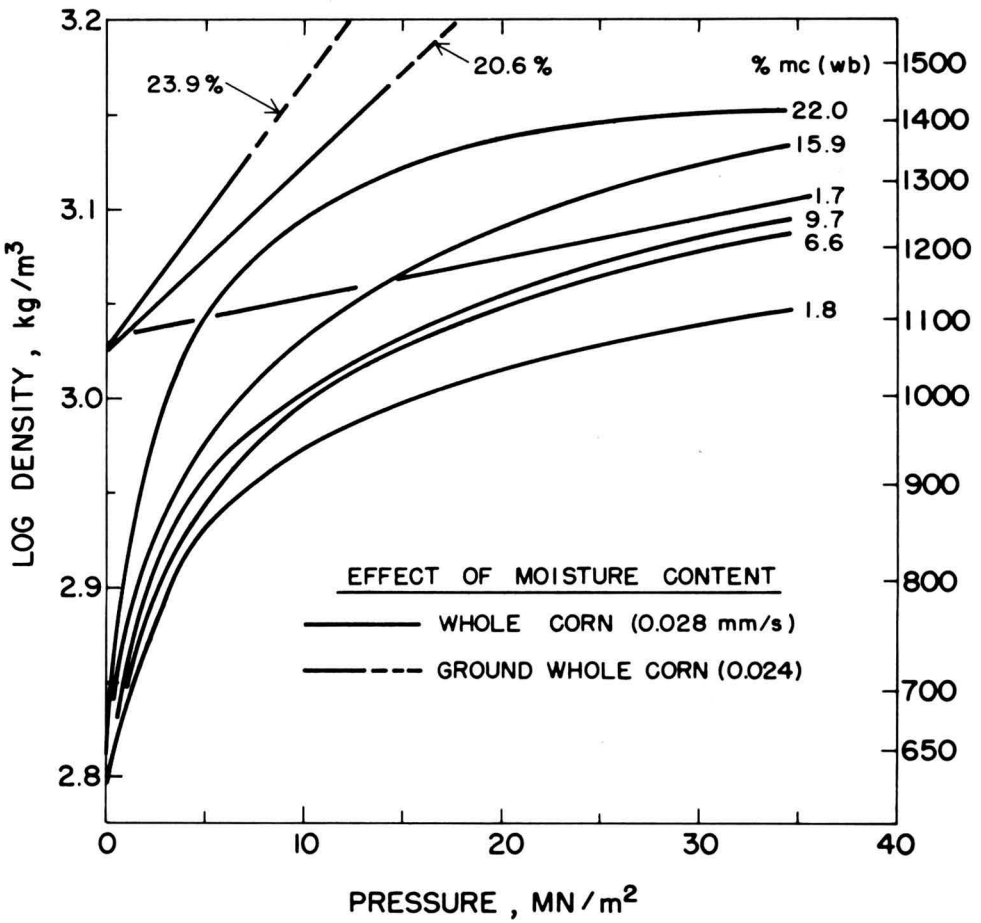

FIG. 4. EFFECT OF MOISTURE CONTENT ON THE COMPACTION BEHAVIOR OF WHOLE CORN AT A LOADING RATE OF 0.028 MM/S IN AN 18.5 MM DIAMETER DIE AT 28°C AND COMPARISON WITH THE DATA OF KUMAR (1973) ON GROUND WHOLE CORN (RUNS 11, 13, 17, 22, AND 24)

Corn Densities

The bulk and kernel densities were measured by air comparison pycnometer as previously described. All other density parameters were arithmetic averages of the densities measured during low, medium, and high loading rate compaction studies. Figure 7 also includes data at 24.2% mc (w.b.) collected in a previous study (McNulty and Mohsenin 1977).

The loose fill bulk density ρ_o in the compaction dies is in all cases

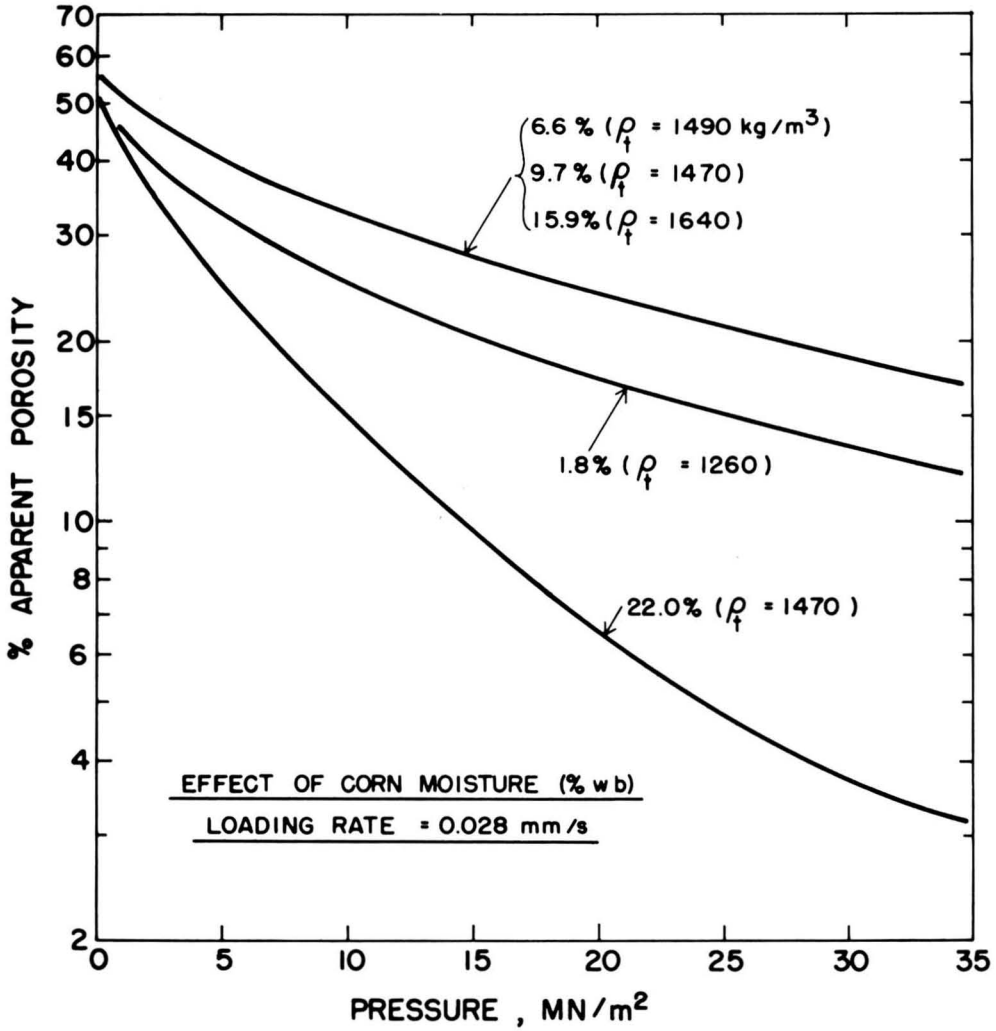

FIG. 5. EFFECT OF MOISTURE CONTENT ON THE COMPACTION BEHAVIOR OF WHOLE CORN AT A LOADING RATE OF 0.028 MM/S IN AN 18.5 MM DIAMETER DIE AT 28°C (RUNS 11, 13, 17, 22, AND 24)

slightly lower than the standard bulk density measured by pycnometer as expected. The kernel density, ρ_k decreases as moisture content increases as expected because the density of water is 996 kg/m^3 at 28°C. The values for kernel density are in close agreement with those reported by Thompson and Isaacs (1967) as shown in Fig. 10. In the absence of internal tissue gas, the kernel densities would represent the

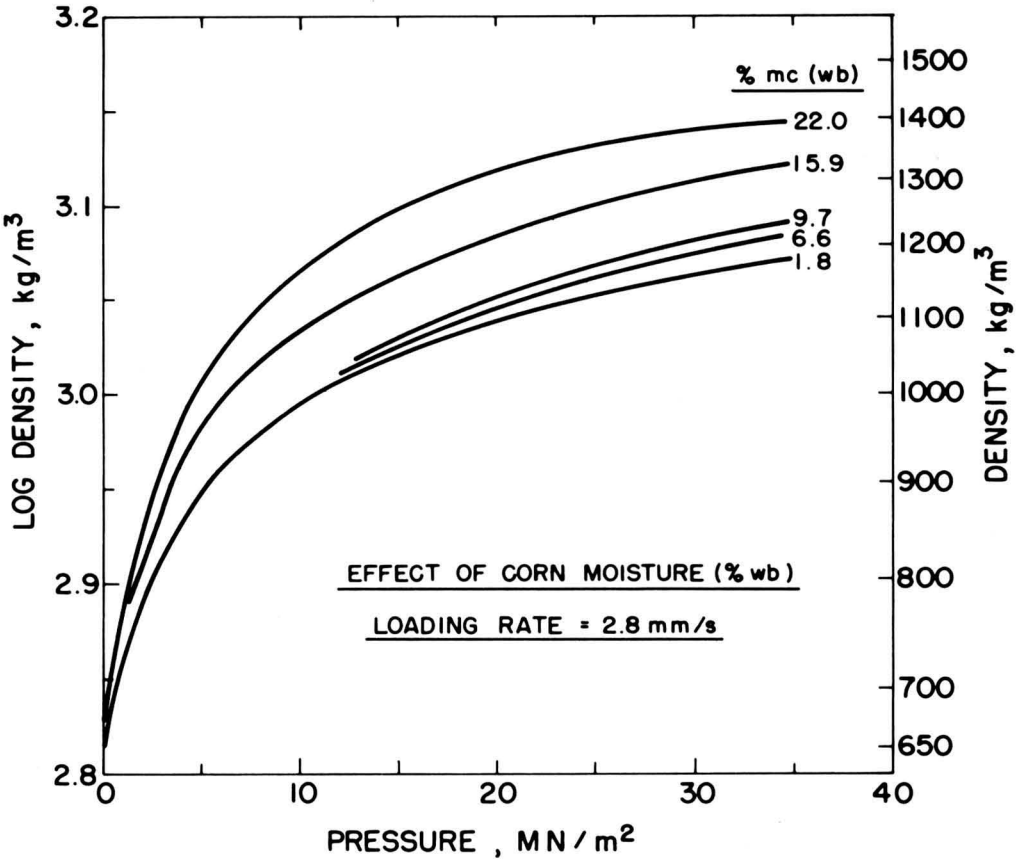

FIG. 6. EFFECT OF MOISTURE CONTENT ON THE COMPACTION BEHAVIOR OF WHOLE CORN AT A LOADING RATE OF 2.8 MM/S IN AN 18.5 MM DIAMETER DIE AT 28°C (RUNS 15, 16, AND 19–21)

a. Density plot.

maximum densities to which whole corn kernel could be compacted.

However, we have previously shown that substantial quantities of internal tissue gas exists in 6.6 and 24.2% mc (w.b.) corn kernels (McNulty and Mohsenin 1977). Figure 7 shows that as moisture content increases the average "at pressure" final density increases almost linearly up to 22.0% moisture after which it decreases i.e. the extent of "at pressure" compaction using the same maximum applied pressure increases as moisture content increases. However, it also appears that the zero pressure final density, ρ_{fP_o}, measured after load removal, will never exceed the kernel density. Thus, the maximum effectiveness of

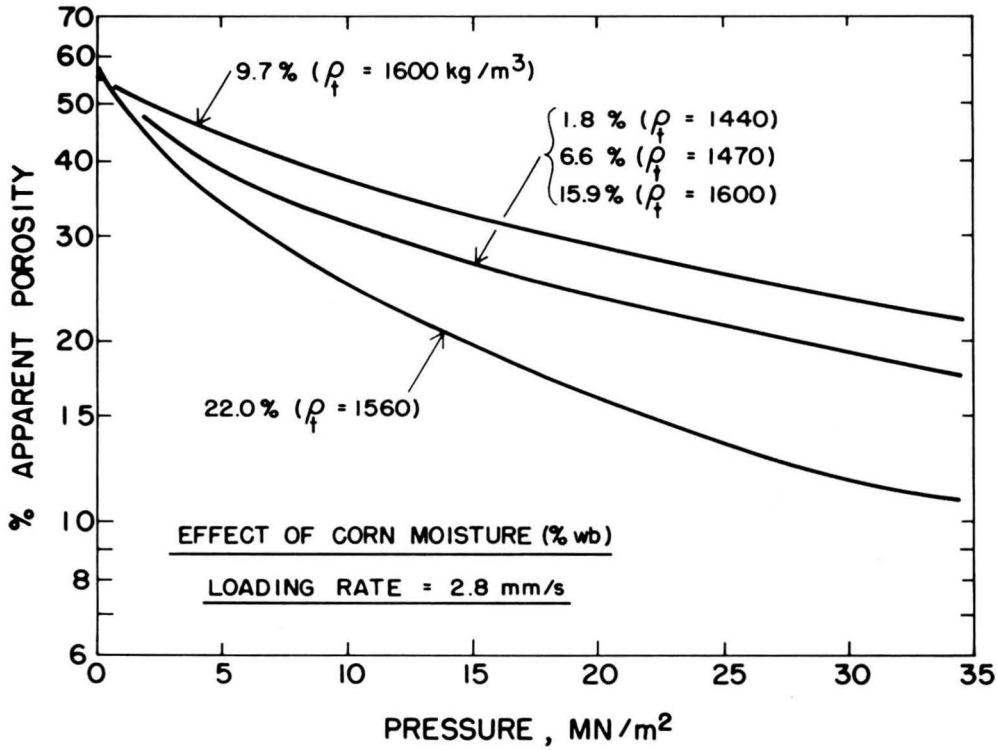

FIG. 6. EFFECT OF MOISTURE CONTENT ON THE COMPACTION BEHAVIOR OF WHOLE CORN AT A LOADING RATE OF 2.8 MM/S IN AN 18.5 MM DIAMETER DIE AT 28°C (RUNS 15, 16, AND 19–21)

b. Porosity plot.

compaction as shown in Fig. 7 or as indicated by CR_{P_o} in Table 3 occurs at 22.0% and appears to decline thereafter.

The estimated compact densities show a maximum at 15.9% mc (w.b.). These data may be used to estimate the internal tissue gas in corn kernel using the following relationships:

$$U = U_e + U_i \tag{5}$$

where U = total porosity = fractional void volume; U_i = internal kernel porosity based on total bulk volume. The external porosity, U_e, is given by Equation 3.

The internal kernel porosity defined as the fractional volume of voids in the kernel itself is given by:

$$U_k = 1 - \rho_k/\rho_t \tag{6}$$

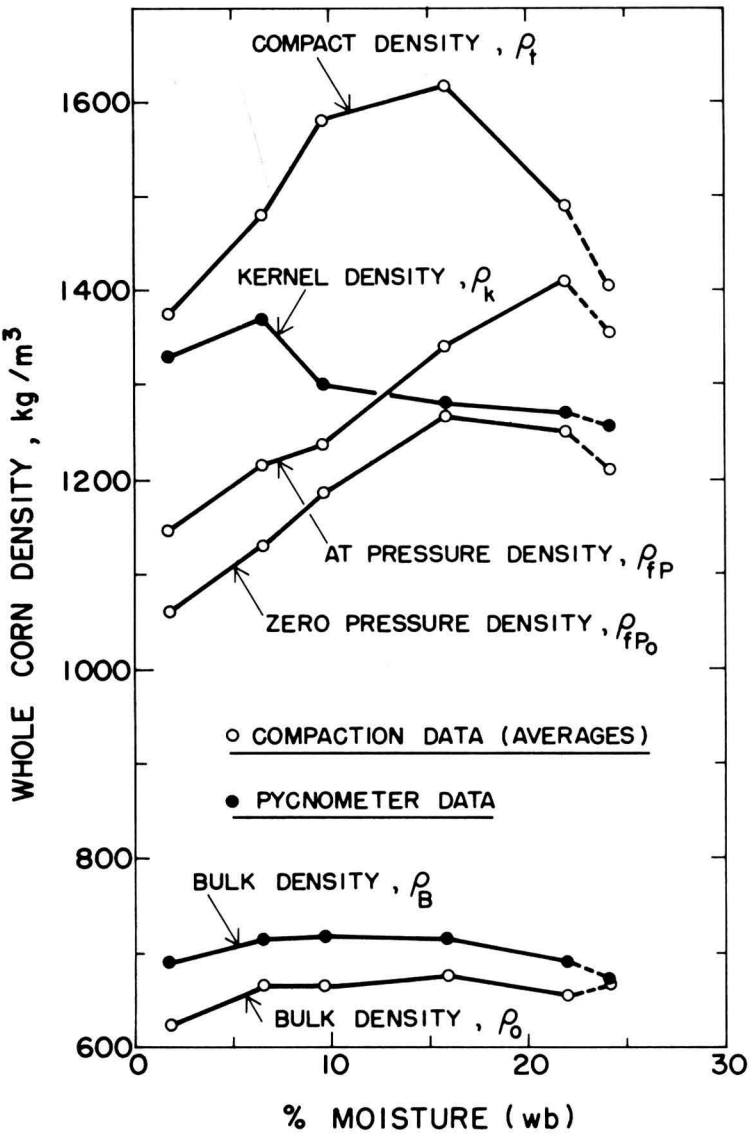

FIG. 7. EFFECT OF MOISTURE ON DENSITY OF WHOLE CORN BEFORE AND AFTER AXIAL COMPACTION AT 28°C

All compaction data are arithmetic average of the results from the three loading rates used. All data were evaluated in this study except those at 24.2% mc which were abstracted from the first paper in this series.

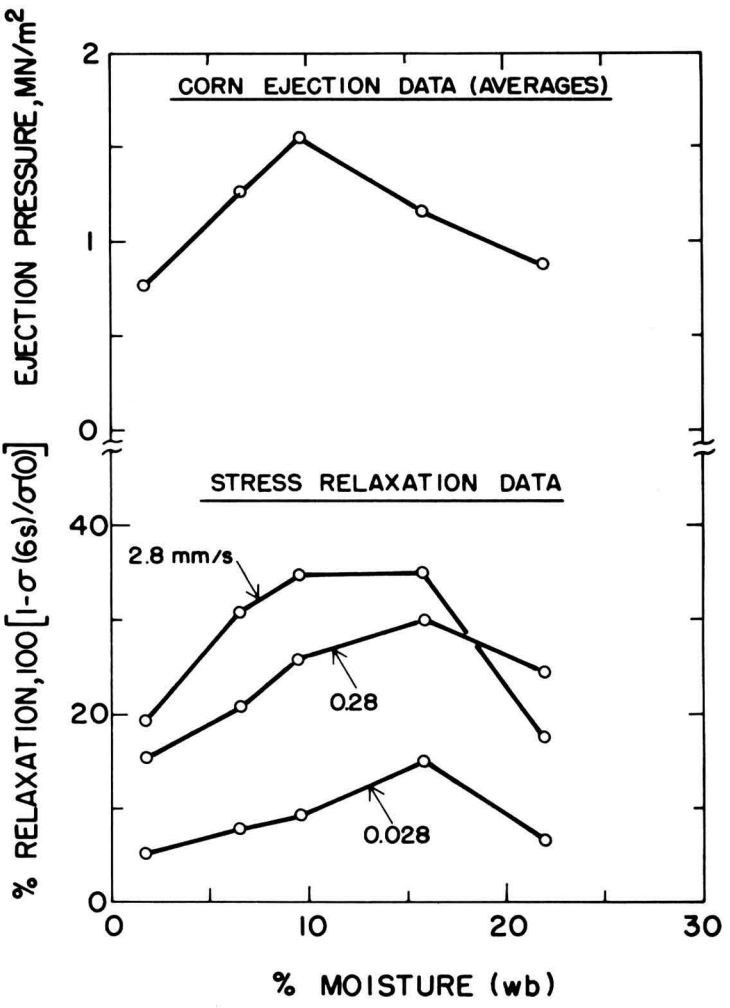

FIG. 8. EFFECT OF MOISTURE AND LOADING RATE ON RELAXATION OF STRESS IN COMPACTED WHOLE CORN (MAX. APPLIED PRESSURE = 34.6 MN/m^2) AND ON THE MAXIMUM PRESSURE REQUIRED TO EJECT COMPACTED SAMPLES FROM THE DIE

Ejection data are arithmetic averages of the results from the three loading rates used. Percent relaxation = % stress relaxed of initial value after 6 s.

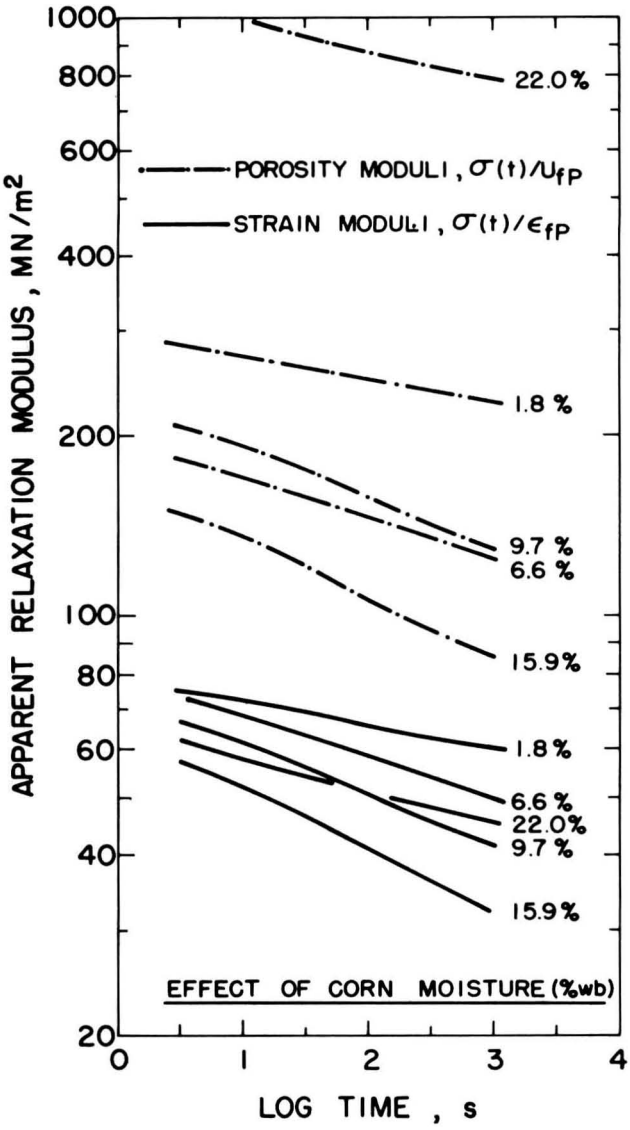

FIG. 9. EFFECT OF MOISTURE CONTENT ON STRESS RELAXATION BEHAVIOR OF COMPACTED WHOLE CORN SUBJECTED TO A MAXIMUM PRESSURE OF 34.6 MN/m^2 IN AN 18.5 MM DIAMETER DIE AT 28°C

a. Corn compacted at 0.028 mm/s

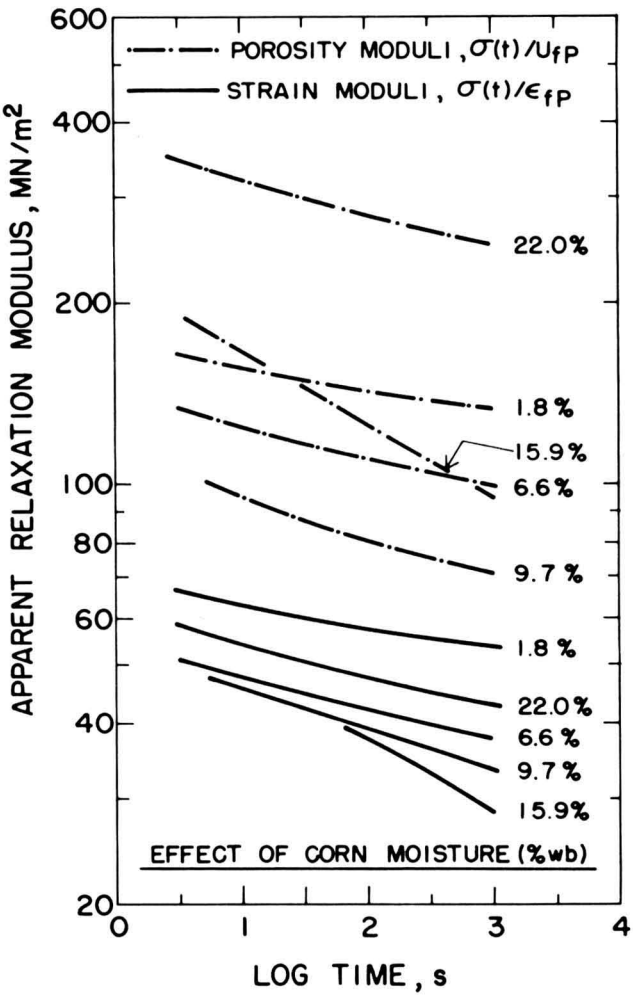

FIG. 9. EFFECT OF MOISTURE CONTENT ON STRESS RELAXATION BEHAVIOR OF COMPACTED WHOLE CORN SUBJECTED TO A MAXIMUM PRESSURE OF 34.6 MN/m^2 IN AN 18.5 MM DIAMETER DIE AT 28°C

b. Corn compacted at 2.8 mm/s

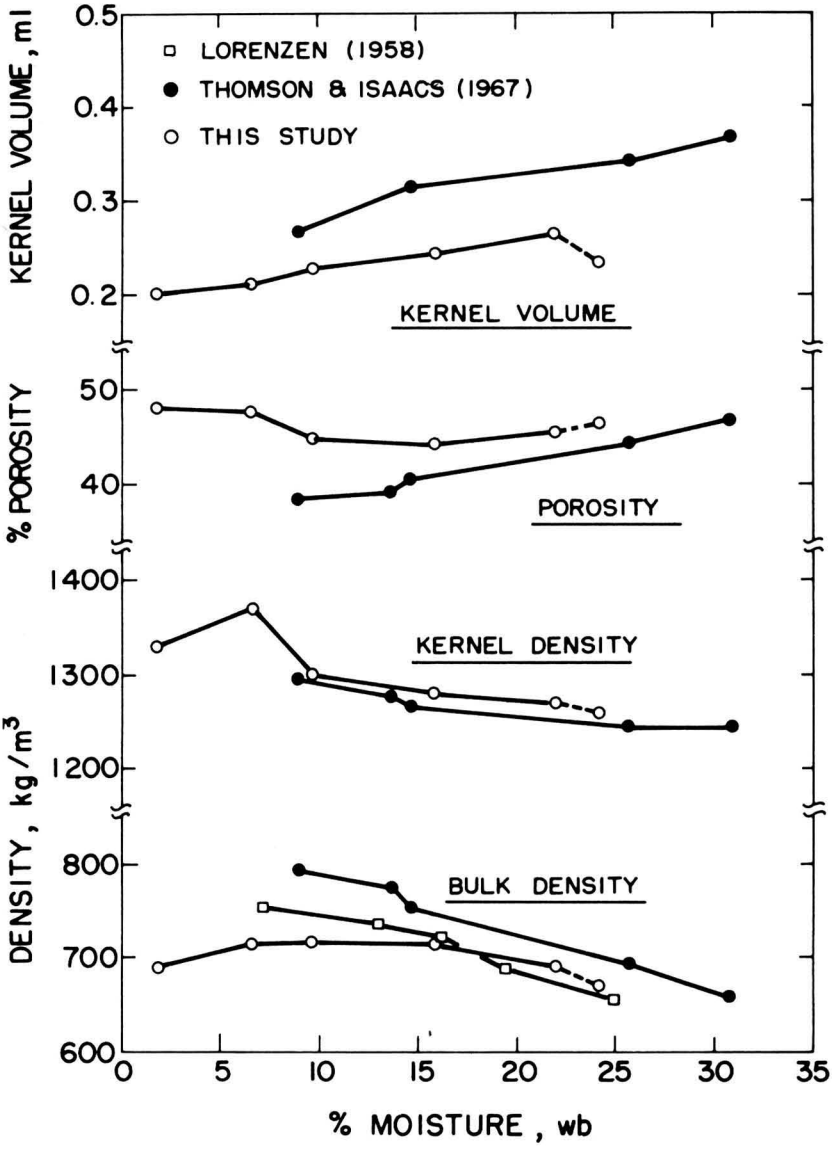

FIG. 10. EFFECT OF MOISTURE CONTENT ON WHOLE CORN PROPERTIES AND COMPARISON WITH SOME LITERATURE DATA

The results are presented in Table 3 which shows that the estimated internal tissue gas varies from 3.6–21.0% with the maximum value at 15.9% moisture content.

Let us now return to Fig. 5 and 6(b) which suggest that the 1.8% moisture corn is compacted more extensively that the 9.7% moisture corn in direct contradiction to the data presented in Fig. 4, 6(a) and 7. The estimated internal tissue gas at 1.8 and 9.7% moisture are respectively, 3.6 and 14.4% (Table 3). These values have been calculated from the apparent compact densities which were estimated by extrapolation from compaction data. The internal tissue gas of 3.6% for the 1.8% moisture corn is almost certainly a gross underestimation due to the unreliability of the extrapolation technique at low levels of product densification as discussed previously (McNulty and Mohsenin 1977). This is dramatically illustrated in Table 3 where compaction of a 6.6% moisture corn to 314 MN/m^2 yields a tissue gas of 14.4% whereas only 7.4% is estimated under compaction to 34.6 MN/m^2. Thus the contradiction between the data in Fig. 5 and 6(b) on the one hand and Fig. 4, 6(a) and 7 is an apparent one based on the experimental constraint that all corn samples were compacted to a similar pressure level of 34.6 MN/m^2. It is interesting to note that no quantitative information on internal tissue gas in corn kernel appeared to be available to us (Wolf 1977), although its structure has been well-established (Wolf *et al.* 1952).

Relaxation and Ejection Behavior

The extent of stress relaxation increased as loading rate increased (Fig. 8), which is due to the fact that considerable relaxation has already occurred during loading at low loading rates.

In contrast loading rate had little effect on ejection pressures (Table 1) where arithmetic averages are plotted in Fig. 8. Both ejection and relaxation data reveal maxima at intermediate moisture levels. In this context it is interesting to note that the most stable compacted corn samples were those produced at the 15.9% moisture level although the compact stability in general was very poor indeed.

The effect of moisture on apparent relaxation moduli is presented in Fig. 9(a) and (b) at respective loading rates of 0.028 and 2.8 mm/s. Two types of moduli were used, namely, strain and porosity moduli defined respectively as:

$$E_t(t) = \sigma(t)/\epsilon_{fP} = Ph_o/(h_o - h_{fP}) \tag{7}$$

$$E'_t(t) = \sigma(t)/U_{fP} = P/U_{fP} \tag{8}$$

where $\sigma(t)$ = stress at time, t; ϵ_{fp} = "at pressure" final strain which varied from a low of 42.3% at 6.6% moisture to a high of 53.8% at 22.0% moisture. In general, the strain moduli decreased systematically as moisture content increased except at 22.0% moisture. It should be noted that the resistance of the material to compaction increases as strain increases i.e. as porosity decreases. Thus, the 22.0% moisture sample which was compacted to the highest strain recorded of 53.8% would be expected to exhibit relatively high relaxation moduli.

The porosity moduli are in all cases considerably higher in magnitude than strain moduli. This is due to the fact that as porosity approaches zero the strength of the material and therefore its relaxation moduli approaches infinity.

Comparison with Literature Data

A comparison of some physical properties of corn measured in this study with data reported in the literature is presented in Fig. 10. The kernel volumes in our study were considerably smaller than those reported by Thompson and Isaacs (1967) for yellow corn of the variety, Pfister Sx29.

At high moisture levels our values of bulk densities ρ_B are in close agreement with the literature data. At low moisture levels, however, our bulk densities are considerably lower. This is due to the fact that our 1.8 and 6.6% moisture samples were oven-dried at 103.5°C overnight prior to testing. Thompson and Isaacs (1967) indicate that such treatment leads to drying damage manifested by lower bulk densities and higher porosities than grain which is dried with unheated air.

Our kernel densities are in close agreement with the literature data.

CONCLUSIONS

(1) Whole corn kernel (1.8–22.0% mc, w.b.) may be compacted to a pressure of 34.6 MN/m^2 at 28°C and at loading rates of 0.028–2.8 mm/s without causing sample failure due to oil expression and/or sample extrusion.

(2) Extensive physical rupture of corn kernels occurred at 1.8% moisture and at lesser but significant levels at 6.6 and 9.7% moisture. At 15.9 and 22.0% moisture, samples were significantly deformed but little macroscopic kernel damage was evident.

(3) The effectiveness of compaction (as indicated by the zero pressure compression ratio) increased dramatically as moisture content increased up to 22.0% and then appeared to gradually decline with further increase in moisture.

(4) Loading rate had little effect on compaction behavior when expressed in terms of density-pressure profiles. In contrast, loading rate appeared to be significant when compaction behavior was expressed in terms of porosity-pressure profiles. This however was an artifact due to underestimation of internal tissue gas at low moisture levels. The average maximum internal tissue gas was estimated as 21% in 15.9% moisture corn kernels.
(5) Powder compaction models reported in the literature did not adequately characterize the compaction behavior of whole corn kernel.
(6) The extent of stress relaxation after termination of compaction increased as loading rate increased and was highest at 15.9% moisture.
(7) The pressures required for the ejection of compacted corn from the 18.5 mm die varied from 0.5 to 2.1 MN/m^2 and revealed an average maximum value at 9.7% moisture. Ejection pressures were substantially independent of loading rate.
(8) The most stable compacted corn samples were those produced at the 15.9% moisture level although the compact stability in general was very poor indeed.

REFERENCES

KUMAR, M. 1973. Compaction behavior of ground corn. J. Food Science *38*, 877–878.

LORENZEN, R. T. 1958. Effect of moisture on weight-volume relationship of small grain. ASAE Paper 58-111, St. Joseph, Michigan.

MCNULTY, P. B. and MOHSENIN, N. N. 1977. High pressure compaction behavior of bulk whole corn kernel under conditions leading to failure. Unpublished observations. (Submitted for publication to Trans. of the ASAE).

MCNULTY, P. B., PETRELL, R. J., FUNG, D. Y. C. and MOHSENIN, N. N. 1977. Effect of high pressure compaction of bulk corn kernel on its microbial activity. (In Preparation).

SHELEF, L. and MOHSENIN, N. N. 1966. Moisture relations in germ, endosperm, and whole corn kernel. Cereal Chem. *43*, 347–353.

THOMPSON, R. A. and ISAACS, G. W. 1967. Porosity determinations of grains and seeds with an air-comparison pycnometer. Trans of the ASAE *10*, 693–696.

WOLF, M. J. 1977. Private communication.

WOLF, M. J., BUZAN, C. L., MACMASTERS, M. M. and RIST, C. F. 1952. Structure of the mature corn kernel. Cereal Chem. *29*, 321–382.

NOTATION

a	constant	
A	area	m^2
CR	compression ratio	
d	diameter	m
D	relative density $= \rho/\rho_t = 1 - U$	
E	relaxation modulus	N/m^2
h	sample height	m
ID	internal diameter	m
k	constant	
m	mass	kg
OD	outer diameter	m
P	pressure	N/m^2
t	time	s
T	temperature	°C
U	porosity	
V	volume	m^3
ρ	density	kg/m^3
ϵ	strain	
σ	stress	N/m^2

SUBSCRIPTS

B	bulk	max	maximum
e	external	o	initial
ext	extrusion	oil	oil expression
f	final	P	at pressure
i	internal	P_o	at zero pressure
k	kernel	s	small
l	large	t	compact

DENSITY TERMINOLOGY IN COMPACTION STUDIES

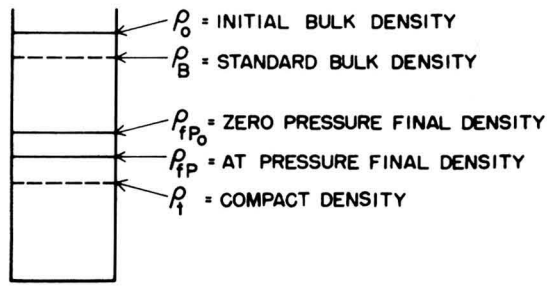

GUIDE FOR AUTHORS

Typewritten manuscripts in triplicate should be submitted to the editorial office. The typing should be double-spaced throughout with one-inch margins on all sides.

Page one should contain: the title, which should be concise and informative; the complete name(s) of the author(s); affiliation of the author(s); a running title of 40 characters or less; and the name and mail address to whom correspondence should be sent.

Page two should contain an abstract of not more than 150 words. This abstract should be intelligible by itself.

The main text should begin on page three and will ordinarily have the following arrangement:

Introduction: This should be brief and state the reason for the work in relation to the field. It should indicate what new contribution is made by the work described.

Materials and Methods: Enough information should be provided to allow other investigators to repeat the work. Avoid repeating the details of procedures which have already been published elsewhere.

Results: The results should be presented as concisely as possible. Do not use tables *and* figures for presentation of the same data.

Discussion: The discussion section should be used for the interpretation of results. The results should not be repeated.

In some cases it might be desirable to combine results and discussion sections.

References: References should be given in the text by the surname of the authors and the year. *Et al.* should be used in the text when there are more than two authors. All authors should be given in the References section. In the Reference section the references should be listed alphabetically. See below for style to be used.

DEWALD, B., DULANEY, J. T. and TOUSTER, O. 1974. Solubilization and polyacrylamide gel electrophoresis of membrane enzymes with detergents. In *Methods in Enzymology*, Vol. xxxii, (S. Fleischer and L. Packer, eds.) pp. 82–91, Academic Press, New York.

HASSON, E. P. and LATIES, G. G. 1976. Separation and characterization of potato lipid acylhydrolases. Plant Physiol. *57*, 142–147.

ZABORSKY, O. 1973. *Immobilized Enzymes*, pp. 28–46, CRC Press, Cleveland, Ohio.

Journal abbreviations should follow those used in *Chemical Abstracts*. Responsibility for the accuracy of citations rests entirely with the author(s). References to papers in press should indicate the name of the journal and should only be used for papers that have been accepted for publication. Submitted papers should be referred to by such terms as "unpublished observations" or "private communication." However, these last should be used only when absolutely necessary.

Tables should be numbered consecutively with Arabic numerals. The title of the table should appear as below:

Table 1. Activity of potato acyl-hydrolases on neutral lipids, galactolipids, and phospholipids

Description of experimental work or explanation of symbols should go below the table proper.

Figures should be listed in order in the text using Arabic numbers. Figure legends should be typed on a separate page. Figures and tables should be intelligible without reference to the text. Authors should indicate where the tables and figures should be placed in the text. Photographs must be supplied as glossy black and white prints. Line diagrams should be drawn with black waterproof ink on white paper or board. The lettering should be of such a size that it is easily legible after reduction. Each diagram and photograph should be clearly labeled on the reverse side with the name(s) of author(s), and title of paper. When not obvious, each photograph and diagram should be labeled on the back to show the top of the photograph or diagram.

Acknowledgments: Acknowledgments should be listed on a separate page.

Short notes will be published where the information is deemed sufficiently important to warrant rapid publication. The format for short papers may be similar to that for regular papers but more concisely written. Short notes may be of a less general nature and written principally for specialists in the particular area with which the manuscript is dealing. Manuscripts which do not meet the requirement of importance and necessity for rapid publication will, after notification of the author(s), be treated as regular papers. Regular papers may be very short.

Standard nomenclature as used in the engineering literature should be followed. Avoid laboratory jargon. If abbreviations or trade names are used, define the material or compound the first time that it is mentioned.

EDITORIAL OFFICE: Prof. D. R. Heldman, Editor, Journal of Food Process Engineering, Michigan State University, Department of Agricultural Engineering, East Lansing, Michigan 48824

JOURNAL OF FOOD PROCESS ENGINEERING VOL. 1, NO. 1 January 1977

CONTENTS